

Mineralogical zonation in chondrules and chemical  
chondrule-matrix complementarities in  
carbonaceous and Rumuruti chondrites

In a u g u r a l - D i s s e r t a t i o n

zur

Erlangung des Doktorgrades

der Mathematisch-Naturwissenschaftlichen Fakultät

der Universität zu Köln

vorgelegt von

**Pia Friend**

aus Solingen

Köln 2017

Berichtersteller: PD Dr. Dominik Hezel  
Prof. Dr. Carsten Münker

Tag der mündlichen Prüfung: 07.07.2017

“The more clearly we can focus our attention on  
the wonders and realities of the universe about us,  
the less taste we shall have for destruction.”

-Rachel Carson

## Table of Contents

Abstract.....	1
Kurzzusammenfassung .....	2
1 Introduction.....	3
1.1 The solar system .....	4
1.1.1 Structure of the solar system .....	4
1.1.2 Formation of the solar system .....	5
1.2 Chondrite classification and components .....	9
1.2.1 Chondrite classification .....	9
1.2.2 Chondrite components.....	13
1.3 Chondrule formation.....	16
1.4 Aims and objectives.....	19
2 The conditions of chondrule formation, Part II: Open system.....	21
Abstract.....	22
2.1 Introduction.....	23
2.2 Methods .....	25
2.3 Results.....	27
2.4 Discussion .....	33
2.4.1 Formation of low-Ca pyroxene rims .....	33
2.4.2 Amount of material added to the chondrules .....	35
2.4.3 Chondrule sizes and bulk compositions .....	35
2.4.4 Unzoned chondrules .....	36
2.5 Conclusions.....	38
References.....	41
3 Chondrule and matrix complementarities in the recently discovered Jbilet Winselwan CM chondrite .....	47
Abstract.....	48
3.1 Introduction.....	49
3.2 Methods .....	52
3.3 Results.....	54
3.3.1 Textures and lithologies of Jbilet Winselwan.....	54
3.3.2 Bulk chondrite composition.....	58
3.3.3 Petrography and elemental composition of chondrules.....	59
3.3.4 Petrography and chemical composition of matrix and fine-grained chondrule rims	61
3.4 Discussion.....	63
3.4.1 Jbilet Winselwan bulk composition .....	63
3.4.2 Aqueous alteration of JW .....	65
3.4.3 Fine-grained chondrule rims.....	66
3.4.4 Complementarities.....	67
3.5 Conclusions.....	71
References.....	74
Supplementary .....	81
4 Complementary element relationships between chondrules and matrix in Rumuruti chondrites.....	84
Abstract.....	85

4.1	Introduction.....	86
4.2	Materials and Methods.....	87
4.2.1	<i>Samples</i> .....	87
4.2.2	<i>Methods</i> .....	88
4.3	Results.....	90
4.3.1	<i>Petrography</i> .....	90
4.3.2	<i>Bulk composition of NWA 753</i> .....	92
4.3.3	<i>Major elements (Fe, Mg, Si) and refractory elements (Al, Ti, Ca) in chondrules and matrix</i> 93	
4.4	Discussion.....	96
4.4.1	<i>Petrologic types of investigated fragments</i> .....	96
4.4.2	<i>Complementarity of major elements (Fe, Mg and Si)</i> .....	97
4.4.3	<i>Complementarity of refractory elements (Al, Ti and Ca)</i> .....	98
4.4.4	<i>Origin of major element complementarities</i> .....	99
4.4.5	<i>Addition of Si in bulk R chondrites</i> .....	100
4.4.6	<i>Origin of refractory element complementarities</i> .....	102
4.5	Conclusions.....	102
	References.....	105
	Supplementary .....	109
5	Discussion.....	112
5.1	Possible mechanisms of complementarities .....	114
5.1.1	<i>Condensation, evaporation and recondensation</i> .....	114
5.1.2	<i>Separation of metal from chondrules</i> .....	116
5.1.3	<i>Differences among precursors and sorting between chondrules and matrix</i> .....	116
5.2	Complementarity and chondrule formation processes.....	117
5.3	Conclusion .....	119
	References for chapter 1 and chapter 5.....	120
	List of abbreviations .....	131
	Danksagung.....	133
	Erklärung zum Eigenanteil an den Publikationen.....	135
	Erklärung.....	136
	Lebenslauf.....	137

## Abstract

Chondritic meteorites ('chondrites') are primitive early solar system materials; the composition of chondrites—especially of CI chondrites—represent the average solar system composition. The two main components of chondrites are (i) chondrules,  $\mu\text{m}$  to mm-sized silicatic melt droplets, and (ii) matrix, an opaque and fine-grained unequilibrium mineral assemblage. The origin of these two constituents, especially for the heat source required for melting chondrules, is still enigmatic. In this work, the genetic link between chondrules and matrix was studied.

A mineralogical zonation with olivine minerals dominating the cores and low-Ca pyroxenes at the margins are present in at least 75% of all chondrules studied in chapter 2. In total, 256 chondrules of 16 different carbonaceous and Rumuriti chondrites (R chondrites) were studied. The low-Ca pyroxene rims were formed by addition of Si to the chondrules (or their precursor) from the surrounding nebula gas, which later condensed to form matrix. Hence, chondrules were open systems and gained 3-15 wt.% material by this process.

In chapters 3 and 4, bulk chondrule, matrix and bulk meteorite compositions of the recently found CM chondrite Jbilet Winselwan (JW) and of three different R chondrites were studied. Bulk chondrule and matrix compositions were obtained with the electron microprobe and bulk meteorite compositions with X-ray spectrometry.

Jbilet Winselwan and the R chondrites show chemical complementarities. Thus, although bulk meteorite compositions are CI chondritic (=solar), chondrules and matrix have different compositions. The amount of matrix in the studied chondrites are at least 50 vol.%. All chondrites have higher than bulk ratios of Fe/Mg, Si/Mg, Al/Ti, Al/Ca in the matrices and vice versa in chondrules. Bulk chondrite ratios are (except Si/Mg in R chondrites) CI chondritic. These complementarities, together with the solar bulk composition of the meteorites, can only be explained when chondrules and matrix formed from a single reservoir.

In chapter 4, complementarity is, to my knowledge, for the first time reported in non-carbonaceous chondrites. It is assumed that carbonaceous and non-carbonaceous chondrites formed in distinct regions within the solar system. A joint formation of chondrules and matrix is required for both reservoirs.

## Kurzzusammenfassung

Chondritische Meteorite („Chondrite“) sind primitive Materialien aus dem frühen Sonnensystem. Ihre Zusammensetzung (insbesondere der CI-Chondrite) repräsentiert die durchschnittliche Zusammensetzung des Sonnensystems. Die beiden Hauptkomponenten der Chondrite sind (i) Chondren,  $\mu\text{m}$  bis mm-große, silikatische Schmelztröpfchen, und (ii) Matrix, ein opakes und feinkörniges Mineralgemisch. Die Entstehung beider Komponenten, insbesondere der Ursprung der Hitzequelle welche die Chondren zum Schmelzen brachte, ist unbekannt. In dieser Arbeit wurde der genetische Zusammenhang zwischen Chondren und Matrix untersucht.

Eine mineralogische Zonierung mit überwiegend Olivinen in den Chondrenzentren und Ca-armen Pyroxenen in den Rändern sind in mindestens 75% der in Kapitel 2 untersuchten Chondren zu finden. Insgesamt wurden 256 Chondren in 16 verschiedenen kohligen sowie Rumuruti Chondriten (R Chondrite) untersucht. Die Pyroxene der Chondrenränder bildeten sich durch Aufnahme von Si aus dem umgebenden Gas, welches später zu Matrix kondensierte. Chondren (oder ihre Vorläufer) fungierten als offene Systeme und erhielten auf diese Weise eine Massenzunahme von 3-15 Gew.%.

In den Kapiteln 3 und 4 wurden mit der Elektronenstrahlmikrosonde die chemische Zusammensetzung von Chondren und Matrix des CM Chondriten Jbilet Winselwan (JW), sowie dreier R Chondrite bestimmt. Die jeweiligen Gesamtgesteinszusammensetzungen der Meteorite wurden außerdem mittels Röntgenfluoreszenzspektrometrie analysiert.

Die untersuchten Chondrite haben mindestens 50 Vol.% Matrix. Die Matrices der Chondrite haben erhöhte Verhältnisse von Fe/Mg, Si/Mg, Al/Ti und Al/Ca gegenüber den Gesamtmeteoriten; Chondren haben entsprechend niedrigere Verhältnisse. Die Gesamtzusammensetzung der Meteorite ist (bis auf Si/Mg in den R Chondriten) CI-chondritisch (solar). Diese komplementären Zusammensetzungen können im Zusammenhang mit den solaren Elementhäufigkeiten der Meteorite nur erklärt werden, wenn sich Chondren und Matrix gemeinsam im gleichen Reservoirs gebildet haben.

In Kapitel 4 wird, zu meinem Wissen, Komplementarität das erste Mal in nicht-kohligen Chondriten beschrieben. Es wird vermutet, dass kohlige und nicht-kohlige Chondrite aus unterschiedlichen Regionen des frühen Sonnensystems stammen. Eine gemeinsame Bildung von Chondren und Matrix muss in beiden Reservoirs angenommen werden.

# 1 Introduction

Meteorites are extraterrestrial lithic fragments that enter Earth's atmosphere and strike its surface. Witnesses that meteorite impacts have always been a part of the Earth are e. g. fossilised meteorites, impact features such as the Chicxulub crater underneath the Yucatan peninsula, or ancient chronicles from China or Crete about meteorite showers. However, in 1794, the German polymath Ernst Chladni realised the extraterrestrial origin of meteorites and thereby laid the foundation for modern meteorite studies.

Most meteorites are found in deserts, because the dry climate prevents extensive weathering and dark rocks are easily visible on light desert ground. Another advantage for finding meteorites in cold deserts is, that meteorites accumulate in response to ice movements. The ice moves until reaching areas with relatively low accumulation but high sublimation rates. Those snow free places, are called 'Blue Ice' areas, because they expose the deeper glacial ice. Meteorites which were carried within the ice remain there after the ice ablated. The Antarctic Search for Meteorites (ANSMET) organises expeditions to those meteorite traps since 1976, and more than 30,000 Antarctic meteorites have been found so far. In 1984, the first lunar rock was discovered and, ten years later, the first Martian rock. However, beside very few samples from Moon and Mars, the vast majority of meteorites that are found on Earth are debris from asteroids. They originate in the asteroid belt, which is located between the planets Mars and Jupiter. Based on whether a meteorite is composed of stone, iron, or stone-iron, two basically distinct types of asteroids are distinguished: (i) differentiated bodies, which became heated and molten, differentiated, and re-solidified after formation, and (ii) undifferentiated asteroids, which were not molten after their accretion and agglomeration in the protoplanetary disc. Meteorites from differentiated bodies are referred to as 'achondrites' and undifferentiated meteorites are called 'chondrites'. The latter are the focus of this work.

The undifferentiated chondrites directly sample the solar nebula (protoplanetary disc), which existed about 4.57 billion years ago (Bouvier and Wadhwa, 2010) and mark the beginning of our solar system. Hence, they record the physical and chemical conditions in the solar nebula.



## 1.1 The solar system

### 1.1.1 Structure of the solar system

Our solar system consists of a central star—the Sun—and eight planets, that orbit the Sun in the same plane (ecliptic) (Fig.1.1). The Sun contains 99.9% of the mass of the solar system (Woolfson, 2000). Hence, the composition of the Sun is representative of the entire solar system. The Sun consists of roughly 99 wt.% of H (~75 wt.%) and He (~24 wt.%), and only less than 2 wt.% of elements heavier than He (Lodders, 2003). As a lower main-sequence star, in its core He is generated by fusion reaction of H, but heavier elements are not produced. Closest to the Sun are the four terrestrial planets of the inner solar system: Mercury, Venus, Earth, and Mars. These, also called 'telluric' or 'rocky' planets, are mainly composed of silicate rocks and metal. Their mean densities are between 5.4 (Mercury) and 3.9 g/cm<sup>3</sup> (Mars) and decrease with increasing distance from the Sun. They are composed of at least two layers: an inner core consisting mainly of Fe and Ni plus minor amounts of other siderophile (iron-loving) elements, and an outer shell that is built up mainly from lithophile (stone-loving) elements, which commonly form silicates. The distance between Sun and Earth is about  $150 \times 10^6$  km, defining 1 AU (Astronomical Unit). Adjacent to the inner solar system, from about 2.0 to 3.4 AU, extends the asteroid belt, which is populated with asteroids and dwarf planets. So far, the orbits of more than 600,000 objects have been recorded in the asteroid belt. Only a few of those objects are more than 100 km in diameter and their total mass is estimated to be about 1/2000 of that of Earth (Chambers, 2014). The

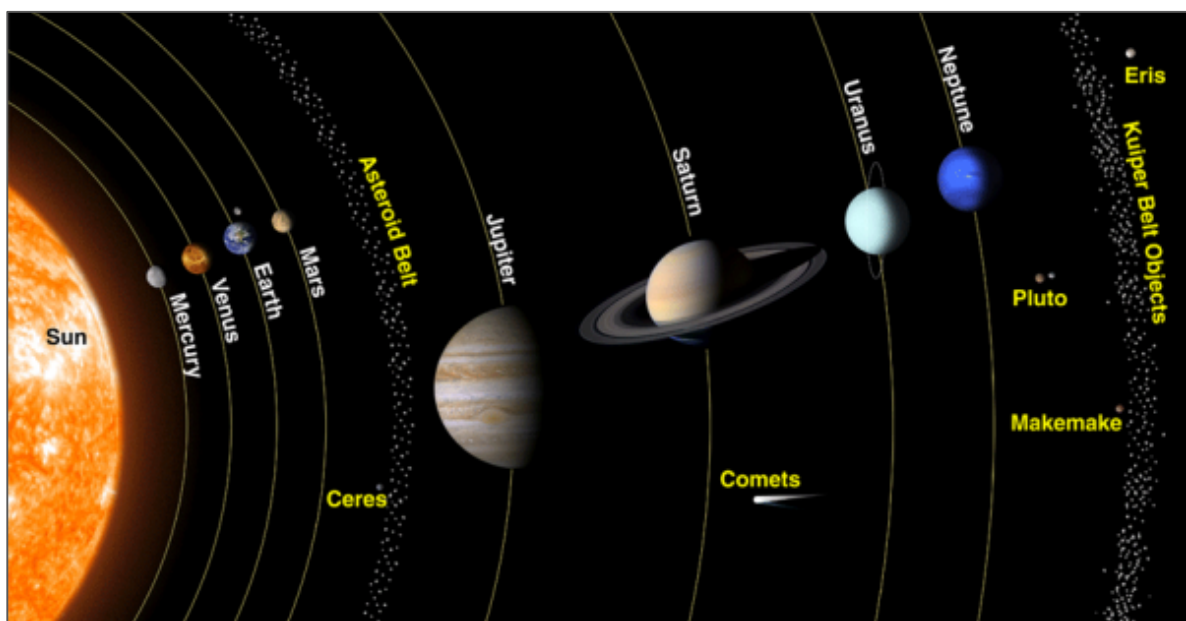


Figure 1.1: Model of the solar system.

(Image credit: NASA's the Space Place, via <http://spaceplace.nasa.gov/ice-dwarf/>)

composition of these objects is not uniform throughout the main asteroid belt. The inner asteroid belt, up to 2.5 AU, is dominated by silicate rich objects which have at some time been partially or even completely molten. At a distance of 2.5 AU the darker and carbon richer objects dominate, which have not, or only mildly, been heated. Behind the asteroid belt lies the outer solar system with the Jovian planets: Jupiter, Saturn, Uranus, and Neptune. These gas giants consist mainly of H and He and their densities are between 0.7 and 1.6 g/cm<sup>3</sup>. Beyond the orbit of Neptune, between 30 and 50 AU, are the objects of the Kuiper belt. The Kuiper belt consists mainly of small objects, which are less than 100 km in diameter, but is also home of three officially recognised dwarf planets—Pluto, Haumea, and Makemake. Additionally, most comets are assumed to originate from the Kuiper belt. Behind the Kuiper belt assumably lies the Oort cloud. The Oort cloud is a hypothetical, and so far, not detected accumulation of astronomic objects in the outermost parts of the solar system.

### 1.1.2 Formation of the solar system

The formation of our solar system and its planetary system is a long-standing question and not yet completely solved. Clues about its formation is basically provided from astronomical observations, cosmochemical studies of meteorites and space missions (Chambers, 2014). Based on these observations, the picture about the formation of the Sun and the planets is constantly refined. I will outline here the basic steps of the beginning and the formation of the solar system.

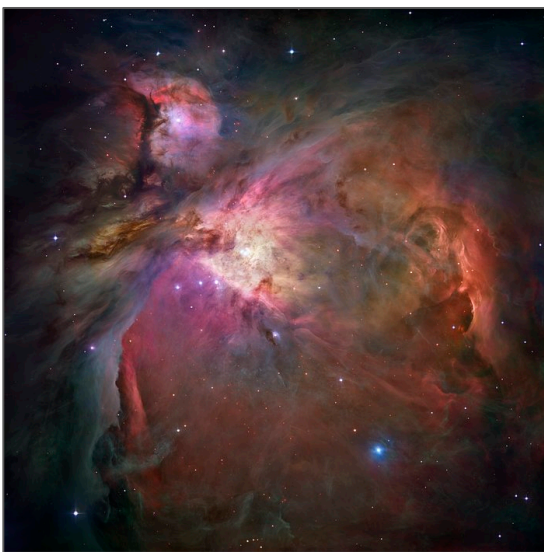


Figure 1.2: Thousands of stars are forming inside the Orion Nebula. (Image credit: NASA/ESA, via [http://spacetelescope.org/.](http://spacetelescope.org/))

The birth of our solar system started in a huge molecular cloud. Molecular clouds are cold and dense ( $T \sim 10$  K;  $n_{H_2} \sim 100$  cm<sup>3</sup>) regions in a galaxy (Ostriker et al., 2001). They consist primarily of molecular hydrogen, mixed with traces of interstellar dust grains and rare organic as well as inorganic molecules (Alves et al., 2001). The largest molecular clouds are visible to the naked eye, appearing as dark patches against a brighter background in the Milky Way. One present region of such a massive star formation in the Milky Way is the Orion Nebula, which is  $1,344 \pm 20$  light years away from Earth (Hirota et al., 2007) (Fig. 1.2).

Such stellar nurseries can contain thousands of young stars and extend hundreds of light years across.

The molecular cloud from which our solar system formed existed for an unknown time, until it collapsed, probably initiated from the shock front of a nearby supernova explosion. The cloud contracted and most of its mass fell into the centre to form the protosun. Due to collapsing, the gravitational potential energy of the cloud was converted into kinetic energy of individual particles. This results in increased collisions of the particles and the kinetic energy was converted into heat. The disc became hottest in its centre, where most of the mass was concentrated in the Protosun. The temperature decreased with increasing distance from the centre. When temperatures in the protosun were as high as  $10^6$  K, nuclear reactions started and the Sun was born, surrounded by a rotating disk. This protoplanetary disk is here called 'solar nebula'. The solar nebula probably lasted for a few million years, until the planets, their moons, the dwarf planets, the asteroids and the comets had finally formed.

When the inner disk cooled, the first solid matter formed as  $\mu\text{m}$  sized objects by condensation. The predicted condensation sequence in a gas of solar composition at pressures of  $10^5$  bar is shown in Fig. 1.3 (Petaev and Wood, 1998). On the x-axis of the diagram, the 'isolation degree' ( $\xi$ ) is given. This variable indicates how much of the already condensed matter is continuously withdrawn from reactive contact with the surrounding gas while condensation proceeds. Hence, at the lower end of the x-axis, condensation under equilibrium condition ( $\xi=0$ ) is displayed, while the rest of the diagram shows condensation with variable degrees of fractionation. The first minerals to form in a cooling gas of solar composition are at temperatures of about 1700 K Ca,Al-rich oxides. These phases make less than 5 % of the total condensable matter (Palme, 2000). With decreasing temperatures, the first silicate to form, slightly above 1300 K, is diopside ( $\text{CaMgSi}_2\text{O}_6$ ), followed by forsterite ( $\text{Mg}_2\text{SiO}_4$ ). Metal, as well as small amounts of anorthitic plagioclase ( $\text{CaAl}_2\text{Si}_2\text{O}_8$ ), start to form at about 1300 K. The composition of the solar nebula is highly reducing and metallic Fe,Ni-phases are the stable condensed form of iron until temperatures of below 800 K (Grossmann et al., 2008). Under equilibrium condensation, also forsterite reacts with gaseous SiO to form enstatite ( $\text{MgSiO}_3$ ) and pure anorthite has been converted to pure albite ( $\text{NaAlSi}_3\text{O}_8$ ), just below 1300 K. As Fe, Mg and Si are the three most abundant elements heavier than oxygen, in the solar nebula, the largest fraction of condensable matter is incorporated into those minerals that condense at temperatures above 1200 K.

The moderately volatile elements, which were not already incorporated into previously

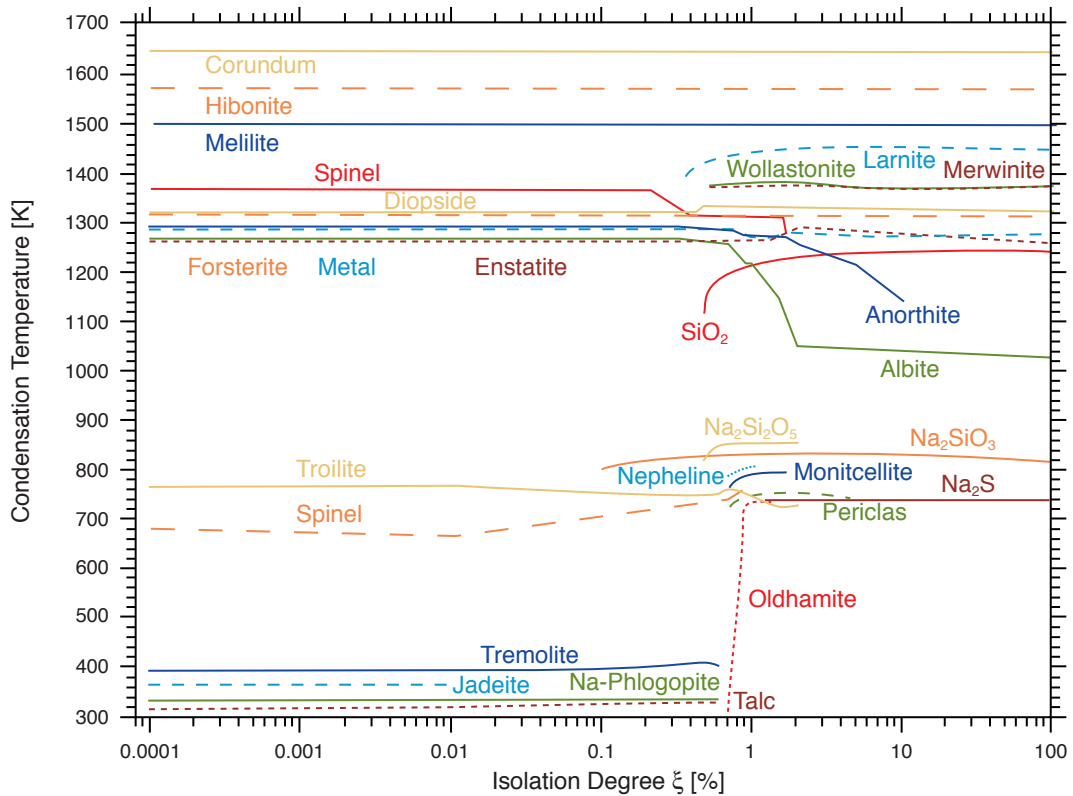


Figure 1.3: Condensation temperatures in a gas of solar composition at a pressure of  $10^{-5}$  bar depending on the isolation degree ( $\xi$ ). Major changes in the condensation sequence take place at isolation degrees between 0.1 and 1 %. (Figure after Petaev and Wood, 1998).

formed minerals, such as e.g. Na in Albite, start to condense at temperatures below 800 K. Sulphur is the most abundant of these moderately volatile elements and condenses by reaction with solid Fe to form sulphides. Under equilibrium condition, other moderately volatile elements condense in solid solution with existing silicates, metal, or sulphide major phases.

Under fractionated condensation, with isolation degrees of  $\xi > 0.1$  %, the condensation sequence changes substantially (Fig.1.3). Values of  $\xi$  between 0.1 and 2.5 seem reasonable to produce the mineral assemblages found in chondrites (Petaev and Wood, 1998).

Accretion of material started already during the formation of the first tiny grains by condensation in the solar nebula. Small amounts of presolar grains were also present in the solar nebula and coagulated with the early condensates. The initial stage of accretion was due to Van der Waals forces, during collisions of the orbiting grains. When particles reach a size of mm or cm, growth is likely to stagnate (Brauer et al., 2008; Zsom et al., 2010), referred to as the 'meter size barrier'. The mechanism which was responsible for the formation of planetesimals remains unclear (Chambers, 2008). However, when planetesimals had once formed, further growth was first mainly due to gravitational focusing ('runaway accretion') and later dominated by oligarchic growth when collisions became more destructive. Both mechanisms lead to increased accretion

rates of larger bodies compared to smaller ones. When planetary embryos had formed, each one had its own annular feeding zone. The temperature gradient away from the Sun in the protoplanetary disc is thereby reflected in the composition of bodies in the different parts of the solar system.

Bodies with a particular diameter or which formed very early got heated, melted and differentiated due to energy that was generated by impacts and the decay of radioactive isotopes such as the short-lived isotope  $^{26}\text{Al}$  (Fig. 1.4). Siderophile elements formed the cores, while lithophile elements accumulated in silicates and formed the mantles and potential crusts of planetesimals. This structure is typical of the terrestrial planets. The main asteroid belt is populated by small bodies, which are mostly unfractionated. Yet, some meteorites derive from differentiated asteroids. These achondrites consist either of the metallic cores, or the olivine-rich mantles, or both, of their parent bodies. Isotope studies on some iron meteorites reveal very old formation ages within 2 Myr after formation of the solar system (Kleine et al., 2005; Markowski et al., 2006, Schersten et al., 2006). Hence, they formed early enough to sustain sufficient amounts of  $^{26}\text{Al}$  for melting. However, most meteorites derive from undifferentiated bodies: the 'chondrites', which represent about 86% of all known meteorites. These objects still contain the solids that have formed at the beginning of our solar system. Chondrites are therefore direct samples of the solid fraction of the solar system and, hence, provide unique insights into its chemical and physical evolution.

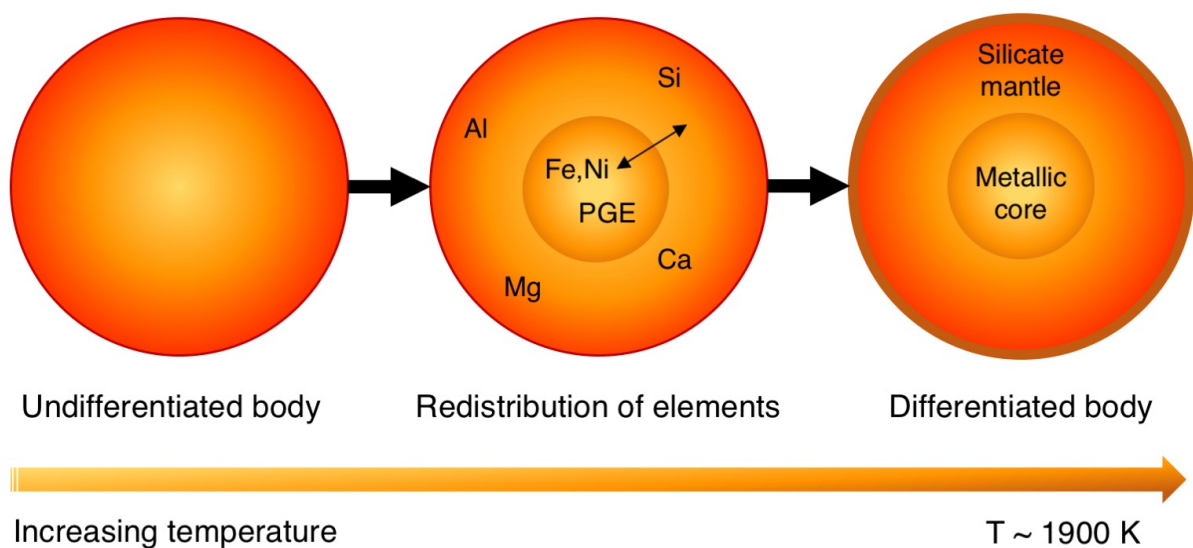


Figure 1.4: Differentiation process: an undifferentiated asteroid gets heated caused largely by the decay of  $^{26}\text{Al}$ . Lithophile elements differentiate into silicates and form the mantle and siderophile elements form the core. Chondrites derive from undifferentiated asteroids.

## 1.2 Chondrite classification and components

### 1.2.1 Chondrite classification

#### *Classification according to primary classification parameters*

Primary classification parameters for chondritic meteorites are their oxygen isotope composition, their bulk chemistry, as well as their petrology and petrography. Based on these parameters, chondritic meteorites are divided into classes, clans and groups (Fig.1.5). The purpose of this classification is to sort the meteorites according to generic similarities, e. g. the same time or same location of formation in the solar nebula or even a common parent body (Krot et al., 2014).

There are 3 *classes* among the chondritic meteorites: ordinary (O), carbonaceous (C), and enstatite (E) chondrites. The chondrites of each class can be charted in a three-oxygen isotope diagram (Fig. 1.6), or on diagrams representing the bulk chemical compositions of the meteorites (Fig. 1.7).

The classes are subdivided into *clans*. Clans unite chondrite groups, which are similar regarding to their chemical, mineralogical and/or isotopic properties; yet have petrologic and/or bulk chemical different characteristics. Meteorites of the same clan may have originated at about the same time and in the same region of the solar nebula (e.g. Kallemeyn et al, 1996).

A *group* consists of at least 5 individual chondrites, which have closely similar whole-rock chemical and oxygen isotope characteristics, and common petrologic features, such as chondrule sizes, chondrule/matrix ratios and mineral compositions. Chondrites of one group have probably originated from the same parent body. Main petrographic characteristics of the individual chondrite groups are listed in Table 1.

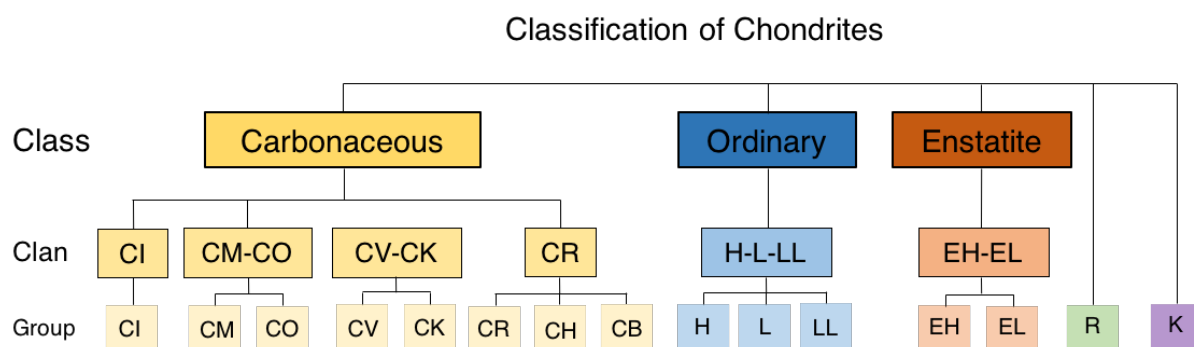


Figure 1.5: Classification scheme of chondrites after Weisberg et al. (2006).

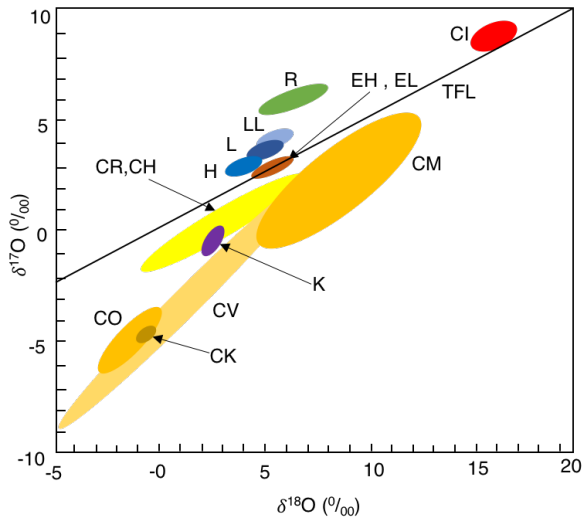


Figure 1.6: Oxygen isotope composition of bulk-rock chondrites. (Data from Clayton and Mayeda, 1996; 1999; Clayton et al., 1991; Clayton, 2003; and references therein)

The eight groups of the *C chondrites* commonly contain rather high percentages of matrix, often with chondrule/matrix ratios around 50:50 (Scott et al., 1996), except CI chondrites which are almost completely composed of matrix. Oxygen isotope compositions of the *C chondrites* plot typically below the terrestrial fractionation line (TFL), except for CI chondrites. The group of CI chondrites represent the most primitive chondrites, with chemical compositions that are identical to the solar photosphere for all but the highly volatile elements (e. g. Anders and Grevesse, 1989,

Lodders 2003, Palme et al., 2014a) (Fig. 1.8). Because of the equal compositions of CI chondrites and the solar photosphere, CI chondrites are used as a reference composition for many solar system materials. Figure 1.7 shows bulk element data of chondrite groups normalised to CI chondrites and to Mg. Other groups of *C chondrites* are enriched in refractory elements by factors 1.0 to 1.4 and depleted in moderately volatile elements, relative to CI chondrites (Scott and Krot,

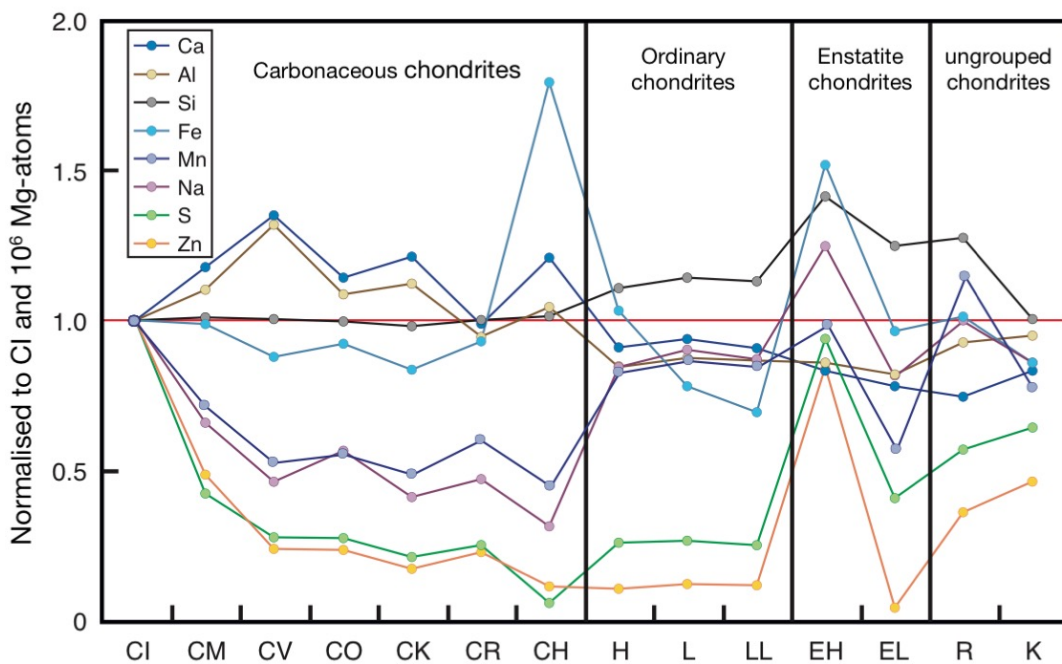


Figure 1.7: Element abundances in chondrite groups normalised to CI chondrites and Mg. (Data from Wolf and Palme, 2001; and references therein).

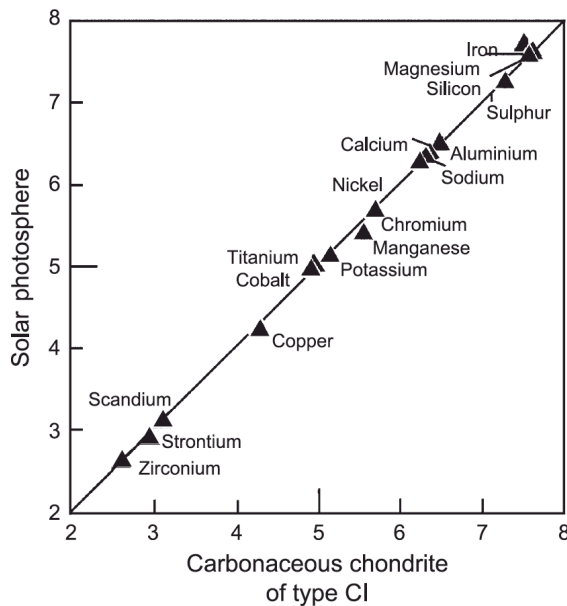


Figure 1.8: Major and trace element abundances of CI chondrites are identical to the composition of the solar photosphere. (Figure from Zanda, 2004)

2003). The major elements Si, Mg and Fe are largely unfractionated among the C chondrites.

The *O chondrites* are with > 80% the most abundant class of meteorites. Their oxygen isotope compositions plot above the TFL on a three-isotope diagram. They generally contain large amounts of chondrules (60-80 vol.%) and opaque phases (7-15 vol.%) but only few amounts of matrix (<15 vol.%) (Scott and Krot, 2003; and references therein). Their subdivision is based on bulk Fe contents (H= high total Fe; L=low total Fe) and oxidation state (LL= low total Fe and low abundance of metal). Ordinary chondrites are

depleted in refractory elements and moderately volatile elements. Silicon and Mg are slightly enriched in all O chondrites, but Fe is enriched in H, and depleted in L and LL Ordinary chondrites with respect to CI chondrites.

*Enstatite chondrites* are highly reduced, with virtually all iron occurring as metal and sulphides. They contain only little matrix material, up to 15 vol.% (Scott et al., 1996). Their oxygen isotopes plot on the TFL in a three-isotope diagram. The group of EH chondrites is characterised by high total Fe and the EL chondrites by low total Fe contents. Silicon is generally enriched in E chondrites, while Ca and Na are enriched in EH, but depleted in EL chondrites, with respect to CI. The refractory element Al as well as the moderately volatile elements Mn, S, and Zn are slightly depleted in EH chondrites and more depleted in EL, compared to CI.

The *Rumuruti (R)* and *Kakangari (K) chondrites* have considerable amounts of matrix, roughly between 40 and 50 vol.% in R chondrites (Bischoff et al., 2011) and up to 70 vol.% in K chondrites (Weisberg et al., 1996). Oxygen isotope data plot above the TFL for R chondrites and below the TFL for K chondrites. In both chondrite groups, bulk rock element data show depletions in refractory and moderately volatile elements, relative to CI chondrites. In R chondrites, Si is enriched, but Mg and Fe are unfractionated. In K chondrites, Fe is depleted, but Si and Mg are unfractionated.

There exist also several mineralogically and/or chemically unique chondrites, which cannot be charted among the existing groups. Those are referred to as *ungrouped* chondrites.



## 1 Introduction

Table 1.1

Main petrographic characteristics of the distinct chondrite groups.

	CAIs (area%)	Chondrules (vol.%)	Matrix (vol.%)	Metal (vol.%)	Chondrule mean Ø (mm)	Petrologic types
<i>Carbonaceous</i>						
CI	<<1	<<1	>99	0	-	1
CM	~1	20	70	0.1	0.3	1-2
CO	~1	48	34	1-5	0.15	3-4
CR	~0.1	50-60	30-50	5-8	0.7	1-2
CH	0.1	~70	5	20	0.02	3
CB	<0.1	30-40	<5	60-70	0.1-20	3
CV	~3	45	40	0-5	1	3-4
CK	0.2	15	75	<0.01	0.7	3-6
<i>Ordinary</i>						
H	0.01-0.2	60-80	10-15	~8	0.3	3-6
L	<0.1	60-80	10-15	~4	0.7	3-6
LL	<0.1	60-80	10-15	2	0.9	3-6
<i>Enstatite</i>						
EH	<0.1	60-80	<0.1	~10	0.2	3-6
EL	<0.1	60-80	<0.1	~10	0.6	3-6
<i>Additional</i>						
R	<0.1	>40	30	<0.1	0.4	3-6
K	<0.1	~30	60	~7	0.6	3

Data are from Krot et al. (2014); except abundance data for CAIs, which are from Hezel et al. (2008) and references therein.

### *Classification according to secondary classification parameters*

Chondrites are primitive solar system materials that originate from unfractionated parent bodies. However, individual chondrites may have undergone secondary alteration processes. Post-accretionary processes are an additional classification parameter for chondrites.

The classification scheme introduced by Van Schmus and Wood (1967) divides chondrites into petrologic types, depending on the degree and nature of secondary alteration that the meteorite experienced on its parent body. This classification is based on mineralogical changes, which occur due to thermal or aqueous alteration. Chondrites of petrologic type 3 represent the least altered material, which have not undergone chemical equilibration processes due to aqueous or thermal overprint. Type 1 and type 2 chondrites underwent aqueous alteration, with the degree

of alteration decreasing from 1 to 2. Type 4 to type 6 chondrites experienced thermal metamorphism of increasing degree from 4 to 6. Typically, carbonaceous chondrites mostly experienced aqueous alteration, with CI chondrites always being of petrologic type 1. The O, E, R and K chondrites are always of petrologic types 3 to 6. The range of petrologic types, which occur in the different chondrite groups is displayed in Table 1. Many chondrites are brecciated rocks (e. g. Bischoff et al., 1983; Bischoff et al., 2011) and their different fragments may have experienced various extents of asteroidal processes. Hence, it is not always possible to label a chondrite with a single petrologic type, and different fragments must be classified individually.

Another secondary classification parameter is the shock stage which indicates the grade of shock pressure that a meteorite experienced during impacts on its parent body. The classification is based on shock effects observed in olivine and plagioclases (Stöffler et al., 1991) or in low-Ca pyroxenes (Rubin et al., 1997). The classification scheme range from S1 (unshocked) to S6 (very strongly shocked).

The degree of terrestrial weathering of individual meteorite finds can also be specified. According to Wlotzka (1993) the progressive alteration stages are from W0 (no visible alteration of minerals) to W6 (massive replacement of primary minerals).

### 1.2.2 Chondrite components

The main components of chondrites are chondrules, matrix, opaque phases and refractory inclusions (Fig.1.9).

*Chondrules* are, together with matrix, the dominant and most prominent component of chondritic meteorites. They are solidified molten spherules, which are normally between 400 µm and 1 mm in size. Chondrules are no direct condensates, but formed from molten precursor material. Major minerals of chondrules are olivines and low-Ca pyroxenes, while minor phases are Ca-pyroxenes and a commonly feldspar-normative glassy or microcrystalline mesostasis. Metal and sulphide grains can also occur in chondrules. Some chondrules are characterised by the presence of thin metal rims, SiO<sub>2</sub>-rich rims, or accretionary dust rims.

Chondrules can be classified based on their texture in porphyritic chondrules, which consist of larger olivine and/or pyroxene crystals set in a fine-grained or glassy mesostasis, and nonporphyritic chondrules (Scott and Krot, 2014). In Fig. 1.10, a porphyritic chondrule and a

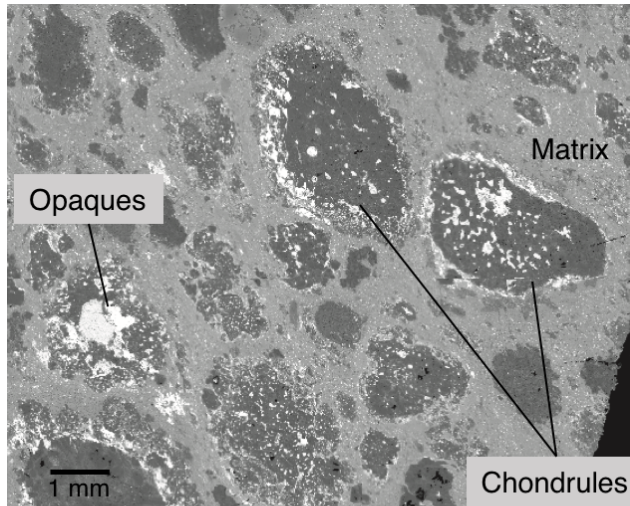


Figure 1.9: Chondrules, matrix and opaque phases are the dominant components in the CV chondrite Bali.

nonporphyritic chondrule are displayed.

Porphyritic chondrules which are dominated by olivine minerals are called porphyritic olivine (PO) chondrules. Those which mainly consist of pyroxene minerals are called porphyritic pyroxene (PP) chondrules, and those containing both minerals are called porphyritic olivine pyroxene (POP) chondrules. Porphyritic chondrules can further be divided according to their oxidation state into FeO-poor chondrules (Type I) and FeO-rich chondrules

(Type II) (Scott and Krot, 2014). The porphyritic structure is due to incomplete melting of chondrule precursor material (Lofgren, 1996; Connolly et al., 1998). Nonporphyritic chondrules have barred olivine (BO), radial pyroxene (RP) or cryptocrystalline (CC) textures. They crystallised from melts that were heated above their solidus long enough to destroy all nuclei.

*Matrix* is the mostly optically opaque mineral mixture wherein chondrules, refractory inclusions and opaque phases are embedded (Scott et al., 1988). The amount of matrix material in chondrites varies significantly among the chondrite groups between 5 and 99 vol.%, but is typically between 5 and 50 vol.% (Table 1.1). Matrix grains are commonly between 10nm and 5µm in size and often represent a disequilibrium assemblage of various mineral phases mixed with presolar material and nebular condensates (Scott and Krot, 2014). Matrix minerals include

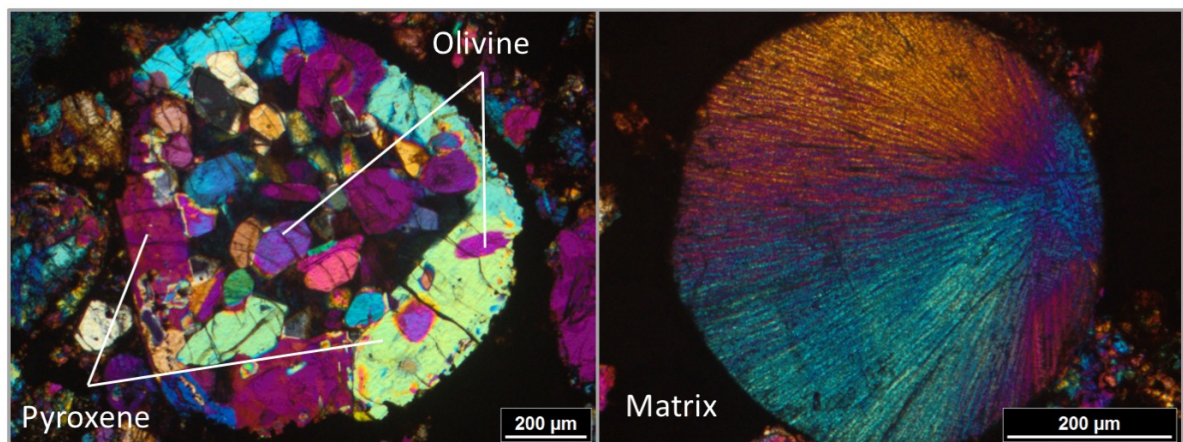


Figure 1.10: Crossed polariser microscope images with “Gips Rot 1” plate. Left: Porphyritic olivine pyroxene chondrule (POP). Large olivine minerals, which enclose olivine minerals poecilitically are primarily in the peripherie of the chondrule. Most olivine minerals are in the chondrule centre. Right: Radial pyroxene chondrule (RP). (Image credit: Addi Bischoff)

amorphous phases as well as crystalline FeO-rich silicates (olivines and pyroxenes), oxides, sulphides, Fe,Ni-metal, and—especially in type 1 and 2 chondrites—phyllosilicates and carbonates. Matrix material is more susceptible to alteration by aqueous fluids and metamorphism on the parent body than other chondritic components, due to the fine grain sizes, the presence of amorphous phases as well as high porosity and permeability. Many of the typical matrix minerals are therefore probably products of secondary processes (Scott and Krot, 2003; Brearley 2003). The two meteorites with the least-altered matrices are Acfer 094 (ungrouped) and ALHA77307 (CO 3.0). Matrices in these meteorites consist of 100-500 nm sized grains of olivine, pyroxene, sulfides, and Fe,Ni-metals which are set in an amorphous material enriched in Si, Al, Ni and S (Huss et al., 2005).

Matrix is usually enriched in FeO relative to average chondrules (e.g. McSween and Richardson, 1977; Bland et al., 2005; Hezel and Palme, 2010). Since matrix is also commonly richer in volatile elements, it is by some authors designated as the 'low-temperature component' of chondrites. However, this is not exactly true, as matrix is a mixture of diverse material, including presolar grains and high temperature nebular condensates (Bland et al., 2007; Scott and Krot, 2014).

*Opaque phases* in chondrites are metals, sulphides and oxides. Two kinds of metals are found in chondrites: grains which are composed of refractory elements that condense at high temperatures ( $>1600$  K) and are associated with CAIs (Palme and Wlotzka, 1976). And metal grains, which are predominantly composed of Fe, Ni and Co and condense with forsterite and enstatite at  $\sim 1350$ - $1450$  K (Campbell et al., 2005). The latter are typically associated with FeO-poor chondrules (Brearley and Jones, 1998), and often affected from low temperature reactions, probably on their parent bodies, which lead to the formation of oxides and sulphides (Scott and Krot, 2014).

The prevalent sulphide phase in most chondritic meteorites is troilite, stoichiometric FeS. However, also other sulphides, such as pyrrhothite and pentlandite, which are not stoichiometric are common in chondrites.

*Refractory inclusions* are direct condensates from the solar nebula. In chondrites, they are either found as calcium-aluminum-rich inclusions (CAIs) or as amoeboid olivine aggregates (AOAs).

CAIs are sub-mm to cm sized clasts, whose major phases are Ca, Al, Mg and Ti-rich oxides and silicates. CAIs were first described about 40 years ago (e.g. Christophe, 1968) and the similarity of their mineral assemblage with those minerals, which are predicted to condense first from a hot gas of solar composition was striking (e.g. Lord, 1965; Grossman 1972). CAIs are

among the oldest material in the solar system, up to 4,568 million years (Bouvier and Whadwa, 2010), and are considered to have been condensed from the solar nebula right at the beginning of its formation.

*AOAs* are irregularly shaped objects, with diameters between 100  $\mu\text{m}$  and up to 5 mm (Chizmadia et al., 2002; Aléon et al., 2002; Komatsu et al., 2001). They consist of fine grained (1-20  $\mu\text{m}$ ) forsterite, Fe,Ni-metal and CAI-like components. AOs are generally rich in  $^{16}\text{O}$ , and therefore considered to have been condensed from an  $^{16}\text{O}$ -rich reservoir in the solar nebula and aggregated with CAI-like objects. AOs are typically less common than CAIs and their occurrence seems to be restricted to type 2-3 C chondrites (Scott and Krot, 2014).

### 1.3 Chondrule formation

Chondrules were probably a substantial part of solid matter in the inner solar system, because of the vast majority of chondrites among the meteorites that are found on Earth, and because chondrules are the dominant objects in most chondrites (e. g. Rubin, 2000). The chondrule forming process, however, is still a major puzzle for meteoritics and intensively discussed since the early 1960s (e. g. Wood, 1962). The overall texture of chondrules, e. g. the presence of euhedral phenocrysts and glassy mesostasis, requires that chondrules formed as melt droplets. However, in particular the heating mechanism required for melting the chondrule precursors remains unknown.

Most authors agree on a nebular origin of chondrules, starting as dust clumps (chondrule precursors) which were heated, melted and subsequently solidified in the solar nebula (e.g Wood 1963; Grossman, 1988; Wasson, 1993; Rubin, 2000; Shu et al., 2001; Alexander et al., 2008; Ruzicka et al., 2012; Hewins and Zanda, 2012). Proposed mechanisms as heat source for chondrule melting include lightning (e.g. Desch and Cuzzi, 2001), interaction with the young Sun (Shu et al., 1996) and nebular shocks (Morris and Desch, 2010). Some works, however, suggest a planetary origin for chondrules during impact events of partially molten planetesimals (e.g. Zook, 1980, 1981; Wänke et al., 1981, 1984; Sanders and Taylor, 2005; Sanders and Scott, 2012; Asphaug et al., 2011; Johnson et al., 2015).

Some critical chondrule properties are not yet fully understood, e.g. chondrule ages and thermal histories of chondrules. Some of the most important chondrule characteristics and their implications are outlined in the following.

- (i) Chondrules were rapidly heated, probably within minutes, to above their solidus temperatures (e. g. Hewins and Connolly, 1996). According to mineral assemblages and mineralogical textures, chondrule peak temperatures must have been between 1750 and 2150 K (e. g. Wasson 1996; Scott et al., 1996).
- (ii) Experiments demonstrated that cooling rates of chondrules were between 10-1000 K/hr, which is faster than cooling of a global nebula and much slower than radiative cooling of isolated spherules (Hewins et al., 2005).
- (iii) The wealth of chondrules in most chondrites suggest that chondrules were produced in large quantities in a hot gas (Desch and Connolly, 2002).
- (iv) The timescales of chondrule formation has not yet been clearly identified. Most studies indicate an age-gap between formation of CAIs and chondrule formation of at least 1 Myr (e.g. Swindle et al., 1996; Mostefaoui et al., 2002; Kita et al., 2005; Budde et al., 2016a). However, some works suggest that chondrule formation started subsequently after formation of CAIs and lasted for about 3 Myr (e.g. Connelly, 2012).
- (v) Chondrules and matrices in individual chondrules are chemically complementary, while the bulk chondrites have solar (CI chondritic) element abundances. (e. g. Klerner and Palme, 1999; Hezel and Palme, 2008; 2010; Palme et al., 2015; Ebel et al., 2016). Additionally, studies of W and Mo isotopes also revealed isotopic complementarities of chondrules and matrix (Becker et al., 2015; Budde et al., 2016a,b) These findings indicate that both components derive from a single, CI chondritic, reservoir of nebular dust.
- (vi) Chondrules were open systems, exchanging material with the surrounding gas (e. g. Tissandier et al., 2002; Grossman et al., 2002; Hezel et al., 2003, 2010; Libourel et al., 2006; Harju et al., 2014). Mesostasis of some chondrules show higher abundances of volatile elements and lower abundances of refractory elements near chondrule rims, and vice versa in the cores (e.g Matsunami et al., 1993; Nagahara et al., 1999). These, volatility related chemical zonings are explained by evaporation and recondensation processes between the chondrules and the surrounding nebula gas during formation. Additionally, a typical occurrence of porphyritic chondrules is, that low-Ca pyroxenes are concentrated at the margins and olivine minerals dominate the centre (Fig. 1.9) (this study, chapter 2). Tissandier et al. (2002) reproduced this characteristic chondrule feature experimentally by reactions of melt with gaseous SiO during crystallisation. Further studies from Chaussidon et al.

(2008) and Harju et al. (2014) on oxygen isotope compositions of minerals also indicate that pyroxenes in the periphery of chondrules developed during chondrule formation by material exchange between chondrule melts and nebula gas.

- (vii) In chondrules, no large mass-dependent fractionations of stable isotopes of e.g. Si, Mg, Fe, and K are observed (Hezel et al., 2010) and bulk chondrules show high Na densities as would be expected by closed system formation of chondrules (e. g. Alexander et al., 2000). However, as explained above, a closed system formation cannot be assumed. High gas densities during chondrule formation are more likely to explain the lack of larger stable isotope fractionation as well as the high Na contents in chondrules (Cuzzi and Alexander, 2006; Alexander et al., 2008).
- (viii) At least some chondrules experienced multiple heating events. The presence of relict grains (e.g Rambaldi, 1981) in some chondrules and igneous rims around some chondrules indicate secondary heating events (Rubin, 2000). Alexander (1996) even proposed that chondrules were generally made by recycling of earlier chondrule generations.

### 1.4 Aims and objectives

This work deals with the condition of chondrule formation. Insights into the chondrule formation process are obtained from mineralogical characteristics of chondrules and chemical compositions of chondrules and matrix.

Mineralogical zonation in chondrules, with olivine minerals in the chondrule centre and low-Ca pyroxene at the chondrule margins, is a well-known characteristic of chondrules and is often mentioned in the literature (e.g. Scott and Taylor, 1983; Grossman, 1996; Grossman et al., 2002; Tissandier et al., 2002; Hezel et al., 2003,2006; Krot et al., 2004; Hewins et al., 2005; Berlin et al., 2006; Lauretta et al., 2006; Chaussidon et al., 2008; Jones, 2012; Hewins and Zanda, 2012; Jaquet et al., 2012; Scott and Krot, 2014; Harju et al., 2014). In many works, it is suggested, that the low-Ca pyroxene rims formed from olivine minerals during recondensation processes of Si from the nebula gas to the chondrules/chondrule precursors. Hence, the chondrules operated as open systems. However, the overall occurrence of these rims in different chondrite groups has never been quantified.

In order to obtain representative information on those mineralogical zonations, the textures of chondrules in several different chondrite groups of C chondrites and in R chondrites will be examined. Therefore element maps of single chondrules will be obtained and converted into 'phase maps'. A phase map shows each mineral phase (olivine, low-Ca pyroxene, Ca pyroxene, mesostases) in a distinct colour. Based on these phase maps, the abundance of mineralogically zoned chondrules, and their characteristics can be studied. These are information about rim thicknesses and the occurrence of poikilolithically enclosed olivine in the low-Ca pyroxene rim minerals. It is the aim to determine the portion of chondrules having a mineralogical zonation. It is then possible to determine the extent to which open system conditions happened during chondrule formation. Also the mean rim thicknesses might be a measurement of the amount of material added from the gas to the chondrules.

Another objective is chemical complementarity in chondrites. There already exist several works on complementarities in carbonaceous chondrites (e.g., Klerner and Palme, 1999; Bland et al., 2005; Hezel and Palme, 2008, 2010; Palme et al., 2014b, 2015; Becker et al., 2015; Kadlag and Becker, 2016; Budde et al., 2016a,b; Ebel et al., 2016). As described in section 1.3, the implication of complementarity is that chondrules and matrix must have formed in a single reservoir. Therefore, complementarity provides a fundamental constraint on the chondrule forming process.



Although a significant body of evidence for complementarity has been reported in the literature, it is still highly discussed or even denied by some authors (e.g. Alexander, 2005; Olsen et al., 2016; Zanda et al., 2017; Connelly et al., 2017). The aim of this work is therefore also to study possible complementarities.

Jbilet Winselwan (JW) is a recently found CM chondrite. There exist so far only few data of bulk chondrules and matrix compositions in CM chondrites. Jbilet Winselwan is a suitable candidate to study complementarity as it is not extensively altered by hydrous fluids on its parent body, compared to most other CM chondrites.

Additionally, complementarity has—to my knowledge—so far never been studied in non-carbonaceous chondrites. Rumuruti chondrites (R chondrites) are suitable non-carbonaceous chondritic meteorites as they contain abundant matrix and their ratios of Fe/Mg, Al/Ti and Al/Ca are CI chondritic. Warren (2011) proposed, that the Rumuruti chondrites originated together with the ordinary and enstatite chondrites in a different region of the protoplanetary disk. Hence, if complementarity is found in R chondrites, it would show that the formation process of chondrules and matrix was similar in both regions, regarding the joint formation of both components.

Chondrules and matrix compositions will be measured with an electron microprobe. Bulk chondrule compositions will be obtained by modal recombination of mineral compositions and their corresponding abundances within each chondrule. To compare these data with the composition of the respective bulk meteorites, bulk meteorites will be measured with X-ray fluorescence spectrometry.

## 2 The conditions of chondrule formation, Part II: Open system

Pia Friend<sup>1</sup>, Dominik C. Hezel<sup>1,2,\*</sup>, Daniel Mucerschi<sup>1</sup>

<sup>1</sup>University of Cologne, Department of Geology and Mineralogy,  
Zùlpicher Str. 49b, 50674 Köln, Germany

<sup>2</sup>Natural History Museum, Department of Mineralogy,  
Cromwell Road, SW7 5BD, London, UK

**\*corresponding author:**

**dominik.hezel@uni-koeln.de**

*Keywords:*

chondrules, open system, zonation, complementarity

*submitted to:*

Geochimica et Cosmochimica Acta

*accepted:*

October, 2015

### **Abstract**

We studied the texture of 256 chondrules in thin sections of 16 different carbonaceous (CV, CR, CO, CM, CH) and Rumuruti chondrites. In a conservative count ~75% of all chondrules are mineralogically zoned, i.e. these chondrules have an olivine core, surrounded by a low-Ca pyroxene rim. A realistic estimate pushes the fraction of zoned chondrules to >90% of all chondrules. Mineralogically zoned chondrules are the dominant and typical chondrule type in carbonaceous and Rumuruti chondrites. The formation of the mineralogical zonation represents a fundamentally important process of chondrule formation. The classic typification of chondrules into PO, POP and PP might in fact represent different sections through mineralogically zoned chondrules. On average, the low-Ca pyroxene rims occupy 30 vol.% of the entire chondrule. The low-Ca pyroxene most probably formed by reaction of an olivine rich chondrule with SiO from the surrounding gas. This reaction adds 3-15 wt.% of material, mainly SiO<sub>2</sub>, to the chondrule. Chondrules were open systems and interacted substantially with the surrounding gas. This is in agreement with many previous studies on chondrule formation. This open system behaviour and the exchange of material with the surrounding gas can explain bulk chondrule compositional variations in a single meteorite and supports the findings from complementarity that chondrules and matrix formed from the same chemical reservoir.

### 2.1 Introduction

In the canonical picture of chondrule formation a dustball is heated to up to 2000 K in minutes to hours. During cooling olivine and pyroxene crystallise from the melt and finally the residual, refractory rich melt is either quenched to glass or a fine-grained mix of pyroxene and plagioclase with rare occurrences of silica. The assorted opaque phases metal and/or sulphide might have been part of the chondrule precursor assemblage. This simplified picture of chondrule formation, while still popular, changed significantly during the past 15 years. Chondrules are now thought to have formed along a more dynamic and complex path, reviewed and outlined at the end of this study.

An individual chondrule might either behave as a closed or an open system during formation. In the closed system case, the chondrule bulk composition is entirely determined by its precursor assemblage (e.g. Hezel and Palme, 2007). In the open system case, the chondrule exchanged material with the surrounding gas during chondrule formation; i.e., the chondrule bulk composition is determined by its precursor assemblage and the material that was exchanged during chondrule formation.

Chondrules may be viewed in two different ways: (i) as individual objects and (ii) as a chondrule population in a single meteorite. The focus of this study is on the latter. Typical and well studied characteristics of chondrule populations are their size distribution or textural type (porphyritic, barred, etc.; e.g. Jones, 2012). A wealth of data exists on chondrule mineral elemental and isotopic composition (e.g. Brearley and Jones, 1998; Scott and Krot, 2014 and references therein). In comparison, bulk chondrule compositional data are sparse (e.g. Gooding et al., 1980; Grossman and Wasson, 1982; Rubin and Wasson, 1988; Jones & Schilk, 2009; Hezel and Palme, 2007, 2010 and references therein).

Type I (i.e. FeO-poor) chondrules are the most abundant in carbonaceous chondrites and a mineralogical zonation with olivine at the centre and low-Ca pyroxene at the rim has been frequently mentioned. In some chondrites an additional outermost silica-rich layer exists (Hezel et al., 2003; Krot et al., 2004). Other chondrule types only rarely show a comparable zonation. A rare chondrule type in ordinary and CH chondrites are silica rich chondrules (SRC), which have silica distributed throughout their entire volume (Brigham et al., 1986; Hezel et al., 2006).

The mineralogical zonation of chondrules was probably first recognised by Scott and Taylor (1983), although a possible process forming such a zonation was already mentioned by Wood (1963). Although well known since then, this mineralogical zonation is usually

only briefly mentioned when reporting chondrule texture in meteorites (e.g. Scott and Taylor, 1983; Grossman, 1996; Grossman et al., 2002; Tissandier et al., 2002; Hezel et al., 2003, 2006; Krot et al., 2004; Hewins et al., 2005; Berlin et al., 2006; Lauretta et al., 2006; Chaussidon et al., 2008; Jones, 2012; Hewins and Zanda, 2012; Harju et al., 2014; Jaquet et al., 2012; Scott and Krot, 2014). The appearance, abundance and general characteristics of this zonation has never been systematically studied across different chondrite types. Only a small number of studies discuss formation scenarios of mineralogically zoned chondrules (Scott & Taylor, 1983; Tissandier et al., 2002; Hezel et al., 2003; Krot et al., 2004, Chaussidon et al., 2008 and Ebel, 2008).

Jacquet et al. (2012) studied trace element patterns in chondrule olivine and enstatite from carbonaceous chondrites and demonstrated that the two minerals must have had different formation histories. The authors suggest the formation of the low-Ca pyroxenes in chondrule margins are distinct from the formation of the olivines, presumably by addition of SiO<sub>2</sub> to the chondrule. Chaussidon et al. (2008) reported O isotope zonation in CV and CR chondrules and concluded that 2/3 of the oxygen in the low-Ca pyroxenes originated from dissolution of precursor olivine, while 1/3 is contributed SiO from the surrounding gas. Harju et al. (2014) measured in situ silicon isotopes in Allende chondrules and also concluded that pyroxene in the chondrule margins was formed by reaction of olivine and an ambient SiO-rich gas. Such gas-melt interaction has previously also been suggested by e.g. Hezel et al. (2003), Krot et al. (2004), Libourel et al. (2006) and experimentally studied by Tissandier et al. (2002), who found that low-Ca pyroxene rims can be formed by the reaction of gaseous SiO with olivine.

It is the general consensus of all of the aforementioned authors that mineralogical, elemental or isotopic zonation in chondrules is the result of chondrule open system behaviour, i.e. interaction of the chondrules with the surrounding gas. A parent body process is never invoked for such zonation. And although the mineralogical zonation is often briefly mentioned in chondrule studies, to our knowledge no systematic study on this fundamental chondrule characteristic exists. This was recognised by Grossman et al. (2002), who emphasised that further systematic research regarding chondrule zonation on a larger number of chondrules is required.

Here we systematically study for the first time the appearance, abundance and general characteristics of mineralogically zoned chondrules in a large set of carbonaceous and R chondrites. The results will provide insights to the origin of chondrule size distributions,

bulk chondrule compositional variations and the origin of the chondrule matrix complementarity.

### 2.2 Methods

Chondrule and mineral compositions were measured with a Jeol JXA-8900RL Superprobe electron microprobe at the University of Cologne and with a Cameca SX100 at the Natural History Museum, London. In both setups, the accelerating voltage was set to 20 kV and the beam current to 20 nA. Peak counting times were 10 or 20 s, and background counting times 5 and 10 s, depending on element. Well characterised natural silicates and oxides were used as standards and ZAF correction was employed to correct for matrix effects. Detection limits for minor elements were: 100 wt-ppm for CaO, TiO<sub>2</sub> NiO and Na<sub>2</sub>O; 200 wt-ppm for Cr<sub>2</sub>O<sub>3</sub>; and 250 wt-ppm for MnO and FeO. Mineral compositions were measured with a focused beam of 1 µm spot size.

Element maps of chondrules were obtained by rastering across the object with a focused beam of 1 µm spot size. Step sizes varied from 2 to 4 µm. The dwell times were in usually 240 ms/pixel. The element maps were then converted into phase maps. These are false colour images of a sample that show each phase in a different colour (cf. Fig. 2.1). Phase maps were obtained with the PHAPS program (Hezel, 2010) as follows: For each chondrule, the Mg and Si element maps were stored as text-files. Each file contains a 2x2 matrix which represents the x- and y-coordinates of the element map, together with the intensity of each coordinate pair. The two files were then imported into PHAPS, which produces a Mg,Si intensity (i) pair  $\{i_{Mg}, i_{Si}\}$  of each pixel of the element map. These intensity pairs are then plotted on a 2 dimensional diagram with Mg on the x- and Si on the y-axis. Points with the same  $\{i_{Mg}, i_{Si}\}$  are stacked on top of each other, and the number of stacked points are displayed as a colour-code. Different phases, such as olivine or low- and high-Ca pyroxenes, plagioclase or mesostasis can be discriminated on this plot. Rectangles are drawn around each phase, and all pixels associated with the points within the rectangle are highlighted with a specified colour. This is then the phase map, which we used to determine parameters such as identification of rims, rim abundance and thickness and etc.

Apparent chondrule diameters and rim thicknesses were measured on the phase maps. Each chondrule was measured along its longest and shortest axis. The average is the reported

chondrule diameter (EA Table 1). In the same way we measured the thinnest and thickest part of a pyroxene rim surrounding a chondrule. Again, the average is the reported rim thickness. We use the apparent chondrule diameters and rim thicknesses to calculate the share the pyroxene rim contributes to the entire chondrule by dividing the volume of the rim, using the rim thickness, through the volume of the inner chondrule, using the apparent chondrule radius minus the rim thickness. The extrapolation of the 2D chondrule and rim area to their respective 3D volumes has an inherent error, as has been pointed out previously by e.g. Hezel & Kießwetter, (2010) and references therein. Taking this into account, the calculated mode (volume fraction) of the pyroxene rim is overestimated by roughly a factor of two relative to the true 3D mode of the pyroxene rim. The reported modes of the pyroxene rims are therefore the calculated modes divided by 2.

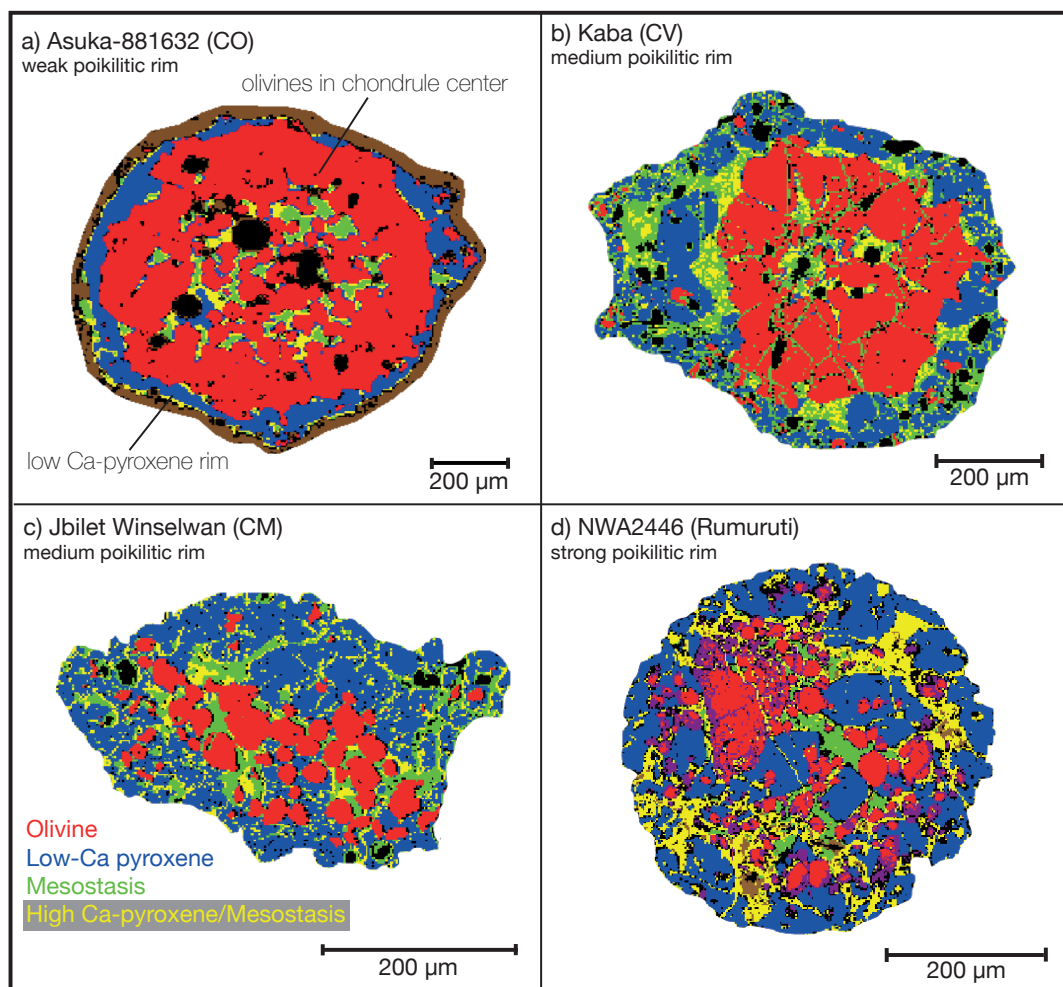


Figure 2.1: Examples of mineralogically zoned chondrules with olivine in the centre and low-Ca pyroxene in the rim. In a few chondrules some low-Ca pyroxene also occurs closer to the chondrule centre. Variable rim thicknesses of low-Ca pyroxene in the centre (b) might be the result of where the chondrule is sectioned.

## 2.3 Results

The focus of this study is on mineralogically zoned chondrules that have olivine concentrated in the center, which is surrounded by an igneous layer rich in low-Ca pyroxene (Fig. 2.1). Previous studies primarily focussed on elemental zonations between core and rim of chondrules (e.g. Ikeda & Kimura, 1996; Nagahara et al., 1999; Grossman et al., 1996). Hereafter, when we talk about zoned chondrules, we always refer to mineralogically zoned chondrules as displayed in Fig. 2.1.

We studied 223 chondrules in 15 different chondrites and from 6 different chondrite groups (CH, CM, CO, CR, CV, R) to constrain the overall systematics (appearance, abundance, etc.) of mineralogically zoned chondrules (Table 2.1). We further included 33 chondrules from Berlin (2009). All studied chondrites are of low petrological types, hence, none of the chondrules experienced extensive thermal metamorphism or recrystallisation on their parent body. As most Rumuruti chondrites are polymict breccias (Bischoff et al., 2013), we only analysed chondrules hosted within their type 3 lithologies.

Table 2.1

Host meteorites of the studied chondrites

Meteorite Type	Meteorite Name	Abbreviation	Petrologic Type	Nr. of Studied Chondrules	Nr. of Zoned Chondrules
CH	Acfer 182	A182	3	5	5
CM	El Quss	EQ	2	11	9
CM	Jbilet Winselwan	JW	2	30	23
CO	Asuka-881632	Asu	3	50	42
CO	Kainsaz**	Kain	3.2	29	18
CR	Al Rais	AR	2	10	10
CR	MET00426*	M426	2	18	15
CR	Renazzo**	Ren	2	11	8
CV	Arch	Arch	3	11	8
CV	Bali	Bali	3	11	8
CV	Kaba	Kaba	3	11	10
CV	Mokoia	Mok	3	14	4
CV	Y86751	Y86751	3	18	18
R	Hughes030	Hug	3-6	7	3
R	NWA753	N753	3.9	10	5
R	NWA2446	N2446	3	10	9

\* Data from Berlin (2009)

\* Data partly from Berlin (2009)



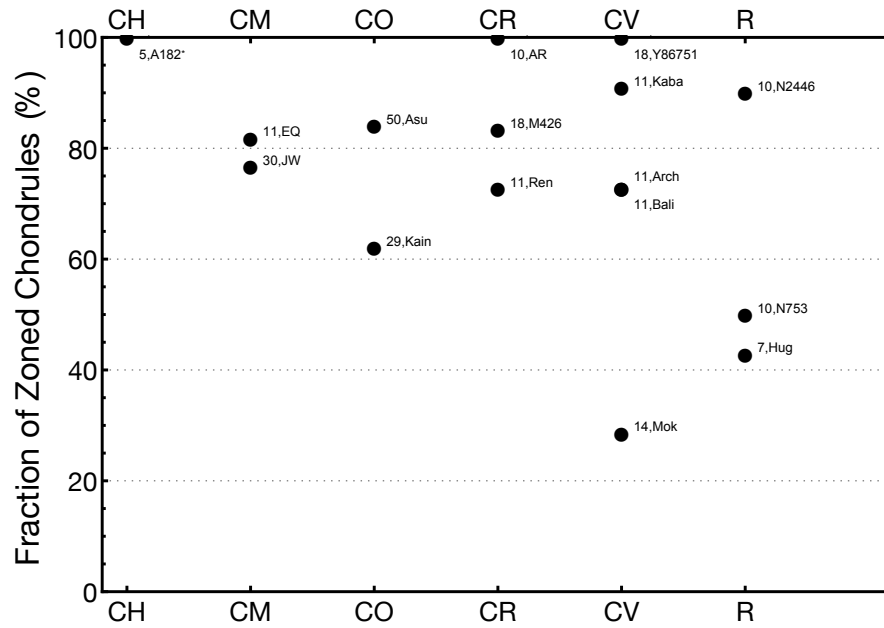


Figure 2.2: Fraction of zoned chondrules in various chondrite classes. On average, almost 75% of all chondrules are zoned. Numbers indicate the total number of chondrules studied in a particular meteorite. Meteorite abbreviations are listed in Table 1. Data for MET00426, 1 Renazzo chondrule and 14 Kainsaz chondrules are from Berlin (2009).

The fraction of zoned chondrules in 12 out of 13 carbonaceous chondrites is between 62 and 100% (Fig. 2.2). On average, the fraction of zoned chondrules in carbonaceous chondrites is almost 80%. The outlier is Mokoia, with a share of only 29% of zoned chondrules. Tomeoka and Onishi (2015) noticed a pseudomorphic replacement of the outermost chondrule layers by secondary minerals, which might have consumed some of the pyroxene.

This low abundance in Mokoia is in stark contrast to the other 4 CV chondrites. Their fraction of zoned chondrules ranges from 74% (Arch, Bali) to 100% (Y-86751), with an average of ~86%. The CH chondrites are an atypical class and the only studied member here, Acfer 182, has a high percentage of cryptocrystalline and skeletal chondrules (e.g. Bischoff et al., 1993; Hezel et al., 2003; Krot et al, 2010). These chondrule types were excluded from the study, leaving only 5 chondrules from Acfer 182 that were studied. Although CH chondrites appear to have a high fraction of zoned chondrules from simple visual inspection, the reported result of 100% is probably not fully representative. The fractions of zoned chondrules in CM, CO and CR chondrites are very similar, and range from 62 to 100%. On average, the fraction is 79%, very similar to CV chondrites. The fraction of zoned chondrules

## 2 The conditions of chondrule formation, Part II: Open system

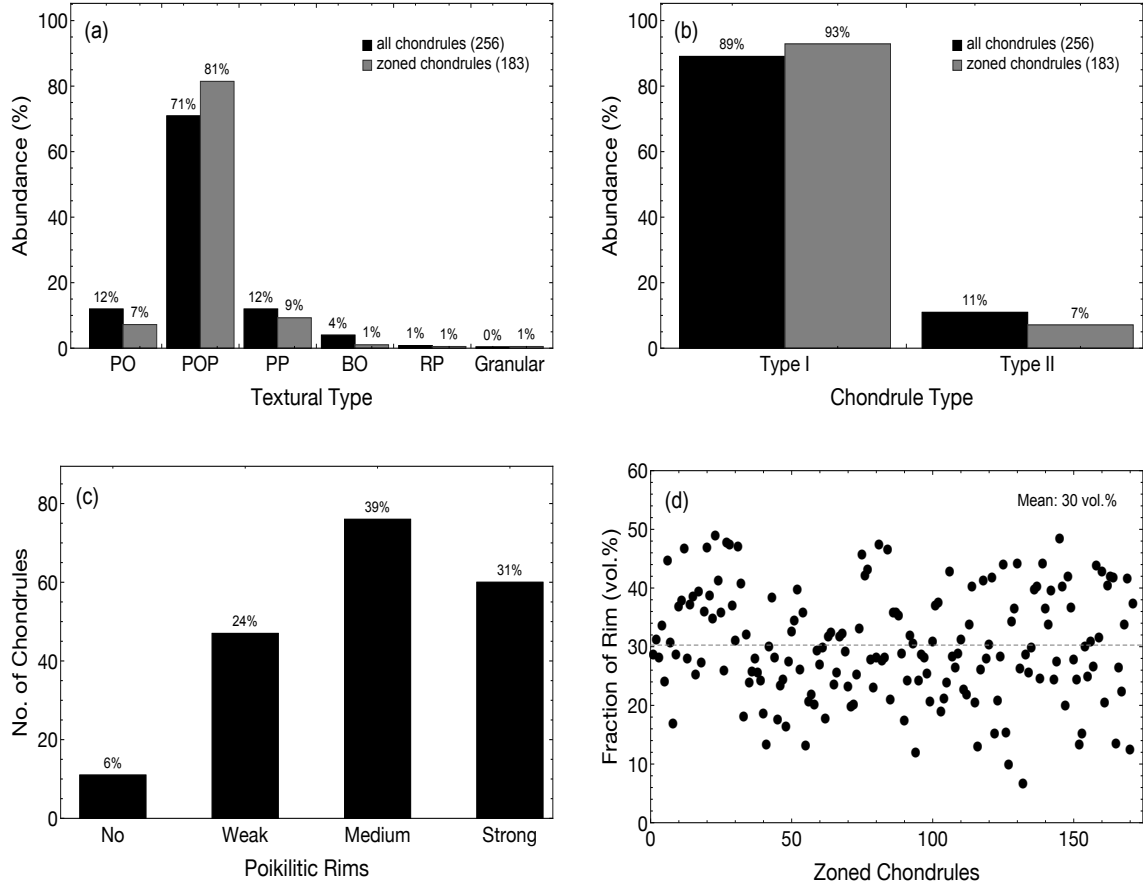


Figure 2.3: (a) Contrary to the entire chondrule population, most zoned chondrules are porphyritic chondrules (97%). PO – porphyritic olivine; POP – porphyritic olivine and pyroxene; PP – porphyritic pyroxene; BO – barred olivine; RP – radial pyroxene. (b) Type II chondrules are usually unzoned. The high abundance here is due to many zoned type II chondrules in Rumuruti. (c) We use a qualitative scheme to discriminate between no, weak, medium and strong poikilitic low-Ca pyroxene rims (cf. Fig. 3.1). The majority of rims is poikilitic, and of those, most are medium poikilitic. (d) The volume fraction of the rim can only be estimated, as the measured 2D thickness depends on where the chondrule is sectioned. The rim fraction varies between 10 and 50 vol.%, with a mean of about 30 vol.%.

in the 3 Rumuruti chondrites is highly variable, from 43% in Hughes030 and 50% in NWA753 to up to 90% in NWA2446.

Figure 2.3a compares the abundance of textural types of the entire chondrule population to the abundance of textural types of the zoned chondrules. Most chondrules are porphyritic (95%), and of those, 71% are porphyritic olivine-pyroxene (POP) chondrules. Almost all zoned chondrules are porphyritic (97%), of which 81% are POP chondrules. This share of POP chondrules within the population of zoned chondrules is somewhat higher than in the entire chondrule population. The percentages of porphyritic olivine (PO) and porphyritic pyroxene (PP) chondrules are each within 12% of the total amount among all studied chondrules. Within the population of zoned chondrules, PO chondrules make up 7% and are somewhat rarer than PP chondrules which make up 9%. Barred olivine (BO) chondrules

(4%), and radial pyroxene (RP) chondrules (1%) are considerably rarer than any other textural type. Their fraction within the zoned chondrules is even lower. In total, only 2% of the zoned chondrules represent one of these textural types.

The majority of chondrules are FeO poor, type I chondrules (89%; Fig. 3b). Only 11% of the entire chondrule population and 7% of the zoned chondrules are FeO rich type II chondrules (cf. zoned type II chondrule in Fig 2.1b). There is a possible difference between carbonaceous and Rumuruti-type chondrites: in Rumuruti 8 out of 12 (i.e. 67%) type II chondrules are zoned, i.e. similar to the 74% in type I chondrules; while in carbonaceous chondrites only 6 out of 16 (i.e. 38%) type II chondrules are zoned. However, this difference could also be a statistical effect due to the low abundances of type II chondrules in carbonaceous chondrites.

Figure 2.1 displays a range of textures of low-Ca pyroxene rims. Many rims have a non-uniform thickness. In most chondrules, the pyroxenes poikilitically enclose olivine. We use a qualitative scheme to discriminate between no, weak, medium and strong poikilitic pyroxene. In Fig. 2.1, plates (a) and (b) display rims that are concentric rings around the olivine-dominated core. The rim in plate (a) is comparatively thin and the pyroxene only occasionally encloses olivine (weak poikilitic). The rim in (b) is much thicker and medium poikilitic, and the enclosed olivine grains are small. There are no low-Ca pyroxenes in the

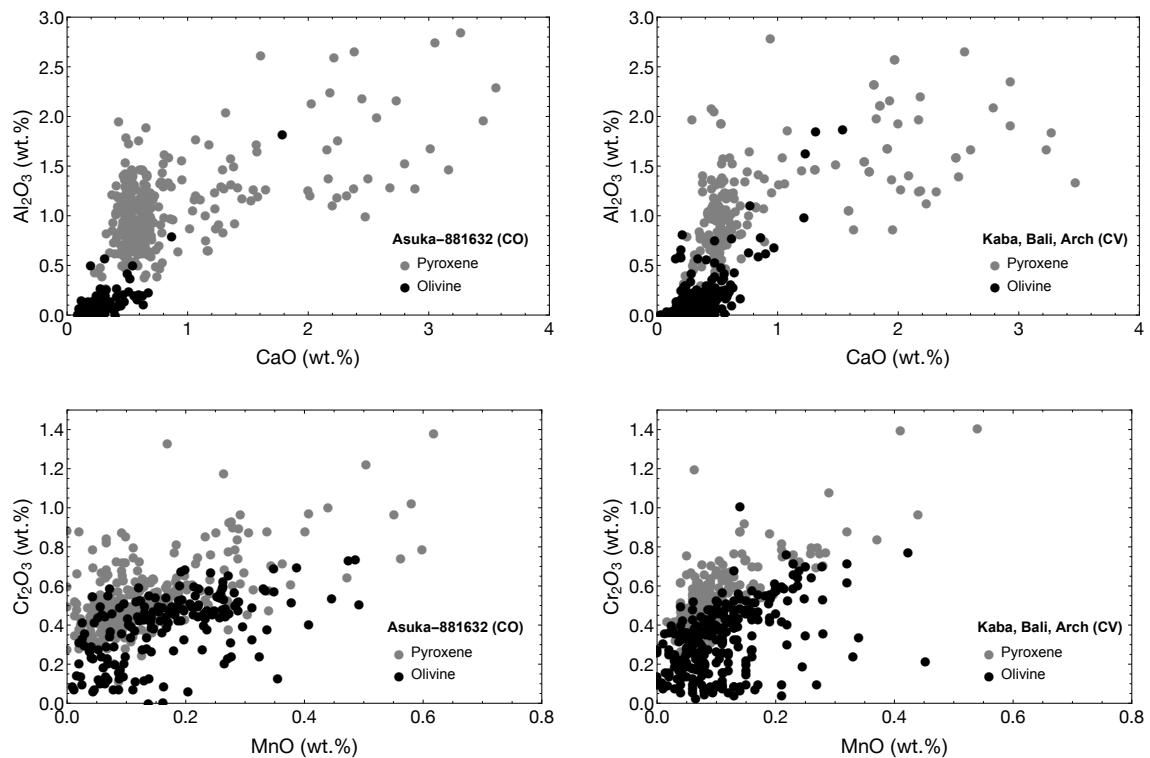


Figure 2.4: Refractory and moderately volatile element composition of olivine and low-Ca pyroxene of two chondrites.

## 2 The conditions of chondrule formation, Part II: Open system

Table 2.2

Representative analyses of chondrule olivine and pyroxene in wt.%.

	Asuka-881632 (CO)				Bali (CV)		Kaba (CV)		Arch (CV)	
<i>Olivine mineral analyses</i>										
SiO <sub>2</sub>	41.83	42.00	41.56	42.03	42.11	42.14	42.23	42.14	41.59	40.73
TiO <sub>2</sub>	0.02	0.09	0.05	0.07	0.09	n.d.	0.12	0.03	0.03	0.01
Al <sub>2</sub> O <sub>3</sub>	0.02	0.25	0.02	0.04	0.15	0.03	0.13	0.05	0.14	0.03
Cr <sub>2</sub> O <sub>3</sub>	0.51	0.24	0.53	0.25	0.26	0.09	0.49	0.32	0.24	0.09
MgO	53.95	56.34	54.23	56.12	56.17	52.68	55.43	55.87	53.93	52.09
FeO	3.31	0.51	3.20	1.16	0.51	4.79	1.06	1.08	3.39	6.52
NiO	0.02	n.d.	n.d.	0.02	0.03	n.d.	n.d.	n.d.	0.02	0.05
MnO	0.10	0.06	0.12	0.07	0.07	0.13	0.17	0.06	0.33	0.10
CaO	0.20	0.51	0.20	0.20	0.42	0.20	0.25	0.26	0.32	0.21
Na <sub>2</sub> O	n.d.	n.d.	n.d.	n.d.	0.03	0.02	n.d.	0.02	0.05	0.02
Total	99.95	100.01	99.92	99.97	99.84	100.08	99.89	99.83	100.04	99.84
<i>Pyroxene mineral analyses</i>										
SiO <sub>2</sub>	58.10	58.07	58.83	57.78	58.97	57.99	58.23	58.24	58.63	58.70
TiO <sub>2</sub>	0.20	0.19	0.18	0.20	0.06	0.20	0.07	0.12	0.22	0.18
Al <sub>2</sub> O <sub>3</sub>	1.47	1.32	0.96	1.19	0.50	1.47	0.76	0.90	0.97	0.92
Cr <sub>2</sub> O <sub>3</sub>	0.38	0.83	0.34	0.69	0.77	0.88	0.00	0.00	0.38	0.38
MgO	38.31	37.14	38.60	37.55	37.47	36.98	37.70	37.83	38.67	38.70
FeO	0.83	1.84	0.46	1.85	1.40	1.77	2.36	2.22	0.50	0.70
NiO	0.09	n.d.	n.d.	0.04	0.02	0.04	0.02	n.d.	n.d.	0.04
MnO	0.09	0.07	0.11	0.07	0.27	0.09	0.23	0.23	0.04	0.02
CaO	0.63	0.53	0.50	0.46	0.37	0.60	0.50	0.47	0.45	0.46
Na <sub>2</sub> O	n.d.	n.d.	0.02	n.d.	0.05	n.d.	0.03	n.d.	n.d.	n.d.
Total	100.10	100.00	100.01	99.83	99.89	100.03	99.88	100.02	99.86	100.10

centre of the chondrule. The olivine bearing part is subround, while the pyroxene dominated chondrule rim buckles to the left. This chondrule rim shows a noticeable amount of mesostasis material, especially between the rim pyroxene and olivine in the core. The chondrule in plate (c) has a thick and medium poikilitic rim. The entire chondrule is elongated, and the rim thickness varies considerably. It is thick parallel to the long axis and almost disappears along the short axis of the chondrule. The boundary between the olivine-rich core and pyroxene-rich rim is less clearly developed than in the chondrules of plate (a) and (b). The pyroxene in the chondrule of plate (d) is strongly poikilitic not only in the rim, but throughout the chondrule section. If this is a section cut close to the chondrule border, the pyroxene appearing at the chondrule centre would in fact also be rim pyroxenes. Rim thicknesses vary according to where a chondrule is sectioned.

In total, about 6% of the zoned chondrules have none poikilitic rims; 24% have weak poikilitic rims; 39% have medium and 31% have strong poikilitic rims (Fig. 2.3c). Figure 3d displays the rim fraction corrected for 3D as outlined in the Methods section. The average

rim fraction is 30 vol.% of the entire chondrule. Individual fractions vary from about 10 to 50 vol.%.

Figure 2.4 displays  $\text{Al}_2\text{O}_3$  vs.  $\text{CaO}$  and  $\text{Cr}_2\text{O}_3$  vs.  $\text{MnO}$  compositions for olivines and low-Ca rim pyroxenes from zoned chondrules in the CO chondrite Asuka-881632 and the CV chondrites Kaba, Bali and Arch (cf. Table 2.2). The element distributions are similar in all meteorites: the low-Ca pyroxenes are generally slightly enriched in  $\text{Al}_2\text{O}_3$  and in cases also in  $\text{CaO}$  compared to the olivines. In contrast, the  $\text{MnO}$  and  $\text{Cr}_2\text{O}_3$  concentrations are about similar, maybe slightly enriched in low-Ca pyroxenes compared to olivines.

The unzoned chondrules have variable appearances, but share many features of the zoned chondrules (Fig. 2.5). The PO chondrule in Fig. 2.5, plate (a) lacks any low-Ca pyroxene. This is the typical appearance of ~40% of the unzoned chondrules, which only vary in their mesostasis abundances. About 25% of the unzoned chondrules have low-Ca pyroxene scattered throughout them (plate b), and would be typically designated POP chondrules.

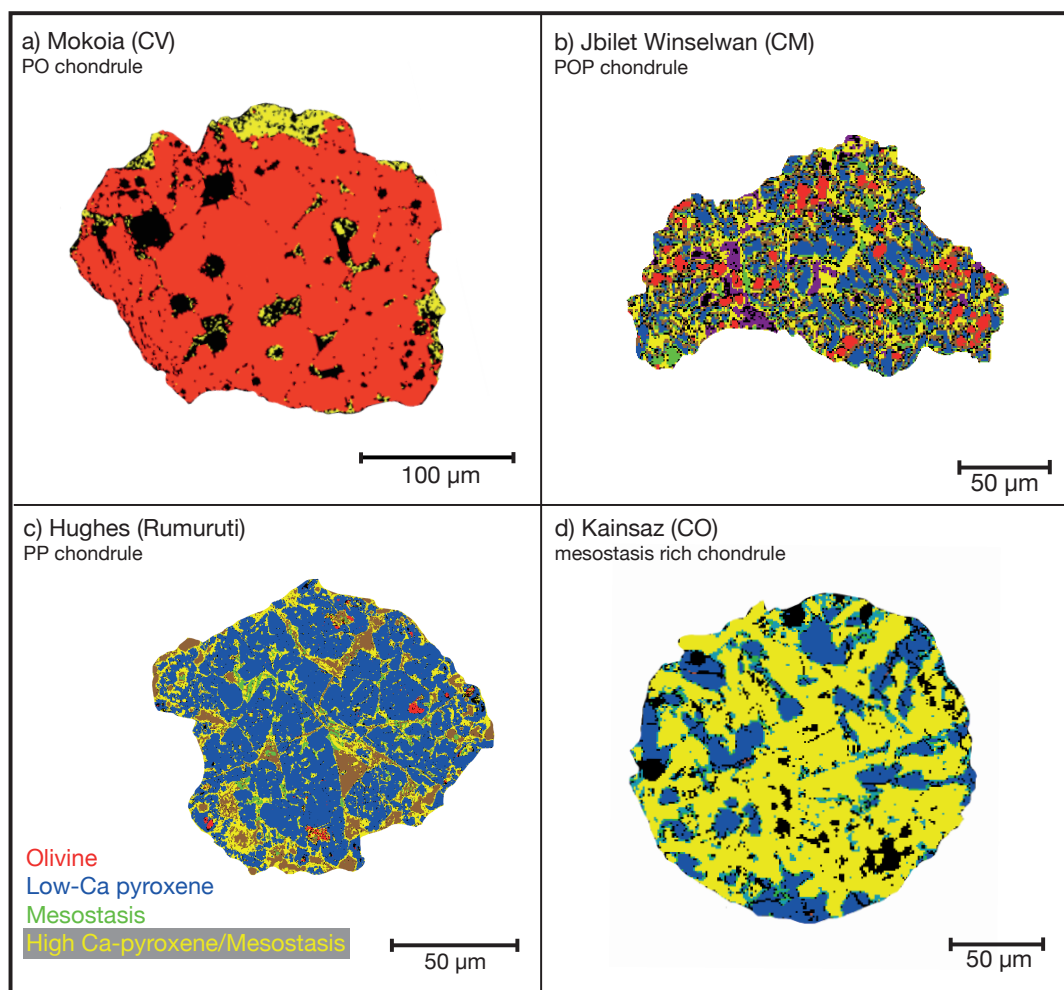


Figure 2.5: Examples of four typical types of unzoned chondrules. (a) PO chondrule, (b) POP chondrule, (c) PP chondrule, (d) mesostasis rich chondrule.

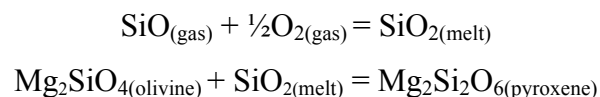
Plate (c) displays an almost pure PP chondrule, which is the appearance of about 12% of the unzoned chondrules. All have only small amounts of mesostasis and some have minor contents of olivine, similar to the one displayed in plate (b). The last, comparatively abundant unzoned chondrule type is dominated by mesostasis and has a share of about 10% (plate d). The remaining 7 unzoned chondrules are mainly atypical chondrules. For example, two have barred pyroxene structures. Another has a complex zonation with pyroxene in the centre, surrounded by olivine. Others are rather fragmented and a clear typification is difficult.

## 2.4 Discussion

### 2.4.1 Formation of low-Ca pyroxene rims

Chondrules were once molten silicate droplets. These droplets most probably cooled from their edge to their center. Hence, olivine, the first mineral to crystallise, would crystallise at the droplet rim, and pyroxene, the next mineral to crystallise would crystallise in the droplet center. Yet, the opposite is observed: olivine is in the centre of chondrules and pyroxene forms the rim. Hence, the observed mineralogical zonation cannot be the result of simple chondrule melt crystallisation.

Mineralogical zonation is not observed in experimental attempts to reproduce chondrule crystallisation textures (e.g. Connolly & Hewins, 1996; Hewins et al., 2005). However, this may be due to the selection of the starting material, which does not match the abundant type I carbonaceous chondrite chondrules. Tissandier et al. (2002) performed open system experiments in which partially molten chondrule analogues were exposed to high  $\text{SiO}_{(\text{g})}$  partial pressures. The results were mineralogically zoned textures, similar to those reported in this study. Recent open system experiments by Di Rocco and Pack (2015) showed that as much as 50% of oxygen can be exchanged between a molten chondrule and the surrounding gas within a few ten to few hundred minutes. This is consistent with results of in-situ oxygen isotope measurements in chondrule olivine and low-Ca pyroxene by Chaussidon et al. (2008). They found that olivine and pyroxene are not co-magmatic, instead about 2/3 of the oxygen hosted in the pyroxenes was derived from dissolved precursor olivine and 1/3 from the addition of SiO from the surrounding gas. The respective equations for this reaction are:



We find that almost all chondrules in carbonaceous and Rumuruti chondrites are zoned (see below). This supports previous findings and suggestions that mineralogical zonation and low-Ca pyroxene formed by the interaction of liquidus olivine with the surrounding gas during cooling. Chondrules were open systems, and this is a fundamental process of the formation of the chondrules in carbonaceous chondrites and Rumuruti type chondrules.

All studied chondrules are hosted in type 2 or 3 chondrites or lithologies, respectively. None of the studied chondrules experienced extensive thermal heating events on their parent bodies. The metamorphic reaction of olivine + SiO<sub>2</sub> = pyroxene requires high temperatures and the transport of SiO<sub>2</sub> to the olivine. Both requirements were not present on the chondrite parent bodies. The formation of the mineralogical zonation on their parent bodies can definitely be ruled out.

It is still unclear precisely how the chondrule precursor aggregates formed (e.g. Hezel & Palme, 2007 and references therein). However, the results presented here strongly suggest that the chondrule precursor aggregates consisted of abundant olivine plus refractory, e.g. Ca- and Al-rich material. In a condensing vapour of CI chondritic composition, first refractory, e.g. Ca- and Al-rich material forms. The first silicates are in most condensation calculations diopside, directly followed by olivine (Larimer, 1967; Grossman, 1972; Yoneda & Grossman, 1995; Davis & Richter, 2003; Ebel, 2006). We suggest these materials became the cores of zoned chondrules, consisting of porphyritic olivine with interstitial mesostasis. During cooling after or during chondrule precursor aggregation, the olivine of these chondrule cores reacted with SiO from the surrounding gas to enstatite, forming the low-Ca pyroxene rim grains. Olivine and low-Ca pyroxene have similar refractory and volatile element compositions (Fig. 4), consistent with the formation of low-Ca pyroxene from olivine. Concentrations of Al<sub>2</sub>O<sub>3</sub> and CaO are slightly elevated in low-Ca pyroxene relative to olivine. These might be the remains of mesostasis traces that were consumed during pyroxene formation, as mesostasis is commonly entirely absent in the chondrule rims. The slightly elevated Cr<sub>2</sub>O<sub>3</sub> in pyroxene compared to olivine might have condensed together with the SiO.

The low-Ca pyroxene mantles are typically medium poikilitic, most probably because the pyroxene forms an armour around the olivine, preventing further addition of SiO and complete reaction to pyroxene. There is an indication that zoned chondrules represent a smaller share of the rare type II chondrules in carbonaceous chondrites than the type I chondrules. This might be related to their different conditions of formation as apparent from

their FeO-rich compositions, or type II chondrules must be xenolithic to their host chondrites.

### 2.4.2 Amount of material added to the chondrules

The average thickness of chondrule rims allows an estimate of how much material was added before the reaction  $\text{olivine} + \text{SiO(g)} = \text{pyroxene}$  ceased. The mean volume of pyroxene rich rims is  $\sim 30$  vol.% (Fig. 3d), representing the amount of low-Ca pyroxene that was formed from the addition of SiO to olivine. The molar mass of forsterite is 141 amu, that of enstatite 201 amu, and consequently the mass of the additional  $\text{SiO}_2$  in enstatite is 60 amu. Hence, the rims in zoned chondrules contain on average 30 wt.% of added  $\text{SiO}_2$ . This means, a chondrule with a rim fraction of 30 vol.% contains 10 wt.%  $\text{SiO}_2$  that was added by interaction with the surrounding gas. As the low-Ca pyroxene rim thicknesses range from 10 to 50 vol.%, chondrules gained between 3 and 15 wt.% mass from the surrounding gas after they were molten. Different mineral densities are not considered in this rough calculation, as this effect is negligible compared to the uncertainties of the measured rim thicknesses.

### 2.4.3 Chondrule sizes and bulk compositions

If chondrules started from well mixed  $\mu\text{m}$ -sized precursor grains (e.g. Alexander, 1994; Brearley, 1996; Ciesla, 2005; Libourel and Chaussidon, 2009), the bulk compositions of all chondrule precursor aggregates would be identical (Hezel and Palme, 2007). However, precursor aggregate sizes need not be identical. If chondrules formed from compositionally identical, but variably sized precursor aggregates, their different surface/volume ratios would suffice to produce compositionally variable chondrules during open system gas-melt material exchange (cf. Wood, 1963). It could then be expected that chondrule sizes correlate with their bulk compositions: larger chondrules would gain less, and smaller chondrules would gain more  $\text{SiO}_2$ . Figure 2.6 displays a weak, possible trend between bulk chondrule compositions and apparent chondrule diameters of 50 Asuka-881632 chondrules (EA Table 2). However, this minor trend might well be a sectioning artefact. Chondrule sections closer to the edge will have thicker apparent rims, resulting in higher bulk  $\text{SiO}_2$  concentrations as low-Ca pyroxene has the highest  $\text{SiO}_2$  concentrations among phases up to almost 60 wt.%,



compared to an average 50 wt.% SiO<sub>2</sub> in chondrule mesostases and about 40 wt.% SiO<sub>2</sub> in olivine.

It is also possible that not all chondrules interacted with the surrounding gas at the same time. Isotopic evidence is interpreted to show that chondrules formed over a prolonged period of time (e.g. Kita et al., 2000,2012; Mostefaoui et al. 2002; Amelin et al., 2002; Connelly et al., 2012). In this case no correlation between chondrule size and SiO<sub>2</sub> content would be expected. In fact, Tachibana et al. (2003) showed a correlation between chondrule age and increasing bulk chondrule SiO<sub>2</sub> content. Different bulk chondrule SiO<sub>2</sub> contents would in this case not be a surface/volume, but a chronological effect. In this scenario, chondrules would co-exist and form over a long period of time with the same gaseous material surrounding them. The gas would become enriched in SiO, as the initially formed chondrules are olivine rich. Chondrules might later get selectively re-heated, depending on the chondrule forming process, thereby exchanging material with the SiO-rich gas.

#### 2.4.4 Unzoned chondrules

About 29% of the studied chondrules were classified as unzoned. However, the chondrules displayed in Fig. 2.5 plate (b) and (c) could actually be sections through rims of zoned chondrules. The average chondrule rim thickness is ~24% of a chondrule diameter, which means about ~24% of the chondrules in a chondrite section should be rim sections. About

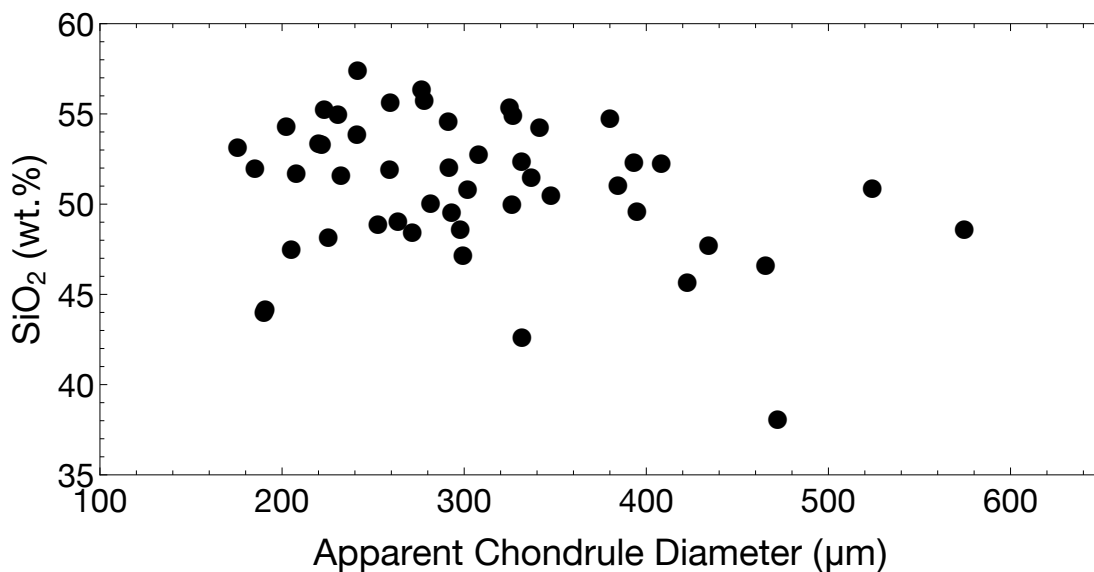


Figure 2.6: The SiO<sub>2</sub> bulk composition of 50 Asuka-881632 chondrules (cf. EA Table 2) decreases slightly with their apparent diameters. This weak trend could also be a sectioning artefact.

40% of the unzoned chondrules (i.e. 12% of all chondrules) have appearances as those shown in Fig. 2.5 plate (b) and (c), i.e. consist mainly of pyroxene, with some poikilitic olivine. Some chondrules, such as the one in Fig. 2.1 plate (d) are obvious sections close to the low-Ca pyroxene rim. It is therefore possible that the chondrules of plate (b) and (c) in Fig. 2.5 are in fact zoned chondrules, and together with chondrules classified as zoned chondrules that are similar to chondrules such as the one in Fig. 2.1 plate (d) add up to the expected 24%. If 40% of the unzoned chondrules are in fact zoned chondrules, it would increase the total share of zoned chondrules to more than 80%. However, as the correct classifications of chondrules as displayed in Fig. 2.5 (b) and (c) are ambiguous, we conservatively classify them as unzoned.

The unzoned PO chondrules as exemplified in Fig. 2.5 (a) are at 40% the second largest fraction of unzoned chondrules. The formation process we suggest for the zoned chondrules starts with olivine rich precursors, to which variable amounts of  $\text{SiO}_2$  are added, converting the olivine to variably thick, low-Ca pyroxene chondrule rims. It seems reasonable within this scenario that a certain share of chondrules received no or only minor amounts of  $\text{SiO}_2$ . The PO chondrules might represent this population or are simply chondrule fragments. It is within this reasoning further possible that at least some low-Ca pyroxene forms a partial rim on these chondrules, but is not sectioned in the studied samples. This is supported by the small number of PO chondrules with only minor amounts of low-Ca pyroxene that are present in the studied meteorites. In these cases, the unzoned PO chondrules might also be in fact part of the zoned chondrules, or at least represent a formation stage of zoned chondrule formation. This would then further increase the total amount of zoned chondrules to >90%.

The mesostasis rich chondrules as exemplified in Fig. 2.5 (d) together with the remaining chondrules of different appearances are difficult to explain in the suggested framework of zoned chondrule formation. These chondrules, however, only contribute about 5% to the total chondrule population. These chondrules might have by chance started with a different bulk composition, by e.g. including a larger fraction of Ca- and Al-rich material. It is also possible that these chondrules are xenoliths from a different region of the protoplanetary disk.

## 2.5 Conclusions

The abundance, appearance and composition of low-Ca pyroxene at the rim of chondrules in various carbonaceous and Rumuruti chondrites has been systematically studied for the first time. Previously, the occurrence of low-Ca pyroxene rims has been only briefly, although frequently, mentioned in publications. Our study clearly reveals that mineralogically zoned chondrules are the dominant chondrule type in carbonaceous and R chondrites. If some of the chondrules here conservatively classified as unzoned chondrules are in fact part of the zoned chondrule population, then >90% of all chondrules in carbonaceous and Rumuruti chondrites are zoned. If this is true, the classic chondrule classification of PO, POP and PP chondrules might simply reflect different sections through zoned chondrules – in other words: most porphyritic chondrules may in fact be PO chondrules with a low-Ca pyroxene rim. Further 3D tomographic studies are required to unequivocally verify this (e.g. Ebel et al., 2007; Friedrich, 2008; Tsuchiyama et al., 2009; Hezel et al., 2013a,b; Uesugi et al., 2013; Friedrich et al., 2015). Because zoned chondrules are the dominant chondrule type in the investigated chondrite groups, the formation of zoned chondrules represents a fundamentally important process of chondrule formation.

Numerous studies have presented evidence for interaction, exchange, evaporation and re-condensation, etc. of material between chondrules and surrounding gas (e.g. Tissandier et al., 2002; Grossman et al., 2002; Krot et al., 2004; Hezel et al., 2003; Libourel et al., 2006; Chaussidon et al. 2008; Hezel et al., 2010; Harju et al., 2012; Jacquet et al., 2012; Di Rocco and Pack, 2015; and cf. introduction). It has also been previously suggested that low-Ca pyroxene rims formed from the reaction of SiO rich gas with chondrule olivine. As almost all type I chondrules have a low-Ca pyroxene rim, almost all chondrules acted as such open systems. The interaction with the surrounding gas added 3-15 wt.% of SiO<sub>2</sub> to these chondrules. Zoned chondrules are in most cases type I porphyritic chondrules. Barred olivine chondrules are likely have cooled too fast to allow reaction of olivine with the surrounding gas. Mineralogically zoned chondrules cannot form from simple cooling, as is evident from experiments designed to reproduce chondrule textures (e.g. Connolly & Hewins, 1996; Hewins et al., 2005). However, experiments specifically designed to simulate open system processes do reproduce mineralogical zonation (Tissandier et al., 2002).

Bulk chondrule compositions in single meteorites show very large scatter in their elemental and isotopic compositions (e.g. Hezel and Palme, 2007 and references therein; Palme et al., 2014). Hezel and Palme (2007) studied in detail the possibility that random

aggregation of compositionally different precursor grains produced these variations (=closed system case). They found this would only be possible if precursor grains were  $>100\ \mu\text{m}$  in size. As there is currently no evidence for such large precursor grains, the closed system case is the least likely explanation for the observed bulk chondrule compositional variations. Relict grains in chondrules that might be considered chondrule precursor grains are commonly comparatively small ( $<40\ \mu\text{m}$ ; Jones, 1996). In contrast, the open system case can produce compositionally variable chondrules, even when their precursor aggregate compositions are the same. Petaev and Wood (1998) showed how condensation with partial isolation in a restricted nebula compartment produces olivine rich solids and SiO rich gas. This persistence of SiO in the gas after Mg has totally condensed is also well known from e.g. Ebel & Grossman (2000). We suggest chondrule precursor aggregates represent olivine rich condensates of different sizes. Then, even if each chondrule gained the same amount of SiO, the relative addition of material would be different due to each chondrule's different surface/volume ratio. It is also possible that if chondrules all had the same initial sizes, the statistical addition of material resulted in variable additions of SiO. Or, as there is evidence for a correlation of bulk chondrule  $\text{SiO}_2$  content and age, the gas became progressively depleted in MgO and later formed chondrules gained more SiO. This means, the first formed chondrules are olivine rich objects, and during subsequent reheating in the same, but then SiO-rich gas, the olivine at the chondrule edge reacted with the SiO to form the pyroxene rim.

The open system scenario suggests that all chondrules from a single meteorite formed from the same chemical reservoir with solar Mg/Si ratio. The remaining gas could then have condensed into the matrix. This scenario would be in agreement with the implications from complementarity, which also suggests that chondrules and matrix formed from a single reservoir (e.g. Bland et al., 2005; Ebel et al., 2008,2016; Hezel and Palme, 2008,2010; Palme et al., 2014,2015; Becker et al., 2015).

It is clear from the results of this study that type I chondrules from carbonaceous and Rumuruti chondrites acted as open systems during their formation. This is a fundamentally important process of chondrule formation. It appears that chondrules formed along a dynamic and complex path, resulting in their diversity.

### **Acknowledgements**

We thank Knut Metzler, Alan Rubin, an anonymous reviewer and the AE Sara Russell for their constructive suggestions that improved the clarity of this paper. We are grateful for the loan of the thin sections Asuka-881632 and Y-86751 from the National Institute of Polar Research, the loan of the Rumuruti sections from Addi Bischoff (Institute for Planetology, Münster) and the loan of Arch, Bali and Kaba from the Natural History Museum in Vienna.

## References

- Alexander C. M. O'D. 1994. Trace element distributions within ordinary chondrite chondrules: implications for chondrule formation conditions and precursors. *Geochimica et Cosmochimica Acta* 58: 3451–3467.
- Amelin Y., Krot A. N., Hutcheon I. D., and Ulyanov A. A. 2002. Lead isotopic ages of chondrules and calcium-aluminium-rich inclusions. *Science* 297: 1678-1683.
- Becker M., Hezel D. C., Schulz T., Elfers B.-M. and Münker C. (2015) The age of CV chondrites from component specific Hf-W systematics. *Earth and Planetary Science Letters*. (in press)
- Berlin J. 2009. Mineralogy and bulk chemistry of chondrules and matrix in petrologic type 3 chondrites: implications for early solar system processes. PhD. thesis, The University of New Mexico, Albuquerque, New Mexico, USA.
- Berlin J., Jones R. H., and Brearley A. J. 2006. Determining the bulk chemical composition of chondrules by electron microprobe (abstract). *37<sup>th</sup> Lunar and Planetary Science Conference*: 2370.
- Bischoff A., and Palme H. 1993. Acfer and paired samples, an iron-rich carbonaceous chondrite: Similarities with ALH85085 and relationship to CR chondrites. *Geochimica et Cosmochimica Acta* 57:2631-2648.
- Bischoff A., Vogel N., and Roszjar J. 2013. The Rumuruti chondrite group. *Chemie der Erde* 37:101-133.
- Bland P. A., Alard O., Benedix G. K., Kearsley A. T., Menzies O. N., Watt L. E., and Rogers N. W. 2005. Volatile fractionation in the early solar system and chondrule/matrix complementarity. *Proceeding of the National Academy of Sciences of the United States of America* 102: 13755-13760.
- Brigham C. A., Murrell M. T., Yabuki H., Ouyang Z., and El Goresy A. 1986. Silica-bearing chondrules and clasts in ordinary chondrites. *Geochimica et Cosmochimica Acta* 50: 1655–1666.
- Brearley A. J. 1996. Nature of matrix in unequilibrated chondrites and its possible relationship to chondrules. In *Chondrules and the Protoplanetary Disk*. Edited by Hewins R. H., Jones J., and Scott E.R.D., Cambridge University Press: 137-152.
- Brearley A. J., and Jones R. H. 1998. Chondritic Meteorites. In *Planetary Materials, Reviews in Mineralogy, vol. 36*. Edited by Papike J. J., The Mineralogical Society of America: 3-001 - 3-398

- Chaussidon M., Libourel G., and Krot A. N. 2008. Oxygen isotopic constraints on the origin of magnesian chondrules and on the gaseous reservoirs in the early Solar System. *Geochimica et Cosmochimica Acta* 72: 1924–19382
- Ciesla F. J. 2005. Chondrule-forming Processes—An Overview. In *Chondrites and the Protoplanetary Disk*. Edited by Krot A. N., Scott E. R. D. and Reipurth B., Astronomical Society of the Pacific: 811-820.
- Connelly J. N., Bizzarro M., Krot A. N., Nordlund A., Wielandt D., and Ivanova M.A. 2012. The absolute chronology and thermal processing of solids in the solar protoplanetary disk. *Science* 388:651-655.
- Connolly H. C., Jr., and Hewins R.H. 1996. Constraints on chondrule Precursor from Experimental Data. In *Chondrules and the Protoplanetary Disk*. Edited by Hewins R. H., Jones J., and Scott E. R. D., Cambridge University Press: 129-135.
- Davis A. M., and Richter F. M. 2003. Condensation and evaporation of solar system materials. In *Treatise on Geochemistry*. Edited by Holland H. D., and Turekian K. K., Elsevier: 407-430.
- Di Rocco T. D., and Pack A. 2015. Triple oxygen isotope exchange between chondrule melt and water vapor: an experimental study. *Geochimica et Cosmochimica Acta* 164: 17-34.
- Ebel D. S. 2006. Condensation of rocky material in astrophysical environments. In *Meteorites and the Early Solar System*. Edited by Kerridge J. F., and Matthews M. S., University of Arizona Press: 253-277.
- Ebel D. S., and Grossman L. 2000. Condensation in dust-enriched systems. *Geochimica et Cosmochimica Acta* 64: 339-366.
- Ebel D. S., and Rivers M. L. 2007. Meteorite 3-dimensional synchrotron microtomography: methods and applications. *Meteoritics and Planetary Science* 42: 1627–1646.
- Ebel D. S., Weisberg M. K., Hertz J., and Campbell A. J. 2008. Shape, metal abundance, chemistry and origin of chondrules in the Renazzo (CR) chondrite. *Meteoritics and Planetary Science* 43: 1725–1740.
- Ebel D. S., Brunner C., Konrad K., Leftwich K., Erb I., Lu M., Rodriguez H., Crapster-Pregont E., Friedrich J. M. and Weisberg M. K. (2016). Abundance, major element composition and size of components and matrix in CV, CO and Acfer 094 chondrites. *Geochimimica et Cosmochimica Acta*. (in press)
- Friedrich J. M. 2008. Quantitative methods for three-dimensional comparison and petrographic description of chondrites. *Computers and Geosciences* 34: 1926–1935.

- Friedrich J. M., Giordano S. A., Tamucci K. A., Ebel D. S., Rivers M. L., and Wallace S. W. 2015. Size-frequency Distributions and Physical Properties of Chondrules from X-Ray Microtomography and Digital Data Extraction (abstract). *46<sup>th</sup> Lunar and Planetary Science Conference*: 1937.
- Gooding J. L., Keil K., Fukuoka T., and Schmitt R. A. 1980. Elemental abundances in chondrules from unequilibrated chondrites: evidence for chondrule origin by melting of pre-existing materials. *Earth and Planetary Science Letters* 50: 171-180.
- Grossman J. N. 1996. Zoning of mesostasis in FeO-poor Semarkona chondrules (abstract). *31<sup>st</sup> Meteorite and Planetary Science Conference*: A55-A56.
- Grossman J. N., and Wasson J. T., 1982. Evidence for primitive nebular components in chondrules from the Chainpur chondrite. *Geochimica et Cosmochimica Acta* 46: 1081-1099.
- Grossman J. N., Alexander C. M. O'D., Wang J., and Brearley A. J. 2002. Zoned chondrules in Semarkona: Evidence for high- and low-temperature processing. *Meteoritics and Planetary Science* 37: 49-73.
- Grossman L. 1972. Condensation in the primitive solar nebula. *Geochimica et Cosmochimica Acta* 36: 597-619.
- Harju E. R., Kohl I. E., Rubin A. E., and Young E. D. 2014. Evaluating silicon condensation in type 1AB chondrules using in-situ silicon isotopes (abstract). *37<sup>th</sup> Lunar and Planetary Science Conference*: 2370.
- Hezel D. C. 2010. A mathematica code to produce maps from the element maps. *Computers and Geosciences* 36: 1097-1099.
- Hezel D. C., and Kießwetter R. 2010. Quantifying the error of 2D bulk chondrule analyses using a computer model to simulate chondrules (SIMCHON). *Meteoritics and Planetary Science* 45: 555-571.
- Hezel D. C., and Palme H. 2007. The conditions of chondrule formation, Part I: Closed system. *Geochimica et Cosmochimica Acta* 71: 4092-4107.
- Hezel D. C., and Palme H. 2008. Constraints for chondrule formation from Ca-Al distribution in carbonaceous chondrites. *Earth and Planetary Science Letters* 265:716-725.
- Hezel D. C., and Palme H. 2010. The chemical relationship between chondrules and matrix and the chondrule matrix complementarity. *Earth and Planetary Science Letters* 294: 85-93.



- Hezel D. C., Palme H., Brenker F. E., and Nasdala L. 2003. Evidence for fractional condensation and reprocessing at high temperatures in CH-chondrites. *Meteoritics and Planetary Science* 38: 1199-1216.
- Hezel D. C., Palme H., Nasdala L., and Brenker F. E. 2006. Origin of SiO<sub>2</sub>-rich components in ordinary chondrites. *Geochimica et Cosmochimica Acta* 70:1548-1564.
- Hezel D. C., Friedrich J., and Uesugi M. 2013a. Looking Inside: 3D Structures of Meteorites. *Geochimica et Cosmochimica Acta* 116: 1-4.
- Hezel D. C., Elangovan P., Viehmann S., Howard L., Abel R. L., and Armstrong R. 2013b. Visualisation and quantification of CV chondrite petrography using micro-tomography. *Geochimica et Cosmochimica Acta* 116: 33-40.
- Hewins R. H., Connolly, H. C., Jr., Lofgren G.E., and Libourel G. 2005. Experimental Constraints on Chondrule Formation. In *Chondrites and the Protoplanetary Disk*. Edited by Krot A. N., Scott E. R. D. and Reipurth B., Astronomical Society of the Pacific: 286-316.
- Hewins R. H., and Zanda B. 2012. Chondrules: Precursors and interactions with the nebular gas. *Meteoritics and Planetary Science* 47:1120-1138.
- Ikeda Y., and Kimura M. 1996. Anhydrous alteration of Allende chondrules in the solar nebula III: alkali-zoned chondrules and heating experiments for anhydrous alteration. *Proceedings of the NIPR Symposium on Antarctic Meteorites* 9: 51-68.
- Jacquet E., Alard O., and Gounelle M. 2012. Chondrule trace element geochemistry at the mineral scale. *Meteoritics and Planetary Science* 47: 1-20.
- Jones R. H. 1990. Petrology and mineralogy of Type II, FeO-rich chondrules in Sermakona (LL3.0): Origin by closed-system fractional crystallization, with evidence for supercooling. *Geochimica et Cosmochimica Acta* 54: 1785-1802.
- Jones R. H. 1996. Relict grains in chondrules: Evidence for chondrule recycling. In *Chondrules and the Protoplanetary Disk*. Edited by Hewins R. H., Jones J., and Scott E.R.D., Cambridge University Press: 163-180..
- Jones R. H. 2012. Petrographic constraints on the diversity of chondrule reservoirs in the protoplanetary disk. *Meteoritics and Planetary Science* 47: 1176–1190.
- Jones R. H., and Schilk A. J., 2009. Chemistry, petrology and bulk oxygen isotope compositions of chondrules from the Mokoia CV3 carbonaceous chondrite. *Geochimica et Cosmochimica Acta* 73: 5854–5883.

- Kita N. T., Nagahara H, Togashi S., and Morishita Y. 2000. A short duration of chondrule formation in the solar nebula: Evidence from  $^{26}\text{Al}$  in Semarkona ferromagnesian chondrules. *Geochimica et Cosmochimica Acta* 64: 3913-3922.
- Kita N. T., and Ushikubo T. 2012. Evolution of protoplanetary disk inferred from  $^{26}\text{Al}$  chronology of individual chondrules. *Meteoritics and Planetary Science* 47: 1108–1119.
- Krot A. N., Libourel G., Goodrich C., and Petaev M. I. 2004. Silica-igneous rims around magnesian chondrules in CR carbonaceous chondrites: evidence for fractional condensation during chondrule formation. *Meteoritics and Planetary Science* 39: 1931–1955.
- Krot A. N., Nagashima K., Yoshitake M., and Yurimoto H. 2010. Oxygen isotopic compositions of chondrules from the metal-rich chondrites Isheyev (CH/CB<sub>b</sub>), MAC 02675 (CB<sub>b</sub>) and QUE 94627 (CB<sub>b</sub>). *Geochimica et Cosmochimica Acta* 74: 2190–2211.
- Larimer J. W. 1967. Chemical fractionation in meteorites-1. Condensation of the elements. *Geochimica et Cosmochimica Acta* 31: 1215-1238.
- Lauretta D. S., Nagahara H., and Alexander C. M. O'D. 2006. Petrology and Origin of Ferromagnesian Silicate Chondrules. In *Meteorites and the early Solar System II*. Edited by Lauretta D. S., and McSween H. Y., University of Arizona Press: 431-459.
- Libourel G., Krot, A. N., and Tissandier, L. 2006. Role of gas–melt interaction during chondrule formation. *Earth and Planetary Science Letters* 251:232–240.
- Libourel G., and Chaussidon M. 2009. Origin of Mg-rich olivine in type I chondrules (abstract). *72<sup>nd</sup> Annual Meteoritical Society Meeting*: 5201.
- Mostefaoui S., Kita N. T., Togashi S., Tachibana S., Nagahara H., and Morishita Y. 2002. The relative formation ages of ferromagnesian chondrules inferred from their initial aluminum-26/aluminum-27 ratios. *Meteoritics and Planetary Science* 37: 421–438.
- Nagahara H., Kita N. T., Ozawa K., and Morishita Y. (1999) Condensation during chondrule formation: Elemental and Mg isotopic evidence (abstract). *30<sup>th</sup> Lunar and Planetary Science Conference*: 1917.
- Palme H., Spettel B. and Hezel D. C. (2014) Siderophile Elements in Chondrules of CV-Chondrites. *Chemie der Erde – Geochemistry* 74: 507–516.
- Palme H., Hezel D. C., and Ebel D. S. 2015. The origin of chondrules: Constraints from matrix composition and matrix-chondrule complementarity. *Earth & Planetary Science Letters* 411: 11–19.
- Petaev M. I., and Wood J. A. 1998. The condensation with partial isolation (CWPI) model of condensation in the solar nebula. *Meteoritics and Planetary Science* 33: 1123–1137.

- Rubin A. E., and Wasson J. T. 1988. Chondrules and matrix in the Ornans CO3 meteorite - possible precursor components. *Geochimica et Cosmochimica Acta* 52: 425-432.
- Scott E. R. D., and Taylor G. J. 1983. Chondrules and other components in C, O, and E chondrites: Similarities in their properties and origins. *Journal of Geophysical Research: Solid Earth* (Supplement)88: B275–B286.
- Scott E. R. D., and Krot A. N. 2014. Chondrites and Their Components. In *Treatise on Geochemistry, 2<sup>nd</sup> edition*. Edited by Turekian, K. K., and Holland H., Elsevier: 65-137.
- Tachibana S., Nagahara H., Mostefaoui S., and Kita N. T. 2003. Correlation between relative ages inferred from <sup>26</sup>Al and bulk compositions of ferromagnesian chondrules in least equilibrated ordinary chondrites. *Meteoritics and Planetary Science*: 38: 939–962.
- Tissandier L., Libourel G., and Robert F. 2002. Gas-melt interactions and their bearing on chondrule formation. *Meteoritics and Planetary Science* 37:1377– 1389.
- Tomeoka K., and Onishi I. 2015. Redistribution of chondrules in a carbonaceous chondrite parent body: A model. *Geochimica et Cosmochimica Acta* 164: 543-555.
- Tsuchiyama A., Nakamura T., Okazaki T., Uesugi K., Nakano T., Sakamoto K., Akaki T., Iida Y., Kadono T., Jogo K., and Suzuki Y. 2009. Three-dimensional structures and elemental distributions of stardust impact tracks using synchrotron microtomography and X-ray fluorescence analysis. *Meteoritics and Planetary Science* 44:1203–1224.
- Uesugi M., Uesugi K., Takeuchi A., Suzuki Y., Hoshino M., and Tsuchiyama A. 2013. Three-dimensional observation of carbonaceous chondrites by synchrotron radiation X-ray CT – quantitative analysis and development for the future sample return missions. *Geochimica et Cosmochimica Acta* 116:17–32.
- Wood J. A. 1963. On the origin of chondrules and chondrites. *Icarus* 2: 152-180.
- Yoneda S., and Grossman L. 1995. Condensation of CaO-MgO-Al<sub>2</sub>O<sub>3</sub>-SiO<sub>2</sub> liquids from cosmic gases. *Geochimica et Cosmochimica Acta* 31: 1215-1238.

### **3 Chondrule and matrix complementarities in the recently discovered Jbilet Winselwan CM chondrite**

Pia Friend<sup>1\*</sup>, Dominik C. Hezel<sup>1,2</sup>, Jean-Alix Barrat<sup>3</sup>, Jutta Zipfel<sup>4</sup>, Herbert Palme<sup>4</sup>, Knut Metzler<sup>5</sup>

<sup>1</sup>University of Cologne, Department of Geology and Mineralogy,  
Zùlpicher Str. 49b, 50674 Köln, Germany

<sup>2</sup>Natural History Museum, Department of Mineralogy,  
Cromwell Road, SW7 5BD London, UK

<sup>3</sup>Université de Bretagne Occidentale, Institut Universitaire Européen de la Mer, CNRS  
UMR 6538, Place Nicolas Copernic, 29280 Plouzané, France

<sup>4</sup>Forschungsinstitut und Naturmuseum Senckenberg, Senckenberganlage 25, D-60325  
Frankfurt am Main, Germany

<sup>5</sup>Institut für Planetologie, Universität Münster, Wilhelm-Klemm-StraÙe 10, 48149  
Münster, Germany

**\*corresponding author:**

**piafriend13@gmail.com**

*Keywords:*

chondrules, matrix, CM chondrites, complementarity, Jbilet Winselwan

*submitted to:*

*Meteoritics & Planetary Sciences*

*submission date:*

*July 2016*

## Abstract

Jbilet Winselwan (JW) is a recently found CM2 chondrite breccia containing two lithologies. The study of 508 chondrules provides the first statistically reliable size distribution for CM chondrites, which is about log-normal with mean chondrule sizes of 149  $\mu\text{m}$  (lithology I) and 141  $\mu\text{m}$  (lithology II). Chondrules are surrounded by fine-grained rims. Chondrule diameters and their rim thicknesses have positive correlations with slopes of 0.12 (lithology II) and 0.18 (lithology I), the latter typical of CM chondrites. JW experienced only mild aqueous alteration and is among the most primitive CM chondrites. Bulk JW element ratios are solar (=CI chondritic) for e.g. Si/Mg (1.12), Fe/Mg (1.80-1.83), Ti/Al (0.053), and about solar for Ca/Al. The 26 studied chondrules have sub-chondritic Si/Mg (0.88) and Fe/Mg ratios (0.21). Complementary, matrix and the fine-grained chondrule rims have super-chondritic Si/Mg ratios with means of 1.34 and 1.41, respectively. The Fe/Mg ratios are also super-chondritic, with means of 2.41 (matrix) and 2.61 (fine-grained rims). The refractory element ratios in chondrules are super-chondritic (Ti/Al: 0.106; Ca/Al: 1.64), and sub-chondritic in the JW matrix (Ti/Al: 0.031; Ca/Al: 0.71) and in the fine-grained rims (Ti/Al: 0.023; Ca/Al: 0.68). Chondrules were open systems, exchanging material with the surrounding gas. The complementary element ratios require formation of chondrules and matrix from the same reservoir. Any chondrule forming processes requiring distinct reservoirs for these components are excluded.

### 3.1 Introduction

In carbonaceous chondrites, chondrules and matrix make up the bulk of the meteorite. Chondrule fractions range from 15-75 vol.%, and matrix accounts for up to 60 vol.% (e.g. Grossman et al. 1988). As chondrule melting requires temperatures as high as 1600 K and above, they are considered high temperature components. Matrix is by some designated as a low temperature component (e.g. Larimer and Anders, 1967; Abreu and Brearley, 2009), predominantly consisting of primitive nebula aggregates, more or less reworked, others believe that matrix largely formed at high temperatures (see Huss et al., 2005). The fundamental questions about the heat source for chondrule melting and the relationship of chondrules and matrix are still cryptical. There are two different principal possibilities regarding the relationship of chondrules and matrix: (i) formation of chondrules and matrix from a single reservoir of solar nebular dust, and (ii) the formation of chondrules and matrix in two or more independent reservoirs and later mixing of appropriate amounts of chondrules and matrix to form chondritic planetesimals.

The major element composition of chondritic meteorites is, except for volatile elements, very similar and fits well with the composition of the solar photosphere (e.g. Wolf and Palme, 2001; Lodders et al., 2009). In particular, ratios among the most abundant non-volatile elements, Mg, Si and Fe are approximately the same in chondritic meteorites as in the Sun. The CI carbonaceous chondrites provide the best fit. Other chondrite types show small deviations from solar ratios. The newly-found CM chondrite Jbilet Winselwan (JW) studied here comes close to the CI composition (Lodders et al. 2009; Palme et al. 2015).

The solar ratios of non-volatile elements in chondritic meteorites are significantly different from the average compositions of matrix and chondrules (e.g. Palme et al., 2015; and references therein). Both components are evidently needed to produce the chondritic bulk composition. Scott et al. (1982, 1984) were presumably the first to reveal a complementary distribution of Fe, Si, and Mg between chondrules and matrix in ordinary and carbonaceous chondrites. Thereon, Wood (1985) noted complementary Fe/Si ratios in chondrules and matrix in the CM chondrite Murchison. Such complementary element distributions are particularly remarkable, as the bulk chondrite has solar (=CI chondritic) ratios for non-volatile elements. The significance of complementarity for the chondrule formation process was fully noticed by Klerner and Palme (1999a,b, 2000), who discovered Si/Mg, Cr/Fe and Ti/Al complementarities in the carbonaceous chondrites Renazzo (CR) and Allende (CV). Hezel and Palme (2008) reported Ca/Al complementarities in two CV

chondrites. Allende and Y-86751 have both CI chondritic bulk Ca/Al ratios. However, in Allende, chondrules have sub- and matrix has super-CI chondritic Ca/Al ratios, while chondrules in Y-86751 have super- and matrix has sub-chondritic Ca/Al ratios. As shown by Ford and Brearley (2008) in the Allende meteorite, there exist some local redistribution of Ca between CAIs and matrix probably due to aqueous fluids. However, Hezel and Palme (2008) demonstrated that the described findings of complementarity cannot result from element redistribution on the parent body. In a further study, Hezel and Palme (2010) reported Si/Mg complementarities between chondrules and matrix in CV, CR, CO and CM chondrites. Palme et al. (2014) found low Ir/Sc and high Ir/Ni in Allende chondrules, which requires complementary ratios in the matrix, as bulk Allende has close to CI chondritic ratios of these elements. Further, Palme et al. (2015) report Fe/Mg complementarities in CR, CO, CV and CM chondrites and Ti/Al complementarities in Renazzo and Mokoia.

Ebel et al. (2016) presented Si, Mg, Ca, Al, Ti and Fe contents of chondrules, CAIs and matrix in CO and CV chondrites as well as in Acfer 094, an ungrouped carbonaceous chondrite. The data were obtained using a new technique based on X-ray intensity maps with low count/pixel ratios. The authors report chondrule-matrix complementarity for Mg, Si, Cr, Ca, Al and Ti in the studied meteorites.

Becker et al. (2015) analysed the trace elements Hf and W, as well as W isotopes in chondrule, matrix and bulk chondrite separates of the CV chondrites Allende, Vigarano and Kaba. All matrix separates have sub-chondritic and the chondrule separates have super-chondritic Hf/W ratios, while the bulk meteorite has a CI-chondritic ratio. In addition, the radiogenic  $^{182}\text{W}$  isotopes are complementary: chondrules have positive and matrix negative  $\epsilon^{182}\text{W}$  when compared to the CI chondritic bulk of Allende. A similar result is presented by Budde et al. (2016). These authors found, in addition, that stable W -isotopes also show the same complementary relationship. Excesses of  $^{183}\text{W}$  were measured in chondrules and depletions in matrix, whereas bulk Allende analyses give the same  $^{183}\text{W}$ , identical to other chondritic meteorites, Earth, Mars and Moon.

Complementarity appears to extend to volatile elements, with bulk meteorite abundances considerably lower than in CI-chondrites. Bland et al. (2005) determined minor and trace element concentrations of volatile elements in matrices of several carbonaceous chondrites. Whereas bulk chondrites show a monotonic decrease of volatile element concentrations with decreasing condensation temperatures, matrices of carbonaceous chondrites display a strongly non-uniform CI-normalised zigzag pattern. Chondrules must have the complementary pattern to achieve the smooth distribution of the bulk meteorite.

Complementary element ratios between chondrules and matrix, together with CI bulk chondrite ratios require a single reservoir, from which chondrules and matrix formed. A stochastic mixture of chondrules and matrix could never produce a chondritic bulk composition. There are already some studies, that treat matrix as an evaporative residue from chondrule formation, considering complementarity (e.g. Wasson, 2008; Abreu and Brearley, 2010). However, many chondrule forming models do not consider matrix at all. Collisions of molten or partially molten planets (e.g. Asphaug et al., 2011; Sanders & Scott, 2012) may produce melt droplets, but there is no explanation for the presence of just the right amount of matrix to balance the non-chondritic composition of chondrules. Such models, ignoring the complementarity argument are still published and we therefore attempt to broaden the evidence for this critical and pivotal argument.

In CM chondrites the idea of complementarity can well be demonstrated. They have abundant matrix and chondrules are in general very Mg-rich and Fe-poor. Thus, one expects low Fe, high Mg chondrules and Si- and Fe-rich matrix. Chondrules Since the borders between Mg-rich and Mg-poor components are generally very sharp in chondrites, element exchange between matrix and chondrules Redistribution of incompatible elements such as Ca, Na and K due to replacement of mesostasis could have affected chondrules in CM chondrites which typically suffered some aqueous alteration. However, since the borders of Mg-rich and Mg-poor chondrules are sharp, similar than in other chondrites, an exchange of these elements between chondrules and matrix on the parent body can be excluded. Only very few data on bulk chondrules, as well as on matrix of CM chondrites exist (e.g. Hezel & Palme, 2010 and references therein) and the newly-found CM chondrite Jbilet Winselwan (JW) appears a suitable candidate for this study, as the findings from Russel et al. (2014) indicate a very low degree of aqueous alteration in most parts of this brecciated meteorite. Additionally, there were five thin sections and plenty enough additional sample material available for our investigations, ensuring a comprehensive data set.

Jbilet Winselwan was found in the Western Sahara in 2013 and classified as CM2 (Ruzicka et al., 2015). Russell et al. (2014) point out distinctly visible chondrules that are surrounded by matrix material or fine-grained dust rims (cf. Fig. 1, 6), and they estimated a ratio of chondrules to matrix of about 50:50. Their studies using X-ray diffraction (XRD) and scanning electron microscopy (SEM) revealed that large parts of this meteorite did not experience significant aqueous alteration. Also, the presence of melilite in CAIs and metal grains within matrix material observed by Russell et al. (2014) indicate a low degree of alteration. Furthermore, these authors emphasise that JW might be a breccia. The results



from Pernet-Fisher et al. (2014) also indicate a brecciated meteorite with various degrees of aqueous alteration, ranging between the petrologic sub-types 2.0 and 2.3 in distinct clasts. Göpel et al. (2015) published bulk meteorite data for minor and trace elements which show abundance patterns typical of CM chondrites, although terrestrial weathering effects are noticeable.

Here we provide a comprehensive set of chemical data for chondrules, inter-chondrule matrix and fine-grained chondrule rims in Jbilet Winselwan. We also present concentrations of major, minor and trace elements of Jbilet Winselwan bulk samples. In addition, we present petrologic and petrographic data, including the first statistically reliable chondrule size distribution among the CM chondrite group. We discuss the results in the context of chondrule-matrix complementarity and describe implications for chondrule formation.

## 3.2 Methods

### *Mineral element analyses*

The elemental composition of minerals and bulk matrix were determined with a JEOL JXA-8900RL electron microprobe at the University of Cologne. The accelerating voltage was set to 20 kV and the beam current to 20 nA. Well-characterised natural silicates and oxides were used as standards and ZAF correction was employed. Detection limits for minor elements were: 100 wt.-ppm for CaO, TiO<sub>2</sub>, NiO and Na<sub>2</sub>O; 200 wt.-ppm for Cr<sub>2</sub>O<sub>3</sub>; and 250 wt.-ppm for MnO and FeO. To verify our reported low Ti abundances, we measured a range of Ti standards.

Mineral compositions were measured with a focused beam of 1 µm diameter. Matrix and dusty rims around chondrules were measured with a defocused beam of 15 µm diameter. Matrix totals were between 75 wt.% and 90 wt.%, with mean totals of 82 wt.% for matrix and 80 wt.% for chondrule rim analyses. These low totals result from (i) the presence of hydrated phases such as phyllosilicates, (ii) the porous matrix structure, and (iii) to a lesser extent from the absence of data on S and P. Since Fe in metals and sulphides is calculated as FeO, this slightly over-determines the reported FeO. This should, however, be negligible, as the modal abundance of opaques in CM chondrites is <3 vol.% (e.g. Rubin et al. 2007). In addition, throughout the paper we focus on element ratios, which are not affected by totals.

#### *Determining bulk chondrule compositions*

Chondrule bulk compositions were obtained using modal recombination (e.g. Berlin et al., 2006; Hezel, 2010; Ebel et al., 2016; Friend et al., 2016). The required element maps were obtained by rastering the chondrules with a focused beam of 1  $\mu\text{m}$  spot size. Step sizes were 2  $\mu\text{m}$  and dwell times 240 ms. As mesostasis in most chondrules was slightly altered during fluid assisted parent body alteration, totals of mesostases analyses are often low (~90 wt.%). Reported bulk chondrule compositions do not include opaque phases. Some of the chondrules contain low abundances of opaques. Their heterogeneous distribution prevents a reliable inclusion in the bulk chondrule composition (Hezel, 2007; Hezel & Kießwetter, 2010; Ebel et al., 2016). This might in some cases underestimate the bulk chondrule Fe content, but does not affect element ratios not involving Fe. The error when using the 2D bulk chondrule composition relative to the true 3D bulk composition of chondrules was calculated using the method of Hezel and Kießwetter (2010).

#### *Bulk chondrites analysis using ICP-AES and ICP-MS*

Two distinct bulk samples of JW (a 1 g chip and a 0.156 mg fragment) were completely powdered using a boron carbide pestle and mortar. Major and trace element concentrations were determined by ICP-AES (inductively coupled plasma-atomic emission spectrometry) and ICP-MS (inductively coupled plasma-mass spectrometry), respectively, at Université de Brest (IUEM, Plouzané) using the procedures described by Barrat et al. (2012, 2014, 2016). The accuracy of major and trace element concentrations is better than 5% (probably better than 3% for all the REEs) based on various standard and sample duplicates.

#### *Bulk chondrite analyses using XRF*

Major and trace elements of bulk samples were measured using a Philips PW 2400 sequential wavelength dispersive X-ray spectrometer at the University of Cologne, Germany. Aliquots of about 120 mg powdered sample were treated with nitrohydrochloric acid for two hours at 130 °C to oxidise metals. After vaporisation of the acid, 3.6 g  $\text{Li}_2\text{B}_4\text{O}_7$  were added as fluxing agent. A glass disk was produced by melting at about 1200 - 1300 °C in a platinum crucible under oxidising conditions. At least 40 standard rock samples, prepared identically, were used for external standardisation of the X-ray spectrometer for each individual element. More details of the analytical procedure are reported in Wolf and Palme (2001). As discussed by these authors, the precision for all elements analysed is below 1%. The accuracy estimated from a comparison with well-determined Allende samples generally is below 2%, except for

Cr, Ni, and P which are accurate to within 3%.

### *Determination of apparent chondrule sizes and apparent fine-grained rim thicknesses*

We measured the apparent size of chondrules and chondrule fragments in two of the studied thin sections and determined the apparent thickness of their fine-grained rims. For these measurements SEM-BSE images were used and the software “Measure” from DatInf GmbH in Tübingen was applied. The apparent diameter of chondrules and fragments was obtained by measuring the area of the cut face and corresponds to the diameter of an equi-sized circle. The apparent thickness of a fine-grained rim was determined by measuring the areas of both, the cut faces of the entire object (chondrule + rim) and that of the enclosed chondrule. For both cut faces the diameters of equi-sized circles were calculated, whereupon the apparent thickness was calculated as the difference between both diameters divided by 2.

## 3.3 Results

### 3.3.1 Textures and lithologies of Jbilet Winselwan

We studied five thin sections of JW (Table 3.1). Figure 3.1 displays the backscattered electron image of one of the larger sections. Jbilet Winselwan appears to be an impact breccia, consisting of two main lithologies: Lithology I is coarse-grained and most of its chondrules are surrounded by fine-grained rims. This lithology is equivalent to the lithic clasts of “primary accretionary rock”, described in Metzler et al. (1992). Lithology II has fewer chondrules, appears fine-grained and clastic and corresponds to the “fine-grained clastic matrix”, described in the above reference. These two lithologies are the typical

Table 3.1: Type and number of measurements obtained from the 5 thin sections of Jbilet Winselwan and from 1 Murchison thin section used in this study.

Section	Mapped chondrules	Bulk chondrule compositions	Chondrule size measurements	Matrix data points	Rim data points
M4 (2) P19398	4	2	-	~30	-
M4 (3) P19399	17	4	-	~30	-
M4 (4) P19400	9	1	-	~30	-
JW S1	6	6	207	~40	18
JW S2	15	12	301	~40	34
Murchison	-	-	-	29	-

lithologies of CM chondrites, and were observed in 12 out of 14 studied samples by Metzler et al. (1992).

In JW, the chondrule to matrix ratio of lithology I is ~45:55 and ~25:75 in lithology II. We observed rimmed chondrules in both lithologies, with significantly higher amounts in lithology I. This textural variety was previously only observed in the CM chondrites Murchison and Murray, while in most other CM chondrites rimmed chondrules were exclusively found in lithology I (Metzler et al., 1992).

Chondrule rims in both lithologies of JW often consist of two distinct layers: The outer layer is characterised by higher abundances of tochilinite-cronstedtite intergrowths (TCI) and sulphides. In addition, rims with distinct Fe-rich and Fe-poor compositions occur in lithology II (Fig. 3.1). Grain sizes are generally larger in the outer layer than in the inner

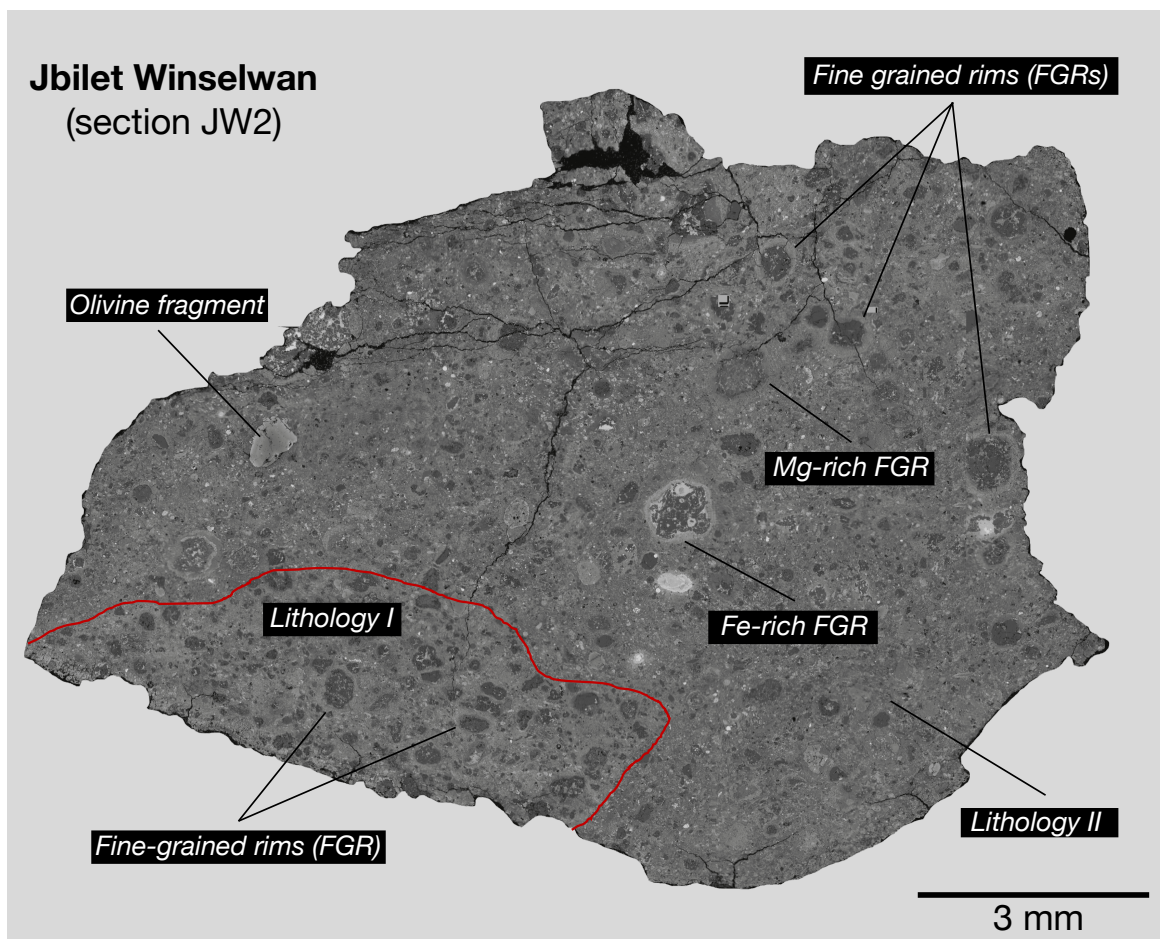


Figure 3.1: Back-scattered electron (BSE) image of Jbilet Winselwan (section JW2). The sample basically consists of two distinct lithologies, where lithology I is enclosed in the shape of lithic clasts in lithology II. Chondrules in both lithologies are commonly small and often surrounded by fine-grained rims. Lithology II contains chondrules with both Fe-rich and Fe-poor rims, as well as large olivine fragments.

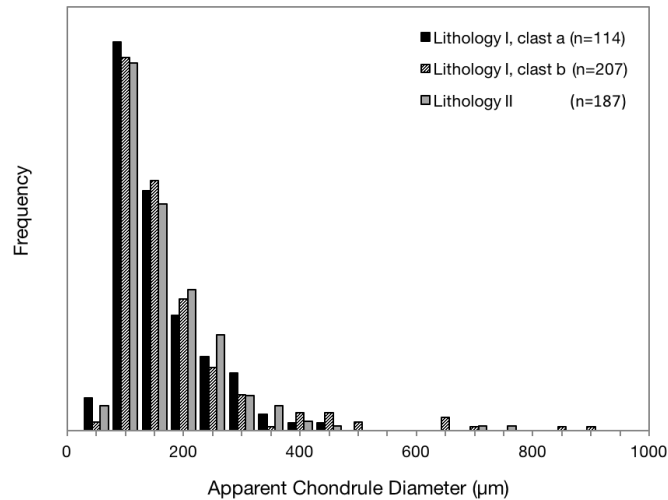


Figure 3.2: Frequency distributions of apparent chondrule diameters (chondrules and chondrule fragments) are about log normal distributed in both JW lithologies. Mean apparent chondrule diameters are about similar in both lithologies, with means of 136  $\mu\text{m}$  (clast a) and 157  $\mu\text{m}$  (clast b) in lithology I and 141  $\mu\text{m}$  in lithology II.

layer. These layered rims are typical of most CM chondrites and were described in detail in Metzler et al. (1992).

We measured the apparent sizes of 508 chondrules and chondrule fragments in two thin sections (321 in two clasts of lithology I and 187 in lithology II). This is, to our knowledge, the first frequency distribution of apparent chondrule sizes in CM chondrites (see Friedrich et al., 2014). The size-frequency distributions are about log-normal (Fig. 3.2), which is typical of chondritic meteorites (Friedrich et al., 2014 and references therein). Measured

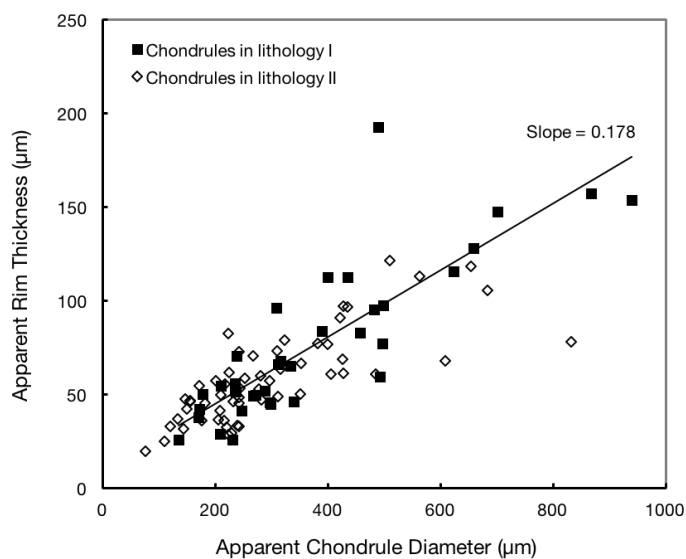


Figure 3.3: Apparent chondrule diameters and apparent rim thicknesses show linear correlations, with a slope of 0.178 in case of lithology I (filled symbols). The slope is somewhat smaller in lithology II (open symbols), which may indicate slightly different formation conditions for the rims in both lithologies.

apparent chondrule sizes in lithology I vary between 45 and 900  $\mu\text{m}$ , while chondrules studied in lithology II range from 45 to 730  $\mu\text{m}$ . The mean apparent chondrule sizes of chondrules in lithology I (clasts a and b) are 136 and 157  $\mu\text{m}$ , respectively, while the mean value of lithology II is 141  $\mu\text{m}$ . The amount of measurable chondrules and fragments is much lower in lithology II since in this case these objects are embedded in large amounts of fine-grained (clastic) material. The above values for apparent chondrule sizes are smaller than those measured by Rubin and Wasson (1986) in the Murray CM chondrite, probably because these authors did not include chondrule fragments.

For 93 out of the 508 chondrules, we further determined the apparent thickness of their fine-grained rims (36 in lithology I, and 57 in lithology II). The apparent thickness of these rims vary between 26 and 193  $\mu\text{m}$  in lithology I and between 20 and 121  $\mu\text{m}$  in lithology II. On average, the rims in lithology I are slightly thicker, with a mean apparent thickness of 76  $\mu\text{m}$ , compared to 59  $\mu\text{m}$  in lithology II. These data are displayed in Figure 3.3, where they are plotted against the apparent chondrule diameters. There is a striking positive correlation between the two parameters, which is evident for chondrules in both lithologies. This correlation is typical of CM chondrites and has been described in detail by Metzler et al. (1992). The slope for lithology I is 0.18 (Fig. 3.3), which is similar to the slopes determined for other CM chondrites (0.17-0.21; Metzler et al. 1992). The slope for chondrules in lithology II is slightly lower with a value of 0.12.

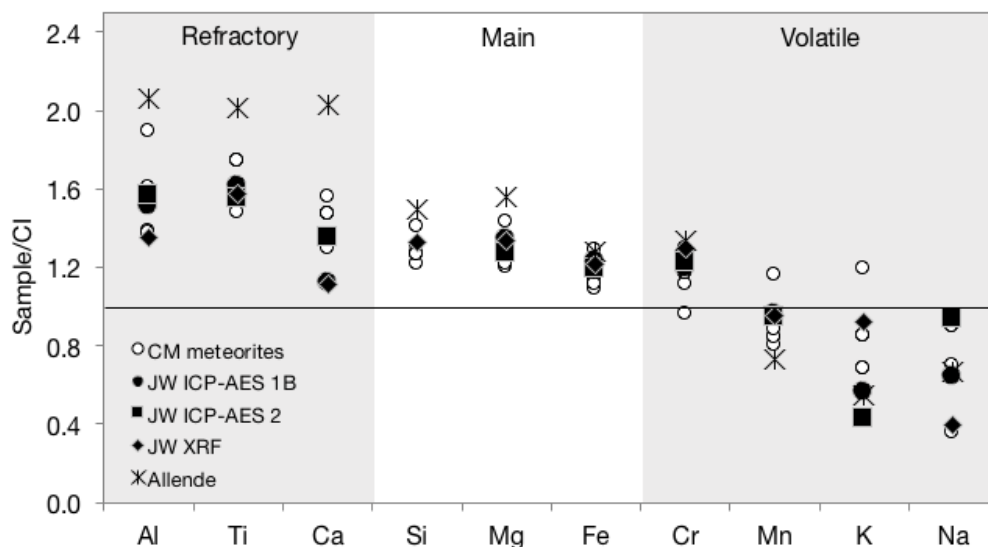


Figure 3.4: Bulk chemical composition (major and minor elements in the order of volatility) of the investigated samples of Jbilet Winselwan. These values are in good agreement with those for other CM chondrites (Jarosewich et al., 1990). Bulk values for Allende (CV3) are shown for comparison.

### 3.3.2 Bulk chondrite composition

The bulk chondrite composition of the major and minor elements in JW are plotted together with literature data for other CM chondrites, and normalised to CI in Figure 3.4 and listed in Supplementary Table 3.1. Data were measured in two different sample splits by ICP-AES (JW 1B and JW 2) and in another sample split that was derived from the same powder as JW 1B by XRF. There is a very good agreement between JW and other CM chondrites, especially for Fe, Mg and Si. The ICP-AES provides a Ca concentration in agreement with other CM chondrites, whereas the Ca concentration obtained with XRF is below this value. The JW data show some discrepancies for K and Na, but are overall similar to the literature values of other CM chondrites.

Figure 3.5 compares the JW trace element data from this study to the data from Göpel et al. (2015). See Supplementary Table 3.2 for data of minor and trace element abundances of the JW splits JW 1A, JW 1B and JW 2 measured by ICP-MS, together with JW bulk chondrite data from Göpel et al. (2015) and other bulk CM chondrites taken from the literature.

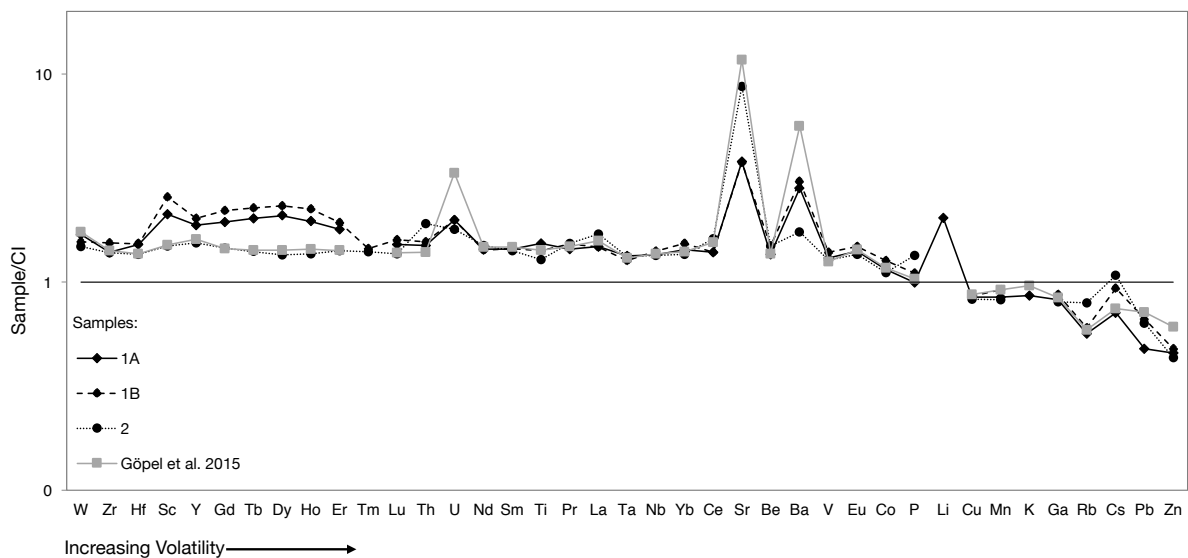


Figure 3.5: Bulk chemical composition (minor and trace elements) of the investigated Jbilet Winselwan samples. The HREE enrichment in one sample aliquot is most probably due to a refractory hibonite grain in this sample. The depletion of volatile elements is typical of CM chondrites. The enrichments in U, Sr, Ba and Li are the result of terrestrial weathering.

### 3.3.3 Petrography and elemental composition of chondrules

We studied 51 chondrules from JW in detail (Table 3.1). Figure 3.6 displays three typical JW chondrules with olivine in the core and low Ca-pyroxene at the rim. These two minerals are the main constituents of chondrules, with abundances between 67 and almost 100 vol.%. Minor constituents are mesostasis and high Ca-pyroxenes with up to 33 vol.%. All studied chondrules are porphyritic: 76% POP, 14% PP and 10% PO. About 92% are FeO-poor type I chondrules (cf. Jones et al. 2005, and references therein). In 71% of the studied chondrules

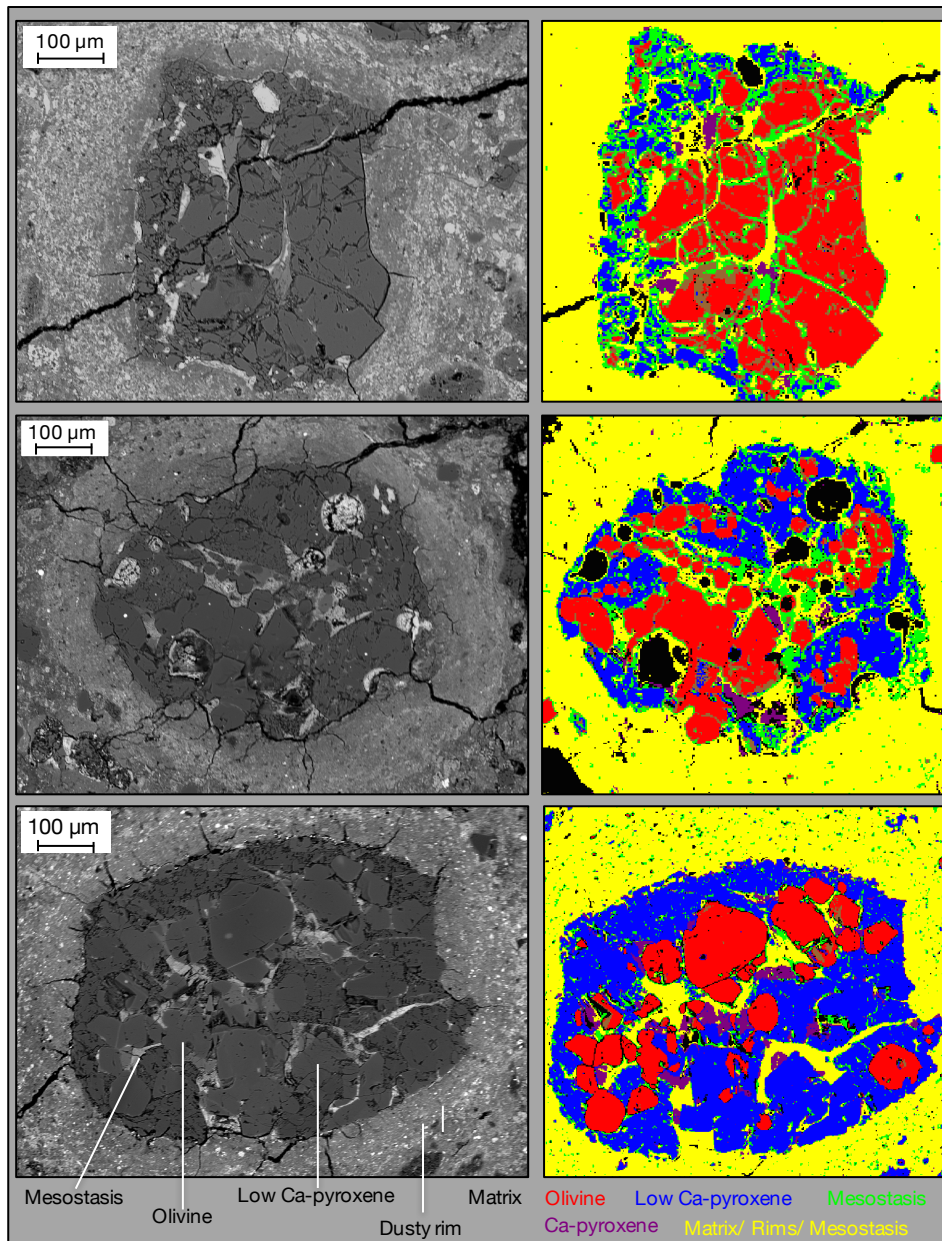


Figure 3.6: Three typical chondrules of Jbilet Winselwan: (a) PO, (b,c) POP chondrules. All chondrules are mineralogically-zoned, with olivine in the core and low Ca-pyroxene at the rim. This zonation is typical for chondrules in Jbilet Winselwan, and CC chondrules in general (Friend et al., 2016).



we found a mineralogical zonation with olivine in the core and low-Ca pyroxene at the rim. This structure of ubiquitously-zoned chondrules is typical of chondrules in all carbonaceous chondrites and was described in detail by Friend et al. (2016).

Chondrule olivine and pyroxene usually do not show any sign of alteration. In contrast, chondrule mesostases are devitrified and to various degrees decomposed to phyllosilicates. Metal grains are primarily located in chondrule olivines. We determined bulk elemental compositions of 26 chondrules (Supplementary Table 3.3). The mesostases of the remaining 25 were too altered to obtain reliable bulk chondrule compositions. Of the 26 studied chondrules, 25 are type I, and one is a type II chondrule. Olivines and pyroxenes in type I chondrules have low FeO contents of  $Fa_{1-6}$  and  $Fs_{1-10}$ , respectively. Olivine in the type II chondrule has an average composition of  $Fa_{35}$ . The elemental bulk chondrule compositions

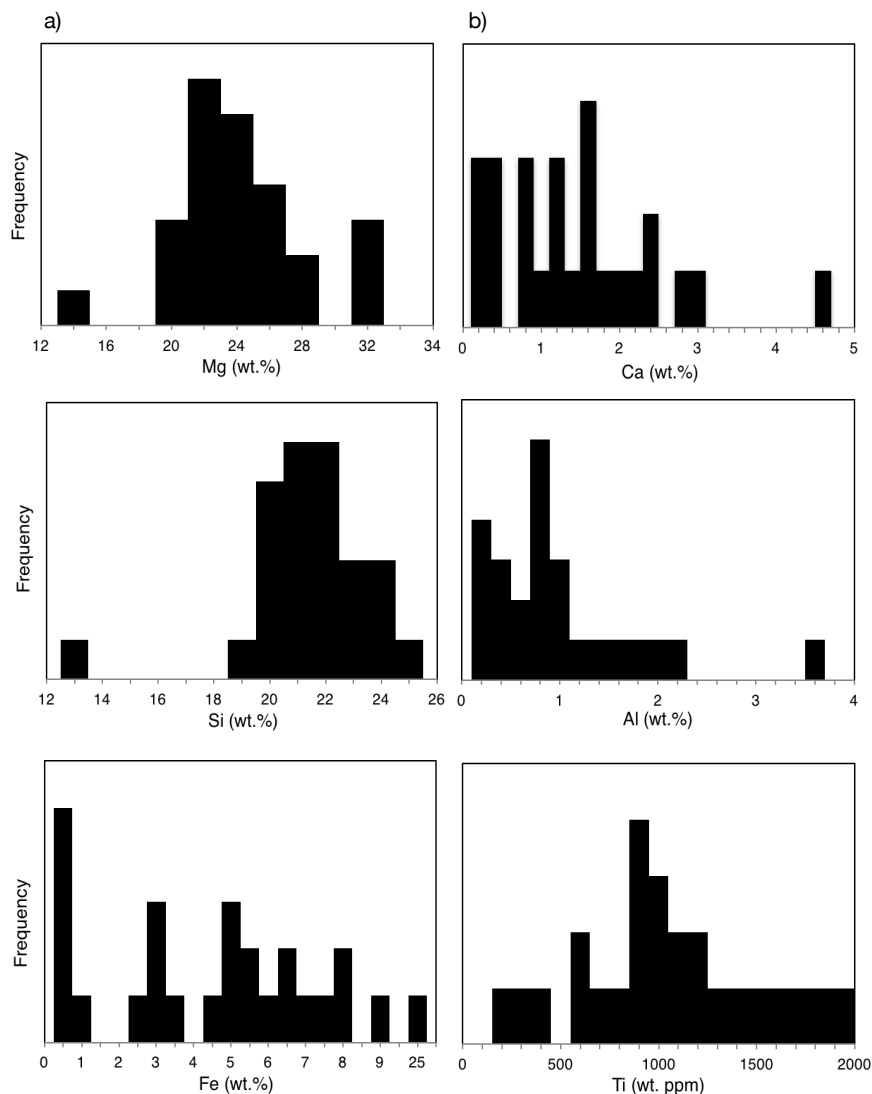


Figure 3.7: Element concentrations (Si, Mg, Al and Ti) of 26 bulk chondrules of Jbilet Winselwan.

Table 3.2: Mean composition and standard deviation of all 25 analysed type I chondrules.

	$\bar{\sigma}$	sd
Na	0.06	$\pm 0.05$
Fe	4.26	$\pm 2.68$
Al	0.91	$\pm 0.54$
Cr	0.35	$\pm 0.14$
Ti	0.10	$\pm 0.05$
Mg	24.93	$\pm 3.43$
Ni	0.07	$\pm 0.13$
Si	21.82	$\pm 1.47$
Mn	0.14	$\pm 0.08$
Ca	1.49	$\pm 1.01$

are generally highly variable. Table 3.2 lists the average contents for the measured elements and respective standard deviations that only include the type I chondrules. Figure 3.7a displays the bulk elemental variations of Mg, Si and Fe of the chondrules. The element with the most narrow range is Si, with a mean of  $21.8 \pm 1.5$  wt.%, not including the type II chondrule, which contains only 13.4 wt.% Si. Seventeen out of the 26 chondrules have Si contents between 21 and 23 wt.%. Chondrules with higher than mean Si

contents have lower olivine modal abundances. Magnesium contents spread across a larger range, from 20 to 32 wt.% Mg, with a mean of  $24.5 \pm 3.9$  wt.%. The type II chondrule contains 14.4 wt.% Mg. The bulk chondrule Mg concentrations are primarily controlled by the modal abundances of mesostasis in the chondrules. The bulk chondrule Fe contents have the largest range, between almost 0 and 9 wt.% in the type I chondrules, and a concentration of 24.6 wt.% in the type II chondrule.

Bulk chondrule concentrations of the refractory minor elements Ca, Al and Ti are displayed in Figure 7b. Calcium is mostly  $<2$  wt.%, but can be as high as 4.7 wt.% in one chondrule with abundant Ca-rich pyroxene. The mean Al content in the FeO-poor chondrules ranges from 0.2 to 2.1 wt.%, and is 3.5 wt.% in the type II chondrule. Bulk chondrule Al concentrations are controlled by mesostasis modal abundances. The bulk chondrule Ti concentrations range from 200 up to 2000 wt.-ppm, with a peak around 1000 wt.-ppm.

Figure 3.8 compares the Ti contents in all phases of the 26 studied chondrules. Titanium concentrations are low in olivines ( $< 500$  wt.-ppm), intermediate in low Ca-pyroxenes as well as in mesostasis (250 to 7000 wt.-ppm), and high in Ca-rich pyroxenes (0.1 to 1 wt.%).

### 3.3.4 Petrography and chemical composition of matrix and fine-grained chondrule rims

Matrix grain sizes are highly variable, ranging from sub- $\mu\text{m}$  to about several  $\mu\text{m}$ . Olivine and pyroxene mineral grains, chondrule fragments, as well as tochilinite-cronstedtite

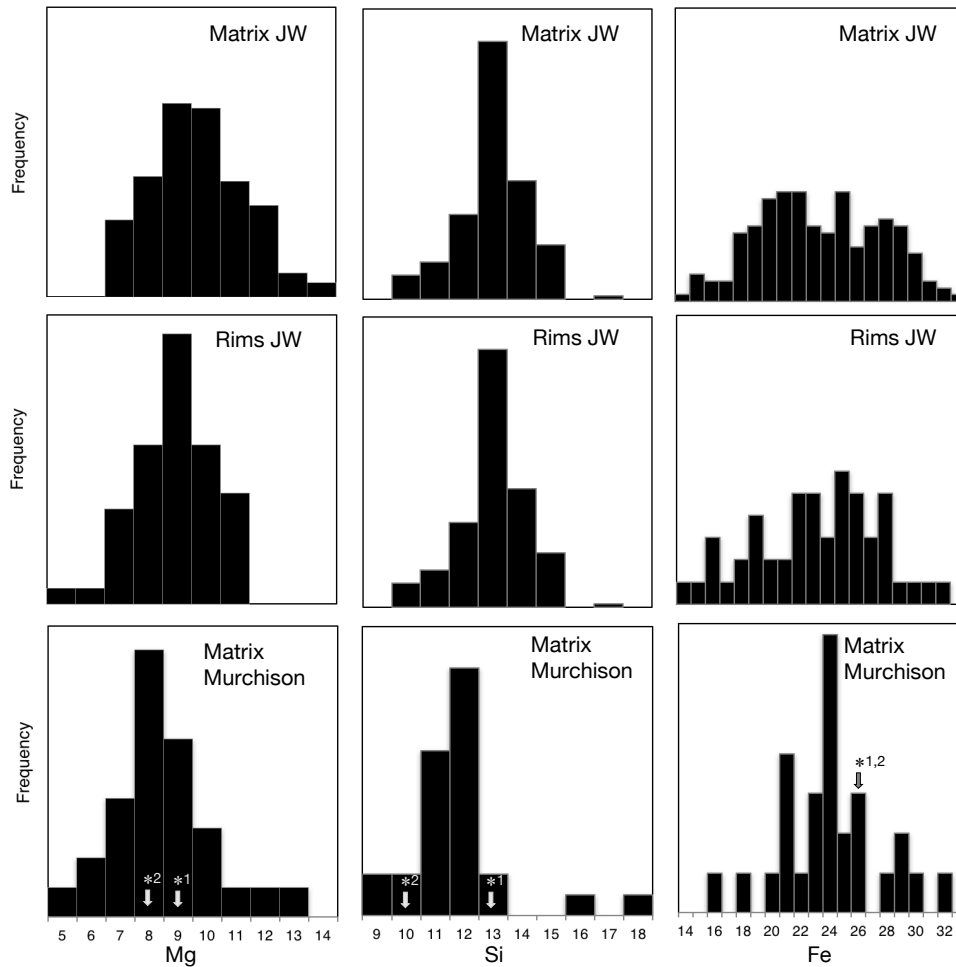


Figure 3.8: Comparison of bulk element compositions between matrix and chondrule rims in Jbilet Winselwan and Murchison matrix. The concentration of Mg, Si and Fe are similar in these three components, although Mg and Si appear somewhat lower in Murchison matrix. Light grey arrows indicate literature data for Murchison matrix (\*<sup>1</sup>Zolensky et al., 1993; \*<sup>2</sup>McSween and Richardson, 1977).

intergrowths (TCI) and sulphides are present in the matrix. Chondrule rims are generally finer grained than matrix. Chondrule rims contain less sulphides and Fe-rich phases than matrix. Also chondrule fragments and larger silicate minerals are markedly rarer in chondrule rims than in matrix.

We made 171 element analyses of interchondrule matrix and 52 in the fine-grained rims around chondrules. In addition, 29 matrix analyses in Murchison were carried out to verify our technique. Table 3.3 lists the mean values and standard deviations of all JW matrix and fine-grained chondrule rim analyses, alongside with respective data for Murchison matrix analyses. The histograms in Figure 3.9 compare the compositional variations of the main elements in the matrix of JW, Murchison matrix and fine-grained rims around JW chondrules. The Mg content in JW matrix ranges from 7 to 14 wt.%. This is slightly higher than the rims around chondrules, which range from 5 to 11 wt.%. Murchison matrix spans the widest range from 5 to up to 13 wt.%. This range is similar to the JW matrix composition,

Table 3.3: Mean compositions and standard deviations of matrix and fine-grained chondrule rims in Jbilet Winselwan and matrix in Murchison.

	Matrix JW		Fine-grained rims JW		Matrix Murchison	
	$\bar{\sigma}$	sd	$\bar{\sigma}$		$\bar{\sigma}$	
Si	13.00	$\pm 1.14$	12.44	$\pm 1.45$	11.78	$\pm 1.66$
Ti	0.05	$\pm 0.02$	0.05	$\pm 0.02$	0.03	$\pm 0.01$
Al	1.53	$\pm 0.37$	2.06	$\pm 0.49$	1.20	$\pm 0.18$
Cr	0.27	$\pm 0.16$	0.26	$\pm 0.06$	0.21	$\pm 0.08$
Mg	9.72	$\pm 1.64$	8.85	$\pm 1.27$	8.47	$\pm 1.66$
Fe	23.42	$\pm 4.13$	23.18	$\pm 4.26$	24.03	$\pm 3.39$
Ni	1.42	$\pm 0.53$	1.54	$\pm 0.30$	1.32	$\pm 0.46$
Mn	0.18	$\pm 0.05$	0.18	$\pm 0.02$	0.17	$\pm 0.06$
Ca	1.09	$\pm 0.38$	1.39	$\pm 0.49$	0.54	$\pm 0.30$
Na	0.39	$\pm 0.14$	0.32	$\pm 0.10$	0.68	$\pm 0.17$

though the peaks are slightly shifted. Silicon contents are indistinguishable in matrix and fine-grained rims of JW, which both have a peak at 13 wt.%. Murchison matrix has slightly lower Si contents with a peak at 12 wt.%. Iron is more homogeneously distributed compared to Mg and Si. In JW, the Fe in matrix and chondrule rims ranges from 14 to 32 wt.%.

### 3.4 Discussion

#### 3.4.1 Jbilet Winselwan bulk composition

The membership of JW to the CM chondrite class is evident from its bulk major, minor and trace element composition. In Figure 3.4, the composition of JW is compared to other CM chondrites analysed by Jarosewich (1990). For comparison, data from the Allende meteorite, representative of CV chondrites, are plotted (Jarosewich, 1990). Allende and other CVs are higher in refractory elements, have different Mg/Fe ratios and lower concentrations of moderately volatile elements, such as Mn (Fig. 3.4). Alkalis are notoriously variable in CM chondrites and cannot be used for classification purposes (e.g. Fuchs et al., 1973). In Fig. 3.10, we show the CI-normalised REE pattern of the various JW samples analysed in this study. The elevated rare earth element abundances from Gd to Er in samples 1A and 1B, both derived from the same powder, are unusual. To our knowledge such a pattern was never observed in a bulk chondrite. It is not a volatility-related pattern, such as the well known group II patterns in fine-grained Allende inclusions (Mason and Taylor, 1982). These

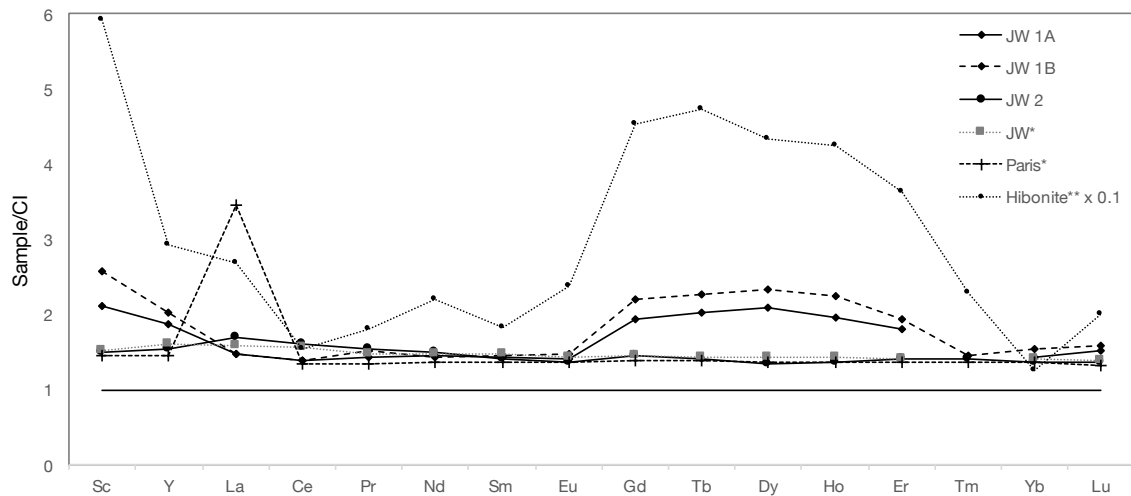


Figure 3.9: Abundances of REE in the investigated samples of Jbilet Winselwan. Samples 1A and 1B, which are both derived from the same powder, are enriched in certain HREEs, showing a pattern that resembles hibonite data (\*\*Fahey et al., 1994). Sample 2 (derived from another powder) as well as literature data for Jbilet Winselwan and the CM chondrite Paris (\*Göpel et al., 2015) have flat REE patterns (except Paris for La).

patterns have high Tm and low Er as well as enrichments in light REE. There is also no smooth dependence of abundances on ionic radius. The closest match to the REE patterns that we could find in the literature are REE patterns of hibonite ( $\text{CaAl}_{12}\text{O}_{19}$ ), a highly Al-rich refractory mineral, second in the canonical condensation sequence after corundum. In contrast to CV chondrites, CM meteorites contain fairly high concentrations of hibonite (Liu et al., 2009). There are large variations in the composition of hibonites, in part related to their origin. Some hibonites may be condensates, whereas others may have crystallised from Al-rich melts (Simon et al., 1996, 1997). The REE pattern of a hibonite grain analysed by Fahey et al. (1994) fits well to the REE pattern found in two of the bulk samples of JW (Fig. 10). It shows basically the same relative abundances of REE as the two bulk samples with the unusual REE pattern. This is suggestive of 'contamination' of the bulk samples with hibonite. Since absolute REE concentrations and REE patterns in hibonites of CM meteorites are quite variable (Simon et al., 1997), it is not possible to make sensible mass balance calculations. There exists simply no single, well defined hibonite component in these meteorites. This applies also to minor elements in hibonite, such as Ti and Al. They may well contribute to the bulk, but their contents in e.g. Murchison are extremely variable (Simon et al., 1997). Nevertheless, the similarity of the REE pattern of some hibonites with the bulk REE patterns of two bulk JW samples suggests that the unusual REE pattern is produced by an overabundance of hibonite grains in the analysed sample.

Figure 3.5 shows the trace element patterns of the JW samples analysed in this study. The elements are arranged in order of decreasing 50 % condensation temperatures (Lodders et al., 2009). Refractory elements, including the siderophile W, have more or less uniform enrichment factors somewhat above the CI abundance level and lower than CV chondrites (see Fig. 3.5). This smooth depletion trend for moderately volatile elements, from Cu to Zn is characteristic of CM chondrites (Palme et al., 1988).

The enrichment of the mobile elements U, Sr, Ba, Li and Pb in the bulk JW chondrite is typical of weathering of the meteorite while residing on the desert surface (Barrat et al. 2003; Al-Kathiri et al., 2005; Saunier et al., 2010; Hezel et al., 2011,2015) .

#### **3.4.2 Aqueous alteration of JW**

The degree of aqueous alteration that JW experienced seems to be variable (e.g. Russell et al, 2014; Kiku et al., 2014; Pernet-Fischer et al., 2014, Grady et al., 2014). Russell et al. (2014) argue that most parts of JW experienced only mild aqueous alteration. Their conclusion is based on the occurrence of melilite in CAIs – which only survives in the least-altered CM meteorites (Lee & Lindgren, 2016) – as well as intact metal grains in the matrix. This is in agreement with our observations of commonly well-preserved mafic minerals in chondrules, where only mesostases are often transformed to phyllosilicates. The alteration of chondrule mesostases is typical of all CM chondrites, and is even present in the least altered CM chondrite, Paris (Hewins et al., 2014). According to Browning et al. (1996), a further indication of a low alteration degree are isolated silicate minerals in CM chondrite matrices. We observed plenty of such isolated olivine and pyroxene grains in the JW matrix. Hence, we propose that significant parts of JW suffered only mild aqueous alteration.

Some authors argue that CM chondrite material was in part aqueously altered in the solar nebular before parent body accretion (e.g. Metzler et al.,1992; Ciesla et al., 2003; Howard et al., 2011). Pernet-Fisher et al. (2014) support this view and argue that the highly variable degrees of aqueous alteration seen in JW chondrules is best explained by pre-accretionary alteration. Our observations support this view. The aqueous alteration of spatially closely associated chondrules within both lithologies show in some cases different degrees of alteration, which is best explained by variable degrees of pre-accretionary alteration.

We further observed TCIs that are surrounded by fine-grained rims. TCIs are products of aqueous alteration, while the rims seemingly accreted free floating anhydrous objects or

grains in the protoplanetary disk. Hence, the rimmed TCIs must have formed by aqueous alteration of metal or sulphide before rim formation and parent body accretion. For a more detailed discussion see Bischoff (1998).

#### **3.4.3 Fine-grained chondrule rims**

Fine-grained rims around CM chondrules have been known for a long time (e.g. Fuchs et al. 1973; Bunch and Chang 1984, Metzler et al. 1992). Many authors advocate formation scenarios in which the rims formed by sticking of fine-grained dust to chondrule surfaces prior to chondrite accretion (e.g. Metzler et al., 1992; Nakamura et al., 1999; Cuzzi, 2004; Ormel et al., 2008; Hanna and Ketchman, 2016). Nevertheless, there is still a dispute on this in the literature. Some authors propose a formation of the chondrule rims by impact events on the parent body (e.g. Trigo-Rodriguez et al., 2005), and based on the investigation of LAP 02342 (CR2), Wasson and Rubin (2014) simply doubt in principle the existence of the fine-grained chondrule rims. They state the “absence of definitive evidence of their presence in CM and other chondrites”.

Our investigation of JW provides further clear evidence that most chondrules in the lithology I and many chondrules in the lithology II are surrounded by well-defined, fine-grained rims. This finding is equivalent to the observations in the two CM chondrites Murchison and Murray, where rimmed chondrules also occur in both lithologies (Metzler et al. 1992). This similarity of JW chondrules to Murchison and Murray may indicate rim porosities around JW chondrules of ~10 vol.% (Beitz et al., 2013). Furthermore, the observed positive linear correlation between the apparent chondrule diameter and apparent rim thickness found here (Fig. 3.3) was noticed earlier in other CM chondrites (Metzler et al. 1992) and was recently confirmed by 3D-measurements using micro x-ray computed tomography (Hanna and Ketchman, 2016). The slope of this correlation in lithology I is within the range of CM literature values. However, the slope for rimmed chondrules in lithology II (Fig. 3) is somewhat smaller than the slope for rimmed chondrules in lithology I. This reflects the tendency to thinner rims in lithology II and may indicate additional processes that were active during the formation of the fine-grained rims.

### 3.4.4 Complementarities

#### 3.4.4.1 Complementary relationships of the major elements Si, Mg, Fe

Plates a & b in Figure 3.11 display element plots of Si vs. Mg and Fe vs. Mg of bulk JW and its components, as well as of Murchison matrix that were all measured in this study. Literature data of bulk CI and CM chondrites as well as bulk chondrule data of El-Quss Abu Said (CM) are included for comparison.

JW has a bulk Si/Mg ratio of 1.12, similar to other CM chondrites and indistinguishable from the CI chondritic Si/Mg ratio of 1.12. All JW chondrules have sub-chondritic Si/Mg ratios with a mean of 0.88. Matrix as well as fine-grained chondrule rims have super-chondritic Si/Mg ratios with means of 1.34 and 1.41, respectively. Hence, matrix and fine-grained chondrule rims have virtually the same Si/Mg. The Murchison matrix plots in exactly the same field as the JW matrix and fine-grained rims, and has a similar super-chondritic mean Si/Mg of 1.39. The similarity in chemical composition of fine-grained rims and interchondrule matrix is typical of carbonaceous chondrites (e.g., Abreu and Brearley, 2010). The bulk chondrule data plot along a trend between forsterite and enstatite in the Si-Mg space (Fig. 3.11a). The mineralogical zonation of most JW chondrules with olivine in the core and low-Ca pyroxene at the border is the result of the reaction of olivine with a Si-rich gas to form low-Ca pyroxene (Friend et al., 2016 and references therein). Chondrule precursors are initially olivine-rich objects and their bulk composition develops during reaction with nebular gas along the olivine – pyroxene joint towards a more Si- & pyroxene-rich composition. A similar mechanism has been found by Hezel et al. (2006) for ordinary chondrite chondrules. Thus, the olivine fraction of chondrules before reaction of chondrule melts with the ambient gas was higher than presently observed, leading to even lower Si/Mg ratios in chondrule precursors and thus amplifying the difference in Si/Mg ratio of chondrules and matrix. The gaseous SiO and Mg that are not locked up in chondrules condense later as constituents of the fine-grained matrix. The bulk CI chondritic Si/Mg ratio is unaffected by this process. This is characteristic of the common reservoir of chondrules and matrix.



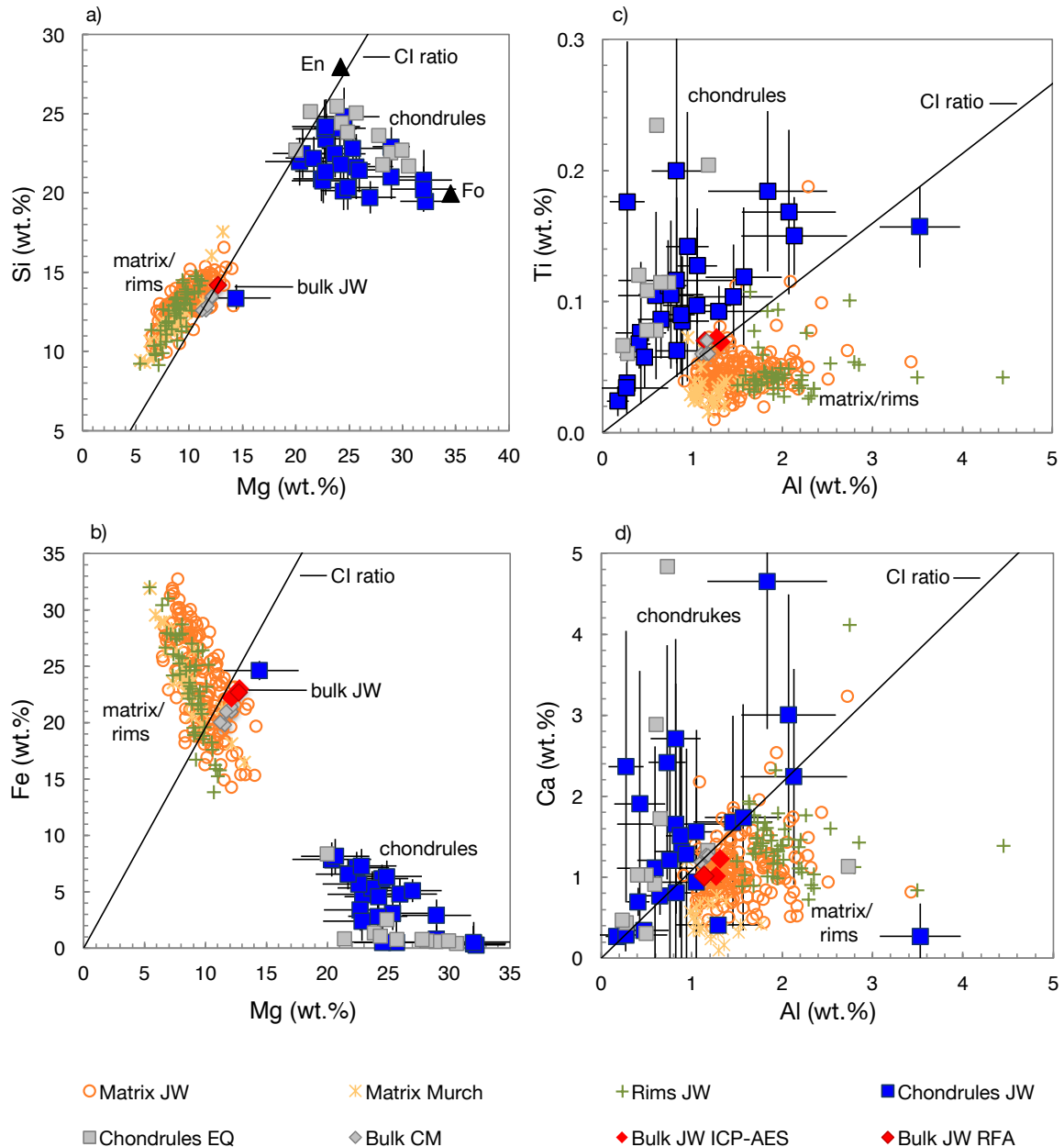


Figure 3.10: Chemical variation diagrams including data from bulk Jbilet Winselwan, 26 bulk chondrules, matrix and fine-grained rims around chondrules, as well as Murchison matrix. a) Mg vs. Si concentrations. En: enstatite composition, Fo: forsterite composition; b) Mg vs. Fe concentrations; c) Ti vs. Al concentrations; d) Ca vs. Al concentrations. For comparison the slope with CI ratio, as well as bulk CM data, bulk chondrules from El-Quss Abu Said (CM), and matrix data of Murchison are added (Wolf and Palme, 2001; Hezel and Palme, 2010; Palme et al., 2014). Chondrules and matrix of Jbilet Winselwan are complementary with respect to Si/Mg, Fe/Mg, Ti/Al and Ti/Ca, while the bulk has chondritic or very close to chondritic ratios.

All JW chondrules have strongly sub-chondritic Fe/Mg ratios (Fig. 3.11b). Even the type II chondrule plots below the CI-chondritic Fe/Mg ratio. We did not include opaque phases in our bulk chondrule analyses, which leads to lower Fe/Mg ratios in chondrules than actually measured. However, opaque modal abundances in CM chondrite chondrules are in most cases below 1 vol.%, thereby increasing the bulk chondrule Fe concentrations of about

5±5 wt.% to rarely more than 7±5 wt.%. Hence, bulk chondrules would still have strongly sub-chondritic Fe/Mg ratios. The matrices of JW and Murchison, as well as the fine-grained rims around JW chondrules all define a single field in the Fe-Mg space, and have super-chondritic Fe/Mg ratios. The mean Fe/Mg of JW matrix is 2.41, Murchison matrix has a ratio of 2.84, and the Fe/Mg ratio of fine-grained chondrule rims in JW is 2.62. These values are all well above the CI-chondritic ratio of 1.96, and the three JW bulk chondrite Fe/Mg ratios of 1.80, 1.82 and 1.83, determined in this study.

Hezel and Palme (2010) and Palme et al. (2015) discuss at length why neither the Si/Mg, nor the Fe/Mg complementarity can be the result of parent body alteration. Anyway, Tomeoka and Buseck (1985) observed that the formation of TCIs from olivine and pyroxene minerals decrease the Fe/Si ratio and increase the Mg/Si ratio in the residual matrix with progressive aqueous alteration. We did not include TCIs which have up to 70 wt.% FeO, but only <10 wt.% Mg (Pignatelli et al., 2016), and occur as larger grains in the matrix (e.g. McSween, 1987) in our matrix analyses. If we embraced TCIs in our matrix measurements, the Fe/Mg ratio would be even more elevated. Hence, aqueous alteration would bring the Fe/Mg and Si/Mg ratios of chondrules and matrix closer together and not further apart – a mechanism opposite to what is required to establish the observed complementary pattern between chondrules and matrix. This reasoning is supported by results from Ebel et al. (2016), who noticed that the extent of Mg/Si complementarities in CO chondrites decrease with increasing petrologic grade.

#### 3.4.4.2 *Complementary relationships of the refractory elements Ca, Al, Ti*

Plates c & d in Fig. 3.11 display element plots of Ti vs. Al and Ca vs. Al for the same samples as in plates a & b. Almost all JW chondrules have super-chondritic Ti/Al ratios. The matrices of JW and Murchison, as well as the fine-grained rims around JW chondrules have complementary, sub-chondritic Ti/Al ratios. The criteria for complementarity is fulfilled, as the bulk JW Ti/Al ratio from the powder with a typical CM REE pattern is 0.053, identical to the CI chondritic Ti/Al ratio of 0.053. The two samples with elevated HREE element patterns have slightly higher than CI chondritic Ti/Al ratios of 0.062 and 0.057, in agreement with the addition of small hibonite grains.

Almost about half of the JW chondrules have super-chondritic Ca/Al ratios, while the other half has about CI chondritic Ca/Al ratios (Fig. 3.11d). Only the single type II chondrule has an extremely low Ca/Al ratio. Neglecting this type II chondrule, the mean Ca/Al ratio of

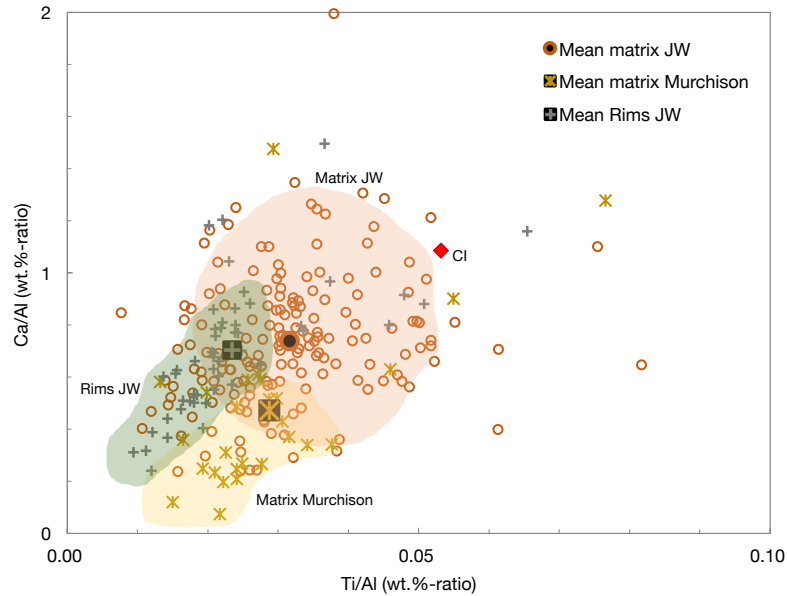


Figure 3.11: Mean refractory element compositions of Jbilet Winselwan matrix, fine-grained chondrule rims in Jbilet Winselwan and Murchison matrix. Each data set comprises a distinct field in the diagram. Mean values of Jbilet Winselwan matrix have the highest Ca/Al and Ti/Al ratios. The values for bulk CI chondrites are shown for comparison.

the chondrules is 1.64. The matrices in JW and Murchison, as well as the fine-grained rims around JW chondrules all have sub-chondritic mean Ca/Al-ratios of 0.71 (JW matrix), 0.68 (fine-grained rims around JW chondrules), and 0.45 (Murchison matrix). The bulk JW Ca/Al ratio is slightly sub-chondritic due to lower than typical Ca concentrations in CM chondrites – that otherwise plot exactly on the CI chondritic ratio line (cf. Fig. 3.11d). It is yet unclear what caused the lower Ca in JW. As CM chondrites typically have CI chondritic Ca/Al ratios, and as the JW bulk Ca/Al ratio is only slightly off the respective CI ratio, it seems reasonable to assume that Ca/Al ratios in chondrules and matrix of JW are complementary.

It appears, there are slight, but systematic differences in the Ca/Al ratios among fine-grained chondrule rims and matrix (Figs. 3.11 & 3.12): (i) JW matrix has the highest Ca/Al and Ti/Al ratios, while (ii) fine-grained rims around JW chondrules have slightly lower Ca/Al and noticeable lower Ti/Al ratios as JW matrix. (iii) Murchison matrix has the lowest Ca/Al ratio and the Ti/Al ratio is intermediate to JW matrix and fine-grained chondrule rims. Hence the ratios for Ti/Al and for Ca/Al of the fine-grained chondrule rims are even more divergent from the CI chondritic ratio than in the matrix of JW (Fig. 3.11). This observation also seems to be true for the Si/Mg and Fe/Mg ratios, which are both slightly higher in the chondrule rims, than in the matrix. We propose, these differences are due to the lower abundances of olivine and pyroxene grains and chondrule fragments in the fine-grained chondrule rims compared to the matrix. The fine-grained rims probably accreted around

chondrules before the matrix formed. Hence, the fine-grained chondrule rims represent the first matrix material.

According to Hidaka et al. (2015) there seems to exist some redistribution of the alkaline elements Rb and Cs on the microscale in chondrules of the CM2 chondrite Samaya caused by intense aqueous alteration within chondrule minerals. However, the elements considered in this study are not likely to be effected by those replacements. Furthermore, these redistributions are limited to the set of minerals within a chondrule and hence would not affect the chondrule bulk composition.

### 3.5 Conclusions

Jbilet Winselwan is a breccia consisting of two lithologies with different chondrule/matrix ratios, but similar size distributions of chondrules and chondrule fragments. Chondrules in both lithologies accreted fine-grained rims, probably while freely floating in the protoplanetary disk. The rims resemble those in Murchison and other CM chondrites (Metzler et al., 1992). The extent of aqueous alteration in JW is comparatively small, and JW is probably one of the least altered CM chondrites. Some aqueous alteration may have occurred in the nebular disk before accretion of the meteorite.

The bulk composition of JW is typical of CM meteorites. Unusual REE patterns in two bulk samples may reflect non-representative proportions of hibonite crystals, which are common in CM meteorites.

Chondrules are often mineralogically zoned, with olivine in the core and low-Ca pyroxene at the rim. This zonation is best explained by an open system exchange reaction of chondrule olivine with a Si-rich gas that formed during fractional condensation (cf. Friend et al., 2016). This indicates that Si/Mg of chondrule precursors (dust aggregates before melting) were even lower in Si/Mg than presently observed.

Bulk JW has CI chondritic Si/Mg, Fe/Mg, Al/Ti and close to CI chondritic Ca/Al ratios. Chondrules have low Si/Mg, and Fe/Mg ratios complementary to high ratios in matrix, typical of most carbonaceous chondrites (Hezel and Palme, 2010; Palme et al., 2015). The formation of Fe-poor refractory olivine and subsequent incorporation into chondrule precursor aggregates is particularly prominent in CM chondrites. Refractory element ratios such as Al/Ti and Ca/Al are also complementary between chondrules and matrix. Preferred

partitioning of Ti into chondrules is frequently observed in carbonaceous chondrites (e.g., Palme et al., 2015). It may indicate preference of perovskite for chondrule precursor aggregates. The fractionation of these two refractory elements requires high temperature processes. Variable and complementary Ca/Al ratios between chondrules and matrix is also observed in several carbonaceous chondrites (Hezel and Palme, 2008). These relationships require the formation of chondrules and matrix from a single reservoir. Arbitrary mixing of chondrules and matrix from different reservoirs will never produce a chondritic bulk meteorite. This excludes an entire set of chondrule formation models, as outlined in some detail by Hezel and Palme, (2010) and Palme et al. (2015).

### **Acknowledgements**

We thank the Natural History Museum in London for the loan of three thin sections and Tadeusz Przylibski of the Wroclaw University of Technology for the loan of two thin sections of Jbilet Winselwan. P. F. is grateful for a fellowship grant No. GSGS-2016B-F01 from the Graduate School of Geosciences (GSGS) of the University of Cologne.

## References

- Abreau N. M., and Brearley A. J. 2010. Early solar system processes recorded in the matrices of two highly pristine CR3 carbonaceous chondrites, MET 00426 and QUE 99177. *Geochimica et Cosmochimica Acta* 74: 1146-1171.
- Al-Kathiri A., Hofmann B. A., Jull A. J. T., and Gnos E. 2005. Weathering of meteorites from Oman: Correlation of chemical and mineralogical weathering proxies with <sup>14</sup>C terrestrial ages and the influence of soil chemistry. *Meteoritics & Planetary Science* 40:1215–1239.
- Asphaug E., Jutzi M., and Movshovitz N. 2011. Chondrule formation during planetesimal accretion. *Earth and Planetary Science Letters* 308: 369-379.
- Barrat J.-A., Jambon A., Bohn M., Blichert-Toft J., Sautter V., Göpel C., Gillet P., Boudouma O. and Keller F. (2003). Petrology and geochemistry of the unbrecciated chondrite Northwest Africa 1240 (NWA 1240): an HED parent body impact melt. *Geochimica et Cosmochimica Acta* 67: 3959-3970.
- Barrat J.-A., Zanda B., Moynier F., Bollinger C., Liozou C., and Bayon G. 2012. Geochemistry of CI chondrites: Major and trace elements, and CU and Zn isotopes. *Geochimica et Cosmochimica Acta* 83: 79-92.
- Barrat J.-A., Jambon A., Ferrière L., Bollinger C., Langlade J. A., Liorzou C., Boudouma O., and Fialin M. 2014. No Martian soil component in shergottite meteorites. *Geochimica et Cosmochimica Acta* 125: 23-33.
- Barrat J.-A., Dauphas N., Gillet P., Bollinger C., Etoubleau J., Bischoff A., and Yamaguchi A. 2016. Evidence from Tm anomalies for non-CI refractory lithophile element proportions in terrestrial planets and achondrites. *Geochimica et Cosmochimica Acta* 176: 1-17.
- Becker M., Hebel D. C., Schulz, T., Elfers B. M., and Münker C. 2015. Formation timescales of CV chondrites from component specific Hf-W systematics. *Earth and Planetary Science Letters* 432: 472-482.
- Beitz E., Blum J., Mathieu R., Pack A., and Hezel D. C. (2013) Experimental investigation of the nebular formation of chondrule rims and the formation of chondrite parent bodies. *Geochimica et Cosmochimica Acta* 116:41-51.
- Berlin J., Jones R. H., and Brearley A. J. 2006. Determining the bulk chemical composition of chondrules by electron microprobe: a comparison of different approaches (abstract). *37<sup>th</sup> Lunar and Planetary Science Conference*: 2370.

- Bischoff A. 1998. Aqueous alteration of carbonaceous chondrites: evidence for pre-accretionary alteration. A review. *Meteoritics and Planetary Science* 33: 1113–1122.
- Bland P. A., Alard O., Benelux G. K., Kearsley A. T., Menzies O. N., Watt L. E., and Rogers N. W. 2005. Volatile fractionation in the early solar system and chondrule/matrix complementarity. *Proceeding of the National Academy of Sciences* 102: 13755-13760.
- Browning L. B., McSween H. Y. Jr., and Zolenski M. E. 1996. Correlated alteration effects in CM carbonaceous chondrites. *Geochimica et Cosmochimica Acta* 60: 2621-2633.
- Budde G., Kleine T., Kruijjer T. S., Burkhardt C., and Metzler, K., 2016. Tungsten isotopic constraints on the age and origin of chondrules. *Proceeding of the National Academy of Science USA* 11: 2886-2891.
- Bunch T. E., and Chang S. 1984. CAI rims and CM2 dust balls: Products of gas-grain interactions, mass transport, grain aggregation and accretion in the nebular?(abstract). *15<sup>th</sup> Lunar and Planetary Science Conference*: 100-101.
- Cuzzi J. N. 2004. Blowing in the wind: III. Accretion of dust rims by chondrule-sized particles in a turbulent protoplanetary nebula. *Icarus* 168: 484-497.
- Ciesla F. J., Lauretta D. S., Cohen B. A., and Hood L. L. 2003. A nebular origin for chondritic fine-grained phyllosilicates. *Science* 299: 549-552.
- Ebel D. S., Brunner C., Konrad K., Leftwich K., Erb I., Lu M., Rodriguez H., Crapster-Pregont E., Friedrich J. M., and Weisberg M. K. 2016. Abundance, major element composition and size of components and matrix in CV, CO and Acfer 094 chondrites. *Geochimimica et Cosmochimica Acta* 172: 322-356.
- Fahey A. J., Zinner E., Kurat G., and Kracher A. 1994. Hibonite-hercynite inclusion HH-1 from the Lancé (CO3) meteorite: The history of an ultrarefractory CAI. *Geochimica et Cosmochimica Acta* 58: 4779-4793.
- Ford R. L., and Brearley A. J. 2008. Element exchange between matrix and CAIs in the Allende meteorite (abstract). *39<sup>th</sup> Lunar and Planetary Science Conference*: 2399.
- Friedrich J. M., Weisberg M. K., Ebel D. S., Biltz A. E., Corbett B. M., Iotzov I. V., Khan W. S., and Wolman M. D. 2014. Chondrule size and related physical properties: A compilation and evaluation of current data across all meteorite groups. *Chemie der Erde* 75: 419-443.
- Friend P., Hezel D. C., and Mucerschi D. (2016). The conditions of chondrule formation, Part II: Open system. *Geochimica et Cosmochimica Acta* 173: 198-209.
- Fuchs L. H., Olsen E., and Jensen K. J. 1973. Mineralogy, mineral-chemistry and composition of the Murchison (C2) meteorite. *Smithsonian Contributions to the Earth*



*Sciences* 10: 1-39.

Göpel C., Birck J.-L., Alber G., Barrat J.-A., and Zanda B. 2015. Mn-Cr systematics in primitive meteorites: Insights from mineral separation and partial dissolution. *Geochimica et Cosmochimica Acta* 156: 1-24.

Grady M. M., Abernathy F. A. J., Verchovsky, A. B., King A. J., Schofield P. F., and Russel S.S. 2014. The Jbilet Winselwan carbonaceous chondrite 2. Light element geochemistry: Strengthening the link between CM and CO meteorites (abstract). *77<sup>th</sup> Annual Meteoritical Society Meeting*: 5377.

Grossman J. N., Rubin A. E., Nagahara H., and King E. A. 1988. Properties of chondrules. In *Meteorites and the Early Solar System*. Edited by Kerridge J. F., and Matthews M. S., University of Arizona Press: 619-659.

Hanna R. D. and Ketcham R. A. 2016. 3D morphology of fine-grained rims in CM Murchison (abstract). *47<sup>th</sup> Lunar and Planetary Science Conference*: 2185.

Hewins R. H., Bourot-Denise M., Zanda B., Leroux H., Barrat J.-A., Humayun M., Göpel C., Greenwood R. C., Franco I. A. Pont S., Lorand J. P., Courède C., Gattacceca J., Rochelle P., Kuga M., Marrocchi Y., and Marty B. 2014. The Paris meteorite, the least altered CM chondrite so far. *Geochimica et Cosmochimica Acta* 124: 190-222.

Hezel D. C. 2007. A model for calculating the errors of 2D bulk analysis relative to the true 3D bulk composition of an object, with application to chondrules. *Computers & geosciences* 33: 1162-1175.

Hezel D. C. 2010. A mathematica code to produce phase maps from two element maps. *Computers & Geosciences* 36: 1097-1099.

Hezel D. C., and Kießwetter R. 2010. Quantifying the error of 2D bulk chondrule analyses using a computer model to simulate chondrules (SIMCHON). *Meteoritics and Planetary Science* 45: 555-571.

Hezel D. C., and Palme H. 2008. Constrains for chondrule formation from Ca-Al distribution in carbonaceous chondrites. *Earth and Planetary Science Letters* 265: 716-725.

Hezel D. C., and Palme H. 2010. The chemical relationship between chondrules and matrix and the chondrule matrix complementarity. *Earth and Planetary Science Letters* 294: 85-93.

Hezel D. C., Palme H., Nasdala L. and Brenker F. E. 2006. Origin of SiO<sub>2</sub>-rich components in ordinary chondrites. *Geochimica et Cosmochimica Acta* 70: 1548-1564.

Hezel D. C., Schlüter J., Kallweit H., Jull A. J. T., Al Fakeer O. Y., Al Shamsi M., and Strekopytov S. (2011). Meteorites from the United Arab Emirates: description,

- weathering and terrestrial ages. *Meteoritics and Planetary Sciences* 46: 327–336.
- Hezel D. C., Poole G., Hoyes J., Coles B. J., Unsworth C., Albrecht N., Smith C., Rehkämper M., Pack A., Genge M., and Russell S. S. (2015). Fe and O isotope composition of meteorite fusion crusts: possible natural analogues to chondrule formation?. *Meteoritics and Planetary Sciences* 50:229–242.
- Hidaka H., Higuchi T., and Yoneda S. 2015. Redistribution of alkaline elements in association with aqueous alteration activity in the early solar system. *The Astrophysical Journal* 815: 76-82.
- Howard K. T., Benedix G. K., Bland P. A., and Cressey G. 2011. Modal mineralogy of CM chondrites by X-ray diffraction (PSD-XRD): Part 2. Degree, nature and settings of aqueous alteration. *Geochimica et Cosmochimica Acta* 75: 2735-2751.
- Huss G. R., Alexander, C. M., Palme H., Bland P. A., and Wasson J. T. 2005. Genetic relationships between chondrules, fine-grained rims, and interchondrule matrix. In *Chondrites and the Protoplanetary Disk*. Edited by Krot A. N., Scott E. R. D. and Reipurth B., Astronomical Society of the Pacific: 701-731.
- Jarosewich E. 1990. Chemical analyses of meteorites: A compilation of stony and iron meteorites analyses. *Meteoritics* 25: 323-337.
- Jones R. H., Grossman J. N., and Rubin A. E. 2005. Chemical, mineralogical and isotopic properties of chondrules: Clues to their origin. In *Chondrites and the Protoplanetary Disk*. Edited by Krot A. N., Scott E. R. D. and Reipurth B., Astronomical Society of the Pacific: 251-285.
- Kiku Y., Ohgo S., and Nishido H. 2014. Characterisation of luminescent minerals in CM'' chondrite (Jbilet Winselwan). *77<sup>th</sup> Annual Meteoritical Society Meeting*: 5300.
- Klerner S., and Palme H. 1999a. Origin of chondrules and matrix in carbonaceous chondrites (abstract). *30<sup>th</sup> Lunar and Planetary Science Conference*: 1272.
- Klerner S., and Palme H. 1999b. Origin of chondrules and matrix in the Renazzo Meteorite. *Meteoritics and Planetary Science* 34: 46-65.
- Klerner S., and Palme H. 2000. Large Titanium/Aluminium fractionation between chondrules and matrix in Renazzo and other carbonaceous chondrites. *Meteoritics and Planetary Science* (Supplement) 35: 89.
- Larimer W. J., and Anders E. 1967. Chemical fractionations in meteorites-II. Abundance patterns and their interpretation. *Geochimica et Cosmochimica Acta* 31: 1239-1270.
- Lee M. R. and Lindgren P. 2016. Aqueous alteration of chondrules from the Murchison CM carbonaceous chondrite: Replacement, pore filling, and the genesis of polyhedral

- serpentine. *Meteoritics and Planetary Science* 51: 1003-1021.
- Liu M. C., McKeegan K. D., Goswami K. K.M., Sahijpal S., Ireland T. R., and Davis A. M. 2009. Isotopic records in CM hibonites: Implications for timescales of mixing of isotope reservoirs in the solar nebula. *Geochimica et Cosmochimica Acta* 73: 5051-5079.
- Lodders K., Palme H., and Gail H. P. 2009. Abundances of the Elements in the Solar System. In Landolt-Börnstein, New Series, vol.VI/4B. Edited by Trümper J. E. Berlin: Springer: 560-598.
- Mason B., and Taylor S. R. 1982. Inclusions in the Allende Meteorite. *Smithsonian Contribution to the Earth Sciences* 25: 1-25.
- McSween H. J. Jr., and Richardson S. M. 1977. The composition of carbonaceous chondrite matrix. *Geochimica et Cosmochimica Acta* 41: 1145-1161.
- McSween H. J. Jr., 1987. Aqueous alteration in carbonaceous chondrites: Mass balance constrains on matrix mineralogy. *Geochimica et Cosmochimica Acta* 51: 2469-2477.
- Metzler K., Bischoff A., and Stöffler D. 1992. Accretionary dust mantles in CM chondrites: Evidence for solar nebula processes. *Geochimica et Cosmochimica Acta* 56: 2873-2897.
- Nakamura T., Nagao K., Metzler K., and Takaoka N. 1999. Heterogeneous distribution of solar and cosmogenic noble gases in CM chondrites and implications for the formation of CM parent bodies. *Geochimica et Cosmochimica Acta* 63: 257-273.
- Ormel C. W., Cucci J. N., and Tielens A. G. G. M. (2008). Co-accretion of chondrules and dust in the solar nebula. *The Astrophysical Journal* 679: 1588-1610.
- Palme H., Larimer J. W., and Lipschutz M. E. 1988. Moderately volatile elements. In *Meteoritics and the early solar system*. Edited by Kerridge J. F., and Matthews M. S., The University of Arizona Press: 436-461.
- Palme H., Lodders K., and Jones A. 2014. Solar system abundances of the elements. In *Treatise on Geochemistry, 2<sup>nd</sup> edition*. Edited by Turekian, K. K., and Holland H., Elsevier: 15-36.
- Palme H., Spettel B., and Hezel, D. C. 2014a. Siderophile elements in chondrules of CV-chondrites. *Chemie der Erde* 74: 507–516.
- Palme H., Hezel D. C., and Ebel D. S. 2015. The origin of chondrules: Constraints from matrix composition and matrix-chondrule complementarity. *Earth and Planetary Science Letters* 411: 11-19.
- Pernet-Fisher J. F., Howarth G. H., Barry P. H., Bodnar R. J., and Taylor L. A. 2014. The extent of aqueous alteration within the Jbilet Winselwan CM2 chondrite (abstract). *45<sup>th</sup> Lunar and Planetary Science Conference*: 2386.

- Pignatelli I., Marrocchi Y., Vacher L. G., Delon R., and Gounelle M. 2016. Multiple precursors of secondary mineralogical assemblages in CM chondrites. *Meteoritics and Planetary Science* 51: 785-805.
- Rubin A. E., and Wasson J. T. 1986. Chondrules in the Murray CM2 meteorite and compositional differences between CM-CO and ordinary chondrite chondrules. *Geochimica et Cosmochimica Acta* 50: 307-315.
- Rubin A. E., Trigo-Rodríguez J. M., Huber H., and Wasson J. T. 2007. Progressive aqueous alteration of CM carbonaceous chondrites. *Geochimica et Cosmochimica Acta* 71: 2361-2382.
- Russell S. S., King A. J., Schofield P. F., Verchovsky A. B., Abernethy F., and Grady M. M. 2014. The Jbilet Winselwan carbonaceous chondrite 1. mineralogy and petrology: strengthening the link between CM and CO meteorites. *77<sup>th</sup> Annual Meteoritical Society Meeting*: 5253.
- Ruzicka A., Grossman J., Bouvier A., Herd D. C., and Agee C. B. 2015. *The Meteoritical Bulletin*. 102. *Meteoritics and Planetary Science* 50.
- Sanders I. S., and Scott E. R. D. 2012. The origin of chondrules and chondrites: Debris from low-velocity impacts between molten planetesimals?. *Meteoritics and Planetary Science* 47: 2170-2192.
- Saunier G., Poitrasson F., Moine B., Gregoire M., and Seddiki A. 2010. Effect of hot desert weathering on the bulk-rock iron isotope composition of L6 and H5 ordinary chondrites. *Meteoritics and Planetary Science* 45:195–209.
- Scott E. R. D., Taylor G. J., and Keil K. 1982. Origin of ordinary and carbonaceous type 3 chondrites and their components(abstract). *13<sup>th</sup> Lunar and Planetary Science Conference*: 1362.
- Scott E. R. D., Rubin A. E., Taylor G. J., and Keil K. 1984. Matrix material in type 3 chondrites-occurrence, heterogeneity and relationship with chondrules. *Geochimica et Cosmochimica Acta* 48: 1741-1757.
- Simon S. B., Davis A. M., and Grossman L 1996. A unique ultra refractory inclusion from the Murchison meteorite. *Meteoritics and Planetary Science* 31: 106-115.
- Simon S. B., Grossman L., Davis A. M. 1997. Multiple generations of hibonite in spinel-hibonite inclusions from Murchison. *Meteoritics and Planetary Science* 32: 259-269.
- Tomeoka K., and Buseck P. R. 1985. Indicators of aqueous alteration in CM carbonaceous chondrites: Microtextures of a layered mineral containing Fe, S, O and Ni. *Geochimica et Cosmochimica Acta* 49: 2149-2163.

- Trigo-Rodriguez J. M., Rubin A. E., and Wasson J. T. 2006. Non-nebular origin of dark mantles around chondrules and inclusions in CM chondrites. *Geochimica et Cosmochimica Acta* 70: 1271-1290.
- Wasson J. T., and Rubin A. E. 2014. Absence of matrix-like chondrule rims in CR2 LAP 02342. *Meteoritics and Planetary Science* 49: 245-260.
- Wolf D., and Palme H. 2001. The solar system abundances of phosphorus and titanium and the nebular volatility of phosphorus. *Meteoritics and Planetary Science* 36: 559-571.
- Wood J. A. 1985. Meteoritic constraints on processes in the solar nebula. Protostars and Planets II. Edited by Black, D.C. and Matthews M.S., The University of Arizona Press: 687-702.
- Zolensky M., Barrett R., and Browning L. 1993. Mineralogy and composition of matrix and chondrule rims in carbonaceous chondrites. *Geochimica et Cosmochimica Acta* 57: 3123-3148.

## Supplementary

Supplementary Table 3.1: Major and minor element abundances in Jbilet Winselwan (this work) and in CI chondrites (Palme et al., 2014).

		CI	Jbilet Winselwan		
			ICP-AES		XRF
			<i>sample 1B</i>	<i>sample 2</i>	
Mg	wt.%	9.54	12.80	12.12	12.70
Al	wt.%	0.84	1.27	1.31	1.41
Si	wt.%	10.70	-	-	14.2
Ca	wt.%	0.91	1.02	1.23	1.02
Ti	wt.-ppm	447	720	690	700
Fe	wt.%	18.66	23.01	22.23	22.7
Na	wt.-ppm	4960	3200	4640	1970
K	wt.-ppm	546	485	726	500
Cr	wt.-ppm	2623	3130	3210	3400
Mn	wt.-ppm	1916	1840	1810	1830
Co	wt.-ppm	513	640	670	660
Ni	wt.%	1.09	1.38	1.39	1.49

### 3 Chondrule and matrix complementarities in the recently discovered Jbilet Winselwan CM chondrite

Supplementary Table 3.2: Minor and trace element abundances (in wt.-ppm) from Jbilet Winselwan (this study and Göpel et al., 2015), CI chondrites (Palme et al., 2014), and the CM2 chondrites NWA 8157 (Göpel et al., 2015) and Paris (Hewins et al., 2014).

	CI	Jbilet Winselwan			Göpel et al.	NWA 8157	Paris
		1A	1B	2			
Li	1.45	2.96				2.69	1.6
Be	0.02	0.03	0.03	0.03	0.03	0.02	0.03
P	985	979	1087	1322	1021		1086
K	546	472			525	1047	380
Sc	5.81	12.31	14.91	8.65	8.77	8.38	8.38
Ti	447	687	634	575	635		628
V	54.6	71.3	76.0	69.5	68.6	67.9	72.1
Mn	1916	1624	1762	1581	1758	1803	1575
Co	513	592	650	570	601	554	651
Cu	133	112.8	113.8	110.0	116.0	115	128
Zn	309	141	148	134	188	142	180
Ga	9.62	7.93	8.40	7.75	8.10	7.63	7.71
Rb	2.32	1.31	1.40	1.84	1.37	1.55	1.72
Sr	7.79	29.58	29.30	68.00	91.35	42.25	10.79
Y	1.46	2.75	2.96	2.26	2.35	2.13	2.11
Zr	3.63	5.06	5.61	5.02	5.14	4.79	4.83
Nb	0.28	0.38	0.40	0.38	0.39	0.37	0.38
Cs	0.19	0.13	0.18	0.20	0.14	0.13	0.13
Ba	2.42	6.87	7.39	4.22	13.61	5.87	3.24
La	0.24	0.36	0.36	0.41	0.38	0.33	0.83
Ce	0.62	0.86	0.86	1.00	0.96	0.84	0.83
Pr	0.09	0.14	0.14	0.14	0.14	0.13	0.13
Nd	0.47	0.68	0.67	0.71	0.70	0.66	0.64
Sm	0.15	0.22	0.22	0.22	0.23	0.21	0.21
Eu	0.06	0.08	0.09	0.08	0.08	0.08	0.08
Gd	0.21	0.40	0.46	0.30	0.30	0.30	0.29
Tb	0.04	0.08	0.09	0.05	0.05	0.05	0.05
Dy	0.26	0.53	0.60	0.35	0.36	0.36	0.35
Ho	0.06	0.11	0.13	0.08	0.08	0.08	0.08
Er	0.17	0.30	0.32	0.23	0.24	0.23	0.23
Tm	0.03		0.04	0.04			0.04
Yb	0.17	0.24	0.26	0.23	0.24	0.23	0.23
Lu	0.03	0.04	0.04	0.03	0.03	0.03	0.03
Hf	0.11	0.16	0.16	0.15	0.15	0.14	0.14
Ta	0.02	0.02	0.02	0.02	0.02	0.02	0.02
W	0.10	0.16	0.15	0.14	0.17	0.12	0.02
Pb	2.62	1.25	1.74	1.66	1.88		1.51
Th	0.03	0.05	0.05	0.06	0.04	0.04	0.04
U	0.01	0.02	0.02	0.01	0.03	0.04	0.01

### 3 Chondrule and matrix complementarities in the recently discovered Jbilet Winselwan CM chondrite

Supplementary Table 3.3: Bulk elemental composition and petrographic type of all studied chondrules in Jbilet Winselwan.

	Chd#2 POP	Chd#5 POP	Chd#6 POP	Chd#9 POP	Chd#21 POP	Chd#24 POP	Chd#32 POP	Chd#33 POP
Si	23.42	22.81	20.15	20.81	20.89	24.04	24.08	22.47
Ti	0.09	0.10	0.14	0.02	0.11	0.08	0.07	0.11
Al	0.89	0.59	0.94	0.17	0.73	0.42	0.41	0.76
Cr	0.28	0.34	0.26	0.16	0.36	0.51	0.54	0.32
Ng	22.87	25.36	24.48	32.01	22.40	22.70	24.13	23.69
Fe	4.78	3.09	6.17	0.41	7.14	3.39	2.83	5.34
Ni	0.02	0.09	0.12	0.01	0.15	0.01	0.01	0.04
Mn	0.08	0.10	0.06	0.03	0.09	0.30	0.16	0.13
Ca	1.32	1.11	1.28	0.27	2.42	1.90	0.70	1.21
Na	<d.l.	0.02	0.03	0.03	0.05	0.05	<d.l.	0.09

	Chd#1b POP	Chd#2b POP	Chd#3b PO	Chd#4b POP	Chd#5b POP	Chd#7b POP	Chd#8b POP	Chd#10b POP	Chd#12b POP
Si	20.30	21.98	19.47	22.92	21.66	20.77	22.49	24.19	24.81
Ti	0.09	0.15	0.18	0.04	0.18	0.17	0.13	0.20	0.12
Al	0.87	2.13	0.27	0.27	1.83	2.07	1.05	0.82	0.82
Cr	0.40	0.49	0.04	0.34	0.41	0.37	0.27	0.60	0.40
Ng	20.49	20.36	32.21	28.96	25.67	22.57	20.64	22.84	24.53
Fe	8.94	7.87	0.29	0.80	0.51	5.69	8.15	2.39	0.54
Ni	0.23	0.13	0.01	0.02	0.01	0.03	0.04	0.02	0.01
Mn	0.23	0.17	<d.l.	0.15	0.10	0.13	0.12	0.26	0.18
Ca	1.51	2.24	2.36	0.31	4.65	3.00	1.56	2.71	1.66
Na	0.05	0.15	<d.l.	<d.l.	<d.l.	0.08	0.21	<d.l.	<d.l.

	Chd#14b POP	Chd#15b POP	Chd#16b PO	Chd#17b POP	Chd#18b POP	Chd#19b POP	Chd#20b POP	Chd#21b POP	Chd#22b PO
Si	21.81	21.46	13.40	22.21	21.37	19.73	20.34	21.02	20.24
Ti	0.09	0.09	0.16	0.10	0.12	0.10	0.06	0.06	0.03
Al	1.29	0.65	3.53	1.46	1.57	1.05	0.83	0.47	0.27
Cr	0.13	0.31	3.78	0.69	0.41	0.29	0.39	0.17	0.24
Ng	24.20	25.95	14.43	21.69	22.80	26.99	24.88	28.96	31.98
Fe	4.57	4.79	24.62	6.56	7.29	5.10	6.36	2.91	0.54
Ni	0.03	0.02	0.05	0.04	0.11	0.02	0.64	0.02	0.01
Mn	0.06	0.15	1.92	0.33	0.20	0.14	0.18	0.09	0.11
Ca	0.41	0.77	0.27	1.68	1.74	0.94	0.81	0.34	0.29
Na	0.06	0.08	0.18	0.07	0.16	0.10	0.05	0.04	<d.l.



## 4 Complementary element relationships between chondrules and matrix in Rumuruti chondrites

Pia Friend<sup>1\*</sup>, Dominik C. Hezel<sup>1,2</sup>, Herbert Palme<sup>3</sup>, Addi Bischoff<sup>4</sup>, Marko Gellissen<sup>5</sup>

<sup>1</sup>University of Cologne, Department of Geology and Mineralogy,  
Zùlpicher Str. 49b, 50674 Köln, Germany

<sup>2</sup>Natural History Museum, Department of Mineralogy,  
Cromwell Road, SW7 5BD London, UK

<sup>3</sup>Forschungsinstitut und Naturmuseum Senckenberg, Senckenberganlage 25, D-60325  
Frankfurt am Main, Germany

<sup>4</sup>Institut für Planetologie, Westfälische Wilhelms-Universität Münster, Wilhelm-Klemm-  
Str. 10, 48149 Münster, Germany

<sup>5</sup>Department of Geosciences, Christian-Albrecht-Universität zu Kiel, Germany

**\*corresponding author:** [piafriend13@gmail.com](mailto:piafriend13@gmail.com)

*Keywords:* chondrules, Rumuruti chondrites, complementarity

*submitted to:* *Earth and Planetary Science Letters*

*submission date:* *March 2017*

### **Abstract**

Chondrule-matrix complementarity has so far only been studied in carbonaceous chondrites. We now determined the chemical composition of 27 bulk chondrules and ~200 matrix spots in unequilibrated fragments of three different Rumuruti (R) chondrites (NWA 2446, NWA 753, Hughes 030). Also the bulk meteorite composition of NWA 753 was determined. Bulk R chondrites have almost CI chondritic (=solar) ratios of Fe/Mg (1.89), Al/Ti (18.62), and Al/Ca (0.94), while chondrules and matrix are complementary to each other. Mean Fe/Mg ratios in chondrules are 0.43 (NWA 2446), 0.36 (NWA 753), and 0.34 (Hughes). The chondrules show depletions of Fe, while matrices are with respective values of 2.46, 2.09, and 2.16 enriched in Fe. The relative low Fe/Mg ratio in NWA 753 matrix is due to abundant large sulphide grains: bulk values for Fe/Mg in NWA 753 can be exactly reproduced by calculating measured compositions and abundances of chondrules, matrix and sulphides. Refractory elements are also complementary: Al/Ti and Al/Ca show depletion of Al and enrichments of Ca and Ti in chondrules (Al/Ti: 10.43 in NWA 753, 12.24 in NWA 2446 and 11.47 in Hughes 030; Al/Ca: 0.66 in NWA 2446, 0.53 in NWA 753, and 0.46 in Hughes 030), while matrices are generally enriched in Al, but depleted in Ca and Ti (Al/Ti: 31.93 in NWA 2446, 34.71 in NWA 753 and 19.14 in Hughes 030; Al/Ca: 2.19 in NWA 2446, 2.40 in NWA 753, and 0.48 in Hughes 030). Calcium in Hughes 030 matrix is enriched due to terrestrial weathering. The data show, that R chondrite components most likely formed from a common reservoir similar to carbonaceous chondrites. Further, super-chondritic Si/Mg ratios in bulk R chondrites must be the result of Si addition to this reservoir, most probably primarily to the chondrules.

## 4.1 Introduction

The two major components of carbonaceous chondrites are chondrules and matrix, with often complementary chemical composition. For example, matrix has high Si/Mg and Fe/Mg ratios, and chondrules have the opposite signature, low Si/Mg and Fe/Mg ratios, while the chondrites have approximately solar or CI chondritic ratios. Wood (1985) already realised that forsterite rich chondrules in CM meteorites require FeO-rich matrix to produce a roughly chondritic Fe/Mg ratio of bulk meteorites. Such complementary element ratios of chondrules and matrix have so far been reported for a number of element pairs in several type 2 and 3 carbonaceous chondrites (CC) (e.g., Klerner and Palme, 2000; Bland et al, 2005; Hezel and Palme, 2008, 2010; Becker et al., 2015; Palme et al., 2014a, 2015; Kadlag and Becker, 2016; Budde et al., 2016a; Ebel et al., 2016).

Complementarity is an important constraint for chondrule formation models. It excludes spatially separated origins of chondrules and matrix, and requires that both components originate from a single reservoir. Carbonaceous chondrites are well suited for studying complementarity, as they have large fractions of matrix, between 30 and 60 vol.%. Ordinary chondrites (OC), as well as enstatite chondrites (EC) only have very low fractions of matrix (< 15 vol.%), and their bulk composition is, hence, largely determined by chondrules (Huss et al., 1981; Palme et al., 2015). The group of Rumuruti chondrites (R chondrites) is chemically and isotopically related to OC and EC (Bischoff et al., 2011; Warren, 2011). In contrast to these two groups, R chondrites contain about 50 vol.% fine grained matrix material. This, and their CI chondritic bulk element ratios of Fe/Mg, Al/Ti, and Al/Ca make the R chondrites ideal candidates to study chemical complementarity.

The R chondrites are a small but growing group of meteorites, so far comprising 173 specimens (data from the “Meteorite Bulletin Database”; <http://www.lpi.usra.edu/meteor/metbull.php>). All listed R chondrites are finds, except for Rumuruti, the only observed fall. The R chondrites exhibit several characteristics that distinguish them from other chondrite groups: (i) they have the highest  $\Delta^{17}\text{O}$  values of all meteorites (e.g., Franchi, 2008; Bischoff et al., 2011). (ii) The chondrule to matrix ratio is ~50:50 and within the same range as in carbonaceous chondrites, but very different from ordinary chondrites (Bischoff et al. 2011). (iii) Mean refractory lithophile element abundances are ~0.95 x CI, hence between those of carbonaceous and ordinary chondrites, and are similar (0.89-1.03 x CI) for the moderately volatile elements Mn and Na (e.g., Kallemeyn et al., 1996; Bischoff et al., 2011). (iv) The mineralogy is highly oxidised, with

~90 vol.% silicates (~70 vol.% olivine, and minor amounts of plagioclase as well as low-Ca and Ca pyroxene), up to 10 vol.% sulphides (mainly pyrrhotite), and negligible amounts of metal (e.g., Kallemeyn et al. 1996; Bischoff et al., 2011). (v) Most R chondrites are breccias, containing clasts with various degrees of internal equilibration, ranging from primitive type 3 fragments up to equilibrated lithologies of petrologic type 5 or 6 (e.g., Bischoff et al., 1994, 2011; Bischoff 2000; Schulze et al., 1994; Kallemeyn et al., 1996).

Here we determine the composition of bulk chondrules and of matrix in R chondrites to find out if a complementary chemical relationship between chondrules and matrix also exist in other types of chondritic meteorites. We studied three unequilibrated, type 3 fragments, each of a different R chondrite and compare the results of to the bulk composition of the R chondrites.

## 4.2 Materials and Methods

### 4.2.1 Samples

Bulk chondrule as well as matrix compositions were studied only in unequilibrated type 3 lithologies in thin sections of NWA 753, Hughes 030, and NWA 2446. The fragment that we investigated from Hughes 030 was described in Bischoff (2000), who suggests a petrologic type of ~3.2 for this clast. Bischoff (2000) points out that Hughes 030 is not considerably shocked and that its primitive fragments, which resemble type 3 carbonaceous chondrites, can clearly be distinguished from the more equilibrated parts of the meteorite. Further, Bischoff et al. (2011) reported on several highly unequilibrated type 3 clasts in NWA 753 as well as in NWA 2446. Detailed investigations of a type 3 fragment of NWA 753 were also done by Kita et al. (2013). They concluded that the fragment is of petrologic type 3.15-3.2.

In addition to these in-situ studies we selected three bulk samples from NWA 753 to determine the bulk composition. These three samples were selected as follows: a several hundred g piece of NWA 753 was cut into 2-3 mm thick slices. The brecciated texture of the rock was clearly visible on these slices in form of dark (type 3) and light (equilibrated) clasts embedded in a clastic matrix. The dark and light fragments were cut out of the slices and the blend was used as the "bulk sample".

#### 4.2.2 Methods

##### *Modal abundances of chondrules, matrix and sulphides*

The modal abundances of chondrules, matrix and sulphides were obtained with the open source image processing program “ImageJ” (Schneider et al., 2012). Each component was thresholded based on its grey value on BSE images and the corresponding area % measured.

##### *EMP analyses of bulk chondrules and matrix*

All analyses were done with a Jeol JXA-8900RL Superprobe at the University of Cologne, operating at 20 kV and a beam current of 20 nA. Well characterised natural minerals were used as standards and the ZAF corrections were applied. Detection limits for minor elements were (by weight): 100 ppm for CaO, TiO<sub>2</sub>, NiO and Na<sub>2</sub>O; 200 ppm for Cr<sub>2</sub>O<sub>3</sub>; and 250 ppm for MnO and FeO. Titanium contents can be very low in the measured mineral phases, and Ti analyses were therefore carefully calibrated as described in Friend et al. (submitted for publication). Mineral compositions were measured with a focused beam of 1 µm, while for matrix analyses a defocused beam of 15 µm diameter was used. The porous structure of the matrices resulted in totals lower than 100 wt.%. Matrix portions with visible sulphide grains were avoided. This may lead to underestimating the total Fe. However, the studied fragments from NWA 2446 and Hughes 030 contain only little sulphide and the effect of underestimating Fe should therefore be small. In the fragment of NWA 753, which contain more abundant sulphide grains, those were measured separately.

Bulk chondrule composition were determined using modal recombination, following the protocol of Hezel (2010). This is an established technique that has been used previously by numerous authors, e.g., Berlin et al. (2006) or Ebel et al. (2009).

##### *Bulk analyses with X-ray fluorescence*

Major, minor, and some trace elements from NWA 753 samples were determined with a Philips PW 2400 sequential wavelength dispersive X-ray spectrometer at the University of Cologne. Aliquots of about 120 mg powdered sample were pre-digested in aqua regia with an HCl to HNO<sub>3</sub> ratio of 3:1 and were equilibrated for two hours at 130 °C to oxidise tiny metal grains that may have survived. After vaporisation of the acid, 3.6 g of Li<sub>2</sub>B<sub>4</sub>O<sub>7</sub> were added as a flux agent to the samples. These were then melted at about 1200 - 1300 °C in platinum crucibles under oxidising conditions. The sample melts were subsequently poured into homogeneous glass disks. The analytical procedure, including external standardisation of the X-ray spectrometer with at least 40 standard rock samples, followed the procedure of

Wolf and Palme (2001). The precision of the reported elements is better than 1% and the accuracy for major and minor elements is estimated to be below 2% (Wolf and Palme, 2001). A well-known Allende standard was also measured to verify the obtained data.

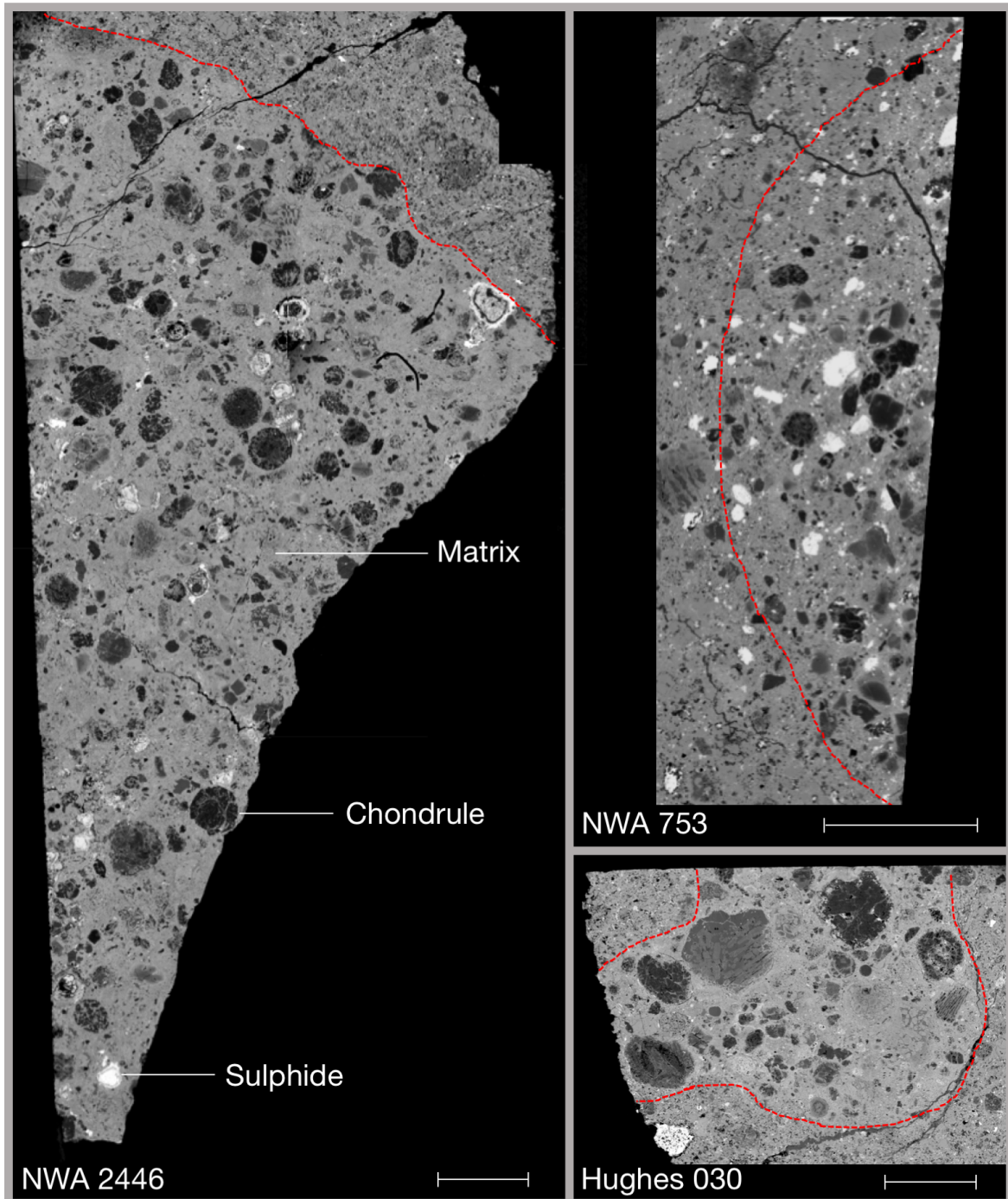


Figure 4.1: Backscatter electron images of the studied type 3 R chondrite fragments, indicated by red dashed lines. Dark chondrules are always easy to identify within lighter matrix material. Sulphides are abundant in NWA 753, while nearly absent in Hughes 030. All scale bars are 1mm.

## 4.3 Results

### 4.3.1 Petrography

Backscatter images of the investigated type 3 lithologies in thin sections of NWA 2446, NWA 753, and Hughes 030 are displayed in Fig. 4.1. All fragments have typical chondritic textures, with roundish chondrules as well as chondrule fragments sitting in a fine-grained matrix. Occasionally, sulphides occur in the matrix. NWA 2446 contains with 28 area% the least amount of chondrules and fragments. Followed by NWA 753, with 34 area% chondrules and fragments. Hughes 030 contains 58 area% chondrules and fragments. Note that given chondrule abundances also comprise chondrule fragments and larger mafic silicate minerals. The latter are probably as well chondrule fragments and are especially abundant in NWA 753 (Fig. 4.1). Only NWA 753 contains larger quantities of sulphides, (~9 area%), followed by significantly lower abundances in NWA 2446 (~2 area%) and Hughes 030 (<1 area%). The latter chondrites are secondary altered by terrestrial weathering, which leads to oxidation of metals and sulphides (Stelzner et al., 1999). The low sulphide abundances are hence most probably due to terrestrial weathering and it is assumable that NWA 2446 and Hughes 030 had initially similar sulphide contents as NWA 753.

Chondrules and chondrule fragments have variable sizes with apparent diameters <600  $\mu\text{m}$ . A total of 27 chondrules were studied, 10 chondrules in each, NWA 2446 and NWA 753, and 7 chondrules in Hughes 030. All chondrules have porphyritic textures: 22 POP, 3 PO, and 2 PP. Among these are 15 type I and 12 type II chondrules. Seventeen chondrules

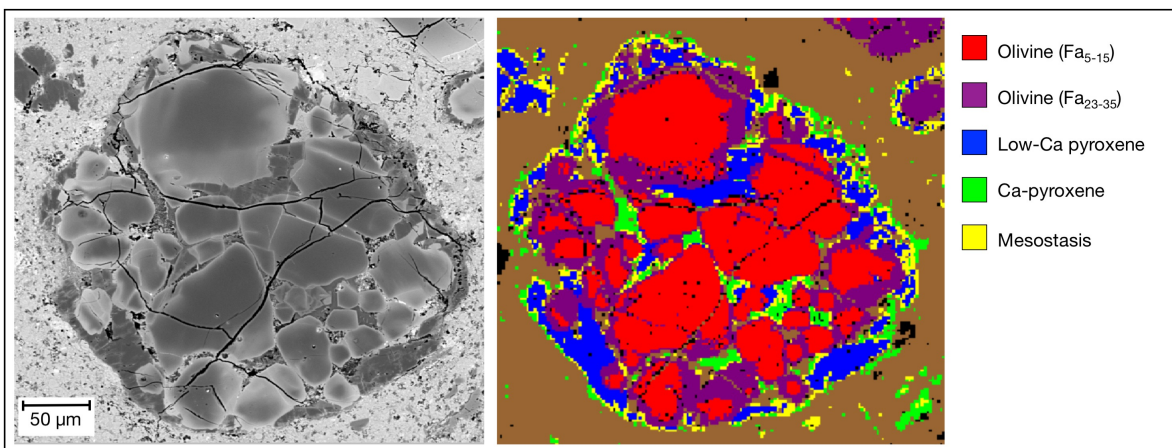


Figure 4.2: Backscatter electron image and the according phase map from a chondrule in NWA 2446. A mineralogical zonation exists, albeit not very prominent. The outermost layer of the chondrule consists of low Ca-pyroxenes, whereas olivine minerals are dominating the interior. Some olivine minerals are in turn chemically zoned, with increasing Fa contents to the margins.

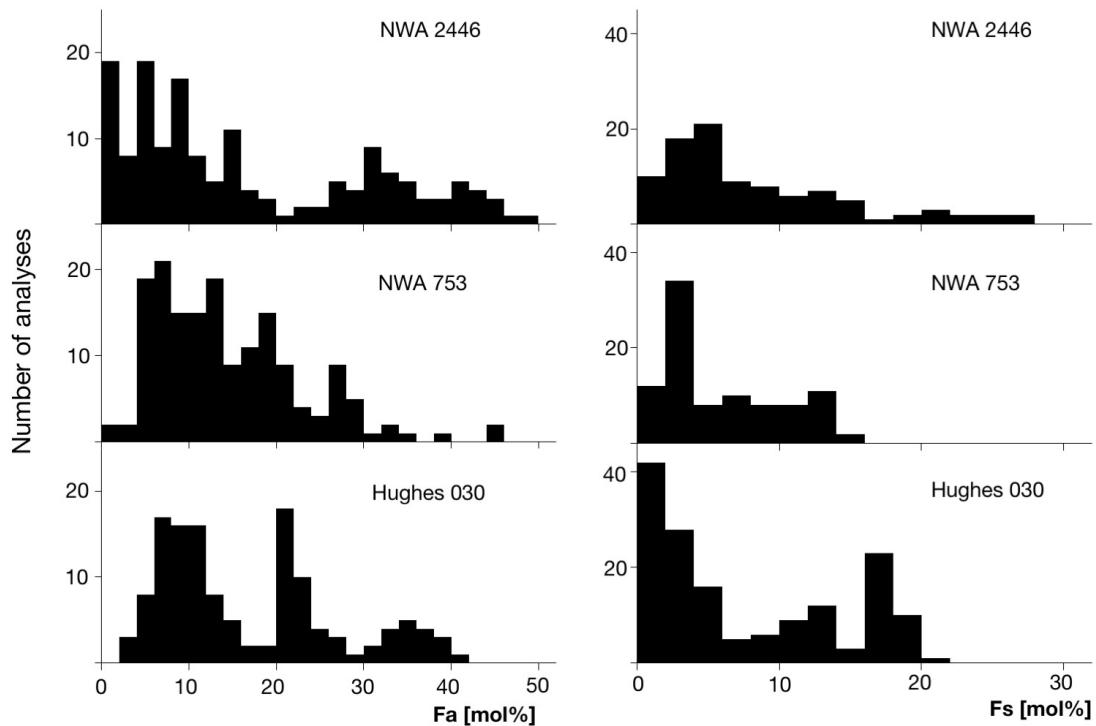


Figure 4.3: Fayalite and respective Fs contents of all interchondrule olivine and low-Ca pyroxene analyses. There is a large compositional range of olivines in all three R chondrites. The range of low-Ca pyroxene compositions is generally more narrow, but still variable, especially in NWA 2446 and Hughes 030.

are mineralogically zoned, with olivine mainly located in the center and low-Ca pyroxenes primarily present at the edge of the chondrules (Fig. 4.2). Such mineralogical zonation results from the reaction of gaseous SiO with chondrule olivine to form pyroxene – a process previously described in carbonaceous and R chondrites (Friend et al., 2016). As discussed by these authors, this reaction reduces compositional differences between chondrules and matrix: Mg-rich chondrules gain Si from the gas phase, thereby increasing their Si/Mg ratios. This means, chondrules were initially Mg-richer, and became more Si-rich during this reaction, i.e. compositionally more like matrix.

Major mineral phases in chondrules and chondrule fragments are olivines and low-Ca pyroxenes, while Ca pyroxenes are less abundant. Mesostasis is present in all chondrules, but is often devitrified. The composition of the mesostasis is generally variable among individual chondrules. Olivines in chondrules are typically forsteritic, and often surrounded by a fine Fa-rich rim (Fig. 4.2). However, also unzoned Fo-rich olivine as well as Fa-rich olivine ( $\sim\text{Fa}_{20-45}$ ) grains are common. Fayalite contents of olivines and Fs contents of pyroxenes have a large spread among chondrules (Fig. 4.3). The largest FeO variations in both minerals were found in NWA 2446 chondrules, ranging from pure forsterite to 49 mol%



Fa and 1 to 27 mol% Fs. Chondrule Fa in NWA 753 ranges between 2 and 46 mol%, but with most grains having Fa-contents between 4 and 20 mol%. Chondrule Fs contents in NWA 753 are much narrower, ranging from 1 to 15 mol%. In Hughes 030, chondrule Fa ranges between 2 and 46 mol% and chondrule Fs between 1 and 21 mol%. Besides abundant Fo-rich olivines ( $Fa_{<10}$ ), a significant number of olivine analyses have Fa-values between 20-25 mol% in this meteorite. Sulphides are absent in chondrules of NWA 2446 and Hughes 030, and only small fractions of sulphides are present in some chondrules of NWA 753.

### 4.3.2 Bulk composition of NWA 753

In NWA 753 we determined the bulk composition of one type 3 lithology, one equilibrated rock fragment, and one large “bulk sample” that contains various lithologies of diverse petrologic types. Two aliquots of each of these samples were measured. The results are illustrated in Fig. 4.4 (and Supplementary Table 4.1) together with a mean bulk composition of R chondrites from Bischoff et al. (2011) and CI data reported in Palme et al. (2014).

The major elements Si, Mg, and Fe have nearly identical concentrations in all three studied NWA 753 samples, and almost identical concentrations as bulk R chondrite literature

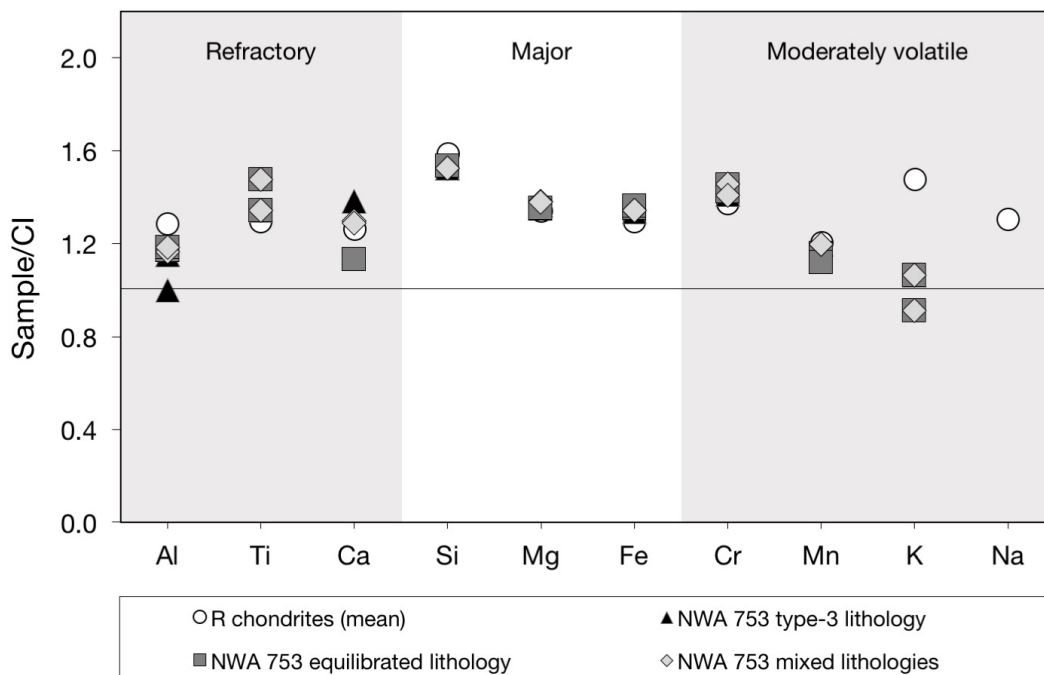


Figure 4.4: Bulk data of all three lithologies from NWA 753 are identical for the main elements. Minor differences are visible for the refractory and the moderately volatile elements. Data from NWA 753 are also generally in good agreement with the mean R chondrite data from Bischoff et al. (2011).

data (e.g., Bischoff et al., 2011). Some variations exist among the refractory elements. In particular, Ca has higher concentrations (1.25 and 1.26 wt.%) in the unequilibrated NWA 753 fragment compared to 1.03 wt.% in the equilibrated NWA 753 fragment, and is intermediate (1.17 and 1.18 wt.%) in the bulk rock sample. The Al concentrations in all measured NWA 753 samples are 0.95-1.00 wt.%, and slightly below the reported mean R chondrite compositions (1.15 wt.%; Bischoff et al., 2011). Our data fit well with literature data for Cr (our data: 3660-3790 ppm; literature data: 3568) and Mn (our data: 2170-2320 ppm; literature data: 2271 ppm). The moderately volatile element K is in most measurements of NWA 753 580 ppm, hence somewhat lower in comparison to mean R chondrite concentrations from the literature (806 ppm). Albeit, one aliquot of NWA 753 equilibrated lithology show a K content of 1000 ppm.

### 4.3.3 Major elements (Fe, Mg, Si) and refractory elements (Al, Ti, Ca) in chondrules and matrix

We studied the bulk element and mineral compositions of 27 chondrules. Matrix was also analysed in each type 3 fragment of the studied R chondrites: 80 matrix analyses in NWA 2446, 63 in NWA 753 and 57 in Hughes 030. The means and standard deviations of all chondrule and matrix analyses of the respective chondrites are listed in Table 4.1. For individual chondrule analyses see Supplementary Table 4.2. The compositions for major (Fe, Mg, Si) and refractory (Al, Ti, Ca) elements of chondrules and matrix are plotted in Fig. 4.5, together with bulk data of the NWA 753 type 3 fragment and bulk R chondrite literature data (Bischoff et al. 2011).

Table 4.1: Mean bulk chondrule and mean matrix compositions in NWA 753, NWA 2446 and Hughes 030.

	NWA 2446		NWA 753				Hughes 030					
	Chondrules (n=10)		Matrix (n=80)		Chondrules (n=10)		Matrix (n=63)		Chondrules (n=7)		Matrix (n=10)	
	Ø	sd	Ø	sd	Ø	sd	Ø	sd	Ø	sd	Ø	sd
Si	22.85	1.75	15.16	0.75	22.18	1.78	15.88	0.55	23.72	2.19	15.23	1.02
Ti	0.09	0.07	0.04	0.03	0.08	0.03	0.03	0.02	0.09	0.08	0.05	0.03
Al	1.09	1.15	1.37	0.49	0.80	0.52	1.10	0.50	0.98	0.71	0.89	0.56
Cr	0.32	0.13	0.29	0.11	0.31	0.14	0.29	0.08	0.39	0.08	0.35	0.20
Mg	20.04	1.94	11.56	1.29	22.20	2.22	12.4	1.21	20.56	0.86	12.54	1.79
Fe	8.56	2.89	28.41	1.30	8.00	2.18	26.1	1.74	6.90	4.60	27.11	1.88
Ni	0.06	0.03	0.65	0.21	0.41	0.13	1.92	0.65	0.03	0.02	0.33	0.12
Mn	0.24	0.12	0.22	0.04	0.23	0.14	0.26	0.03	0.23	0.12	0.27	0.07
Ca	1.64	0.97	0.62	0.48	1.53	0.89	0.46	0.30	2.14	1.01	1.83	1.45
Na	0.56	0.67	0.32	0.25	0.06	0.03	0.16	0.08	0.15	0.21	0.04	0.03

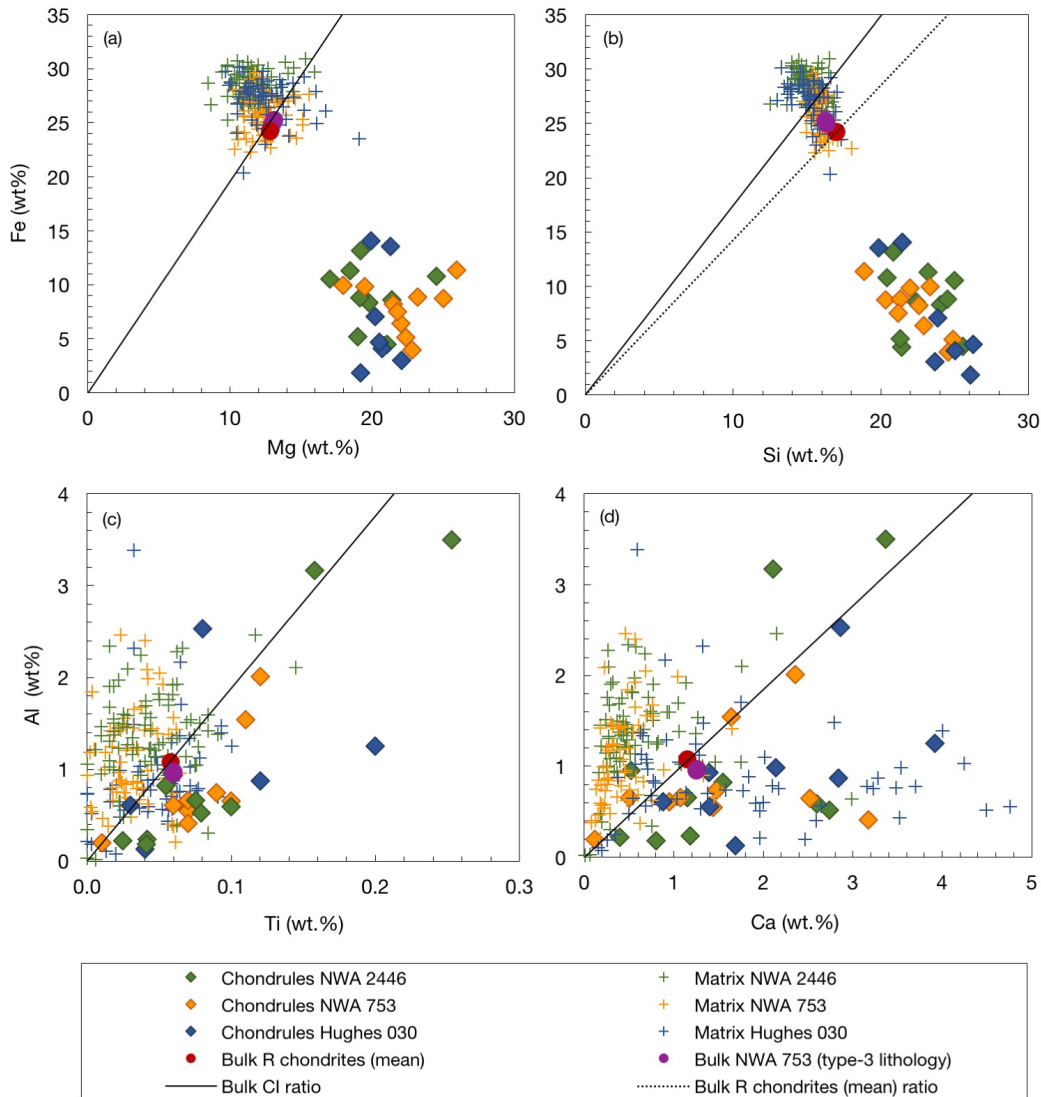


Figure 4.5: A complementary distribution between chondrules and matrix exists for Fe and Mg, as well as Fe and Si within the type 3 lithologies of all three studied R chondrites. Bulk R chondrites have CI chondritic Fe/Mg ratios, yet the Fe/Si ratios are somewhat below the CI chondritic ratio. Also, matrix of the type 3 R chondrite lithologies are generally enriched in Al, while depleted in Ti and Ca. Only Hughes 030 matrix shows large scattering of Ca values with in cases high contents, probably due to terrestrial weathering. Mean R chondrite bulk data are CI chondritic, and bulk data of the unequilibrated NWA 753 fragment are also virtually CI chondritic. Mean bulk data for R chondrites are from Bischoff et al., 2011, and references therein; CI data are from Palme et al., 2014.

The studied fragment of NWA 753 contains substantial amounts of sulphides and isolated olivine and pyroxene minerals, presumably chondrule fragments, dispersed within the matrix. These phases were avoided when measuring matrix, but were measured separately. The obtained data are displayed in Fig. 4.6.

Chondrule compositions for the major elements are quite variable (Fig. 4.5a and 4.5b). Iron contents are between 2 and 14 wt.%, Mg contents between 17 and 26 wt. % and Si contents between 19 and 26 wt. %. Individual matrix analyses are all fairly similar, with

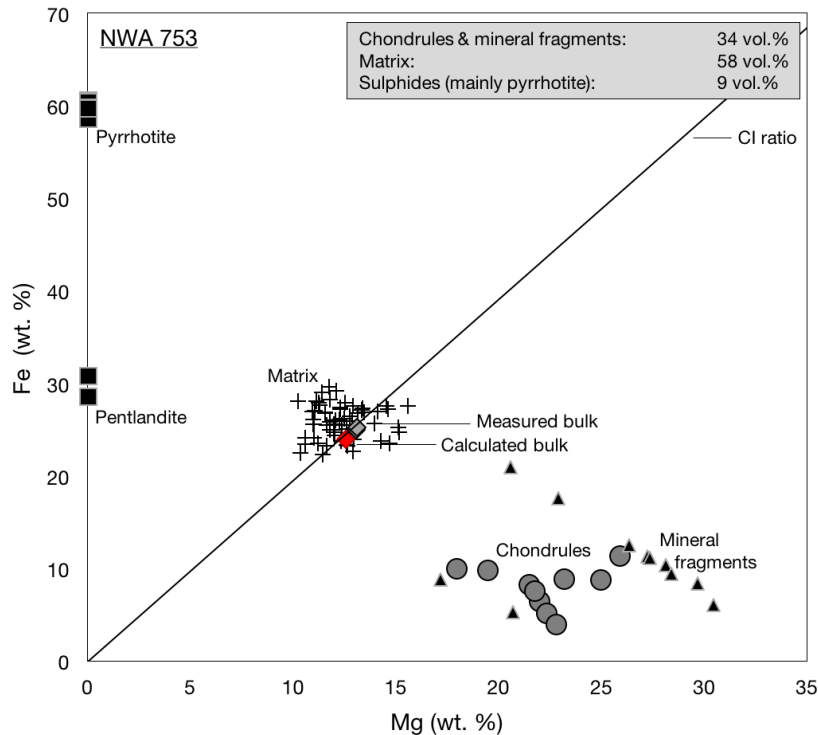


Figure 4.6: Complementarity of Fe and Mg within the type 3 fragment of NWA 753 is not only established between chondrules and matrix, but also includes sulphides and mineral fragments embedded in the matrix. The calculated bulk composition is virtually identical to the measured bulk composition. CI data are from Palme et al., 2014.

mean Fe contents of 28 wt. % in NWA 2446, 26 wt.% in NWA 753 and 27 wt. % in Hughes 030. Mean Mg contents in the matrices of all three chondrites are 12 wt. % and mean Si contents are 15 wt. % in NWA 2446 and Hughes 030, and 16 wt. % in NWA 753. Figure 4.6 displays the Fe and Mg concentrations of all components present in the NWA 753 type 3 lithology. Sulphide minerals are mainly pyrrhotite with ~60 wt. % Fe, but minor amounts of pentlandite with ~30 wt.% Fe are also present. Mineral fragments are olivines and low-Ca pyroxenes, with variable Fe contents between 5 and 21 wt.%.

In Fig. 4.5c and 4.5d, the contents of refractory elements are displayed. Aluminium concentrations of chondrules are commonly <1.0 wt.%, but can be as high as 3.5 wt. %. Titanium concentrations in chondrules are between 100 and 2500 ppm and Ca concentrations are between <1.0 and 3.9 wt.%. Mean Al concentrations of matrix are 1.4 wt.% in NWA 2446, 1.1 wt.% in NWA 753 and 0.9 wt. % in Hughes 030. Mean matrix Ti values are 400 ppm in NWA 2446, 300 ppm in NWA 753 and 500 ppm in Hughes 030. Calcium concentrations in NWA 2446 and NWA 753 are generally low, with mean values of 0.6 wt.% (NWA 2446) and 0.5 wt.% (NWA 753). In Hughes 030, most measured Ca concentrations range between about 1 and 5 wt.%, with a mean value of 1.8 wt.%.

## 4.4 Discussion

### 4.4.1 Petrologic types of investigated fragments

The first indicator, that the studied R chondrite fragments did not experience any extensive thermal metamorphism are their well preserved chondritic textures, with chondrules and matrix in roughly equal amounts. The observed dominance of low-Ca pyroxenes relative to Ca pyroxenes is another characteristic of unequilibrated type 3 R chondrite lithologies (Bischoff, 2000) as well as the variable olivine Fe contents (Fig. 4.3) (Kallemeyn et al., 1996).

Grossman and Brearley (2005) proposed to combine the average and standard deviation of  $\text{Cr}_2\text{O}_3$  contents in ferroan olivines ( $\text{Fo} < 98$ ) of chondrules to determine low petrologic subtypes. Kita et al. (2013) also applied this approach to a fragment of the R chondrite NWA 753. Here, we selected analyses of at least 20 larger ( $\geq 30\mu\text{m}$ ) olivine grains within chondrules of each investigated fragment for petrologic sub-classification (Fig. 4.7). Data from Kita et al. (2013) for another fragment of NWA 753 are also included. The fragment from NWA 2446 plots in the field of the petrologic subtype 3.2, close to the field of subtype 3.15. Data of the NWA 753 fragment suggest a petrologic subtype of 3.15, similar to that from Kita et al. (2013), but plott slightly above the according field. The olivine compositions of Hughes 030 indicate a petrologic subtype of 3.2.

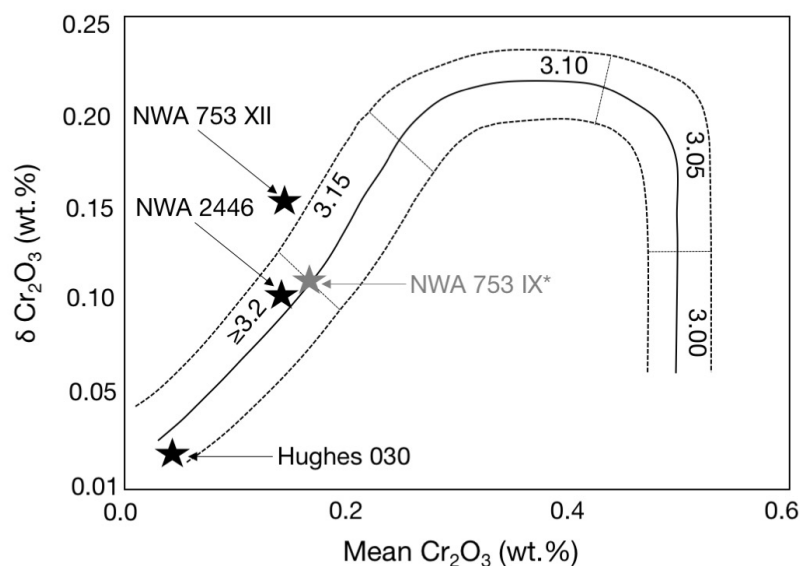


Figure 4.7: The average and mean values of  $\text{Cr}_2\text{O}_3$  in olivine minerals with  $\text{Fo} < 98$  as it is used in Grossman and Brearley (2005). The fragments of NWA 753 and NWA 2446 indicate low petrologic types of  $< 3.2$ , while the fragment of Hughes 030 is slightly more altered. Data for another fragment of NWA 753 (NWA 753 IX) are from Kita et al., 2013.

### 4.4.2 Complementarity of major elements (Fe, Mg and Si)

All studied R chondrites have complementary Fe/Mg ratios between chondrules and matrix, while the bulk composition of the R chondrites have CI chondritic Fe/Mg ratios (Fig. 4.5a). The mean chondrule Fe/Mg values are 0.43 in NWA 2446, 0.36 in NWA 753 and 0.34 in Hughes 030 (Supplementary Table 4.3), and are sub-chondritic. Matrix analyses have generally super-chondritic mean Fe/Mg ratios of 2.46 in NWA 2446, 2.09 in NWA 753, and 2.16 in Hughes 030. Bulk composition of the type 3 lithology of NWA 753 has Fe/Mg ratios of 1.91 and 1.93, and literature data for bulk R chondrites have Fe/Mg ratios of 1.89, both are very close to the CI chondritic Fe/Mg value of 1.96. Complementarity between chondrules and matrix is most pronounced in NWA 2446, with virtually all matrix analyses plotting significantly above the Fe/Mg ratio of CI chondrites and bulk R chondrites. Matrix data of Hughes 030 are slightly closer to, but still higher than bulk R chondrite and CI chondritic Fe/Mg ratios (Fig. 4.5). However, the NWA 753 matrix has a mean Fe/Mg ratio of 2.09, close to the ratio of CI and bulk R chondrites. This is to a large extent, because the larger sulphide grains with an abundance of 9 area% were avoided when measuring matrix. The chondrules in NWA 753 are, however, very Fe-poor, similar to chondrules from NWA 2446 and Hughes 030. Also, the mean Fe/Mg ratio of the individual olivine and low-Ca pyroxene minerals in the matrix is 0.43, slightly higher than the mean Fe/Mg ratio of the chondrules. The bulk chondrite composition calculated from all components is 23.99 wt.% Fe and 12.55 wt.% Mg, resulting in an Fe/Mg ratio of 1.91, which is virtually identical to the measured NWA 753 bulk composition (Fig. 4.6 and Table 4.2).

The difference in Fe/Mg ratios between chondrules and matrix is the strongest case for complementarity. Internal redistribution of Fe and Mg is impossible (Hezel and Palme, 2010; Palme et al., 2015). Forsterite rich chondrules are not the result of FeO-loss from more FeO-rich chondrules. Cation diffusion is impossible at the equilibration temperatures of carbonaceous chondrites. For example, the heavily weathered Mokoia has the same average composition of chondrules as the slightly weathered but more metamorphosed Allende chondrite.

Chondrules and matrix have also different Fe/Si ratios (Fig. 5b). The bulk ratios of the two NWA 753 type 3 lithologies are 1.53 and 1.56. The Fe/Si ratios of chondrules are lower than in bulk R chondrites: 0.37 (NWA 2446), 0.36 (NWA 753) and 0.29 (Hughes 030). Yet, the Fe/Si ratios of the matrices are with 1.87 (NWA 2446), 1.63 (NWA 753) and 1.78 (Hughes 030) significantly higher than in bulk R chondrites. The mean Fe concentration of the NWA 753 matrix is again the lowest, because of the abundant large sulphide grains not

## 4 Complementary element relationships between chondrules and matrix in Rumuruti chondrites

Table 4.2: Parameters for calculating bulk meteorite Fe and Mg composition of NWA 753.

	Chondrules	Matrix	Mineral fragments	Pyrrhotite	Pentlandite
Area%	28	57	6	7	2
Density	2.9	2.9	3.4	4.6	4.8
Av. Fe (wt.%)	8.0	26.1	11.1	59.7	29.7
Av. Mg (wt.%)	22.2	12.4	25.3	-	-
Calculated bulk Fe/Mg: 1.91					

included in the matrix analyses (cf. Fig. 5.6). The Fe/Si ratio of CI chondrites (1.74) is 12 and 10%, respectively, higher than our measured XRF bulk type 3 lithology in NWA 753 of 1.53 and 1.56, and 18% higher than literature R chondrite Fe/Si ratio of 1.4. The reason for this is that the solar reservoir of the R chondrites was enriched in Si.

### 4.4.3 Complementarity of refractory elements (Al, Ti and Ca)

Chondrules in all studied R chondrite fragments have sub-chondritic Al/Ti ratios, while most matrix analyses have super-chondritic Al/Ti ratios (Fig. 4.5c). The Al/Ti ratio for literature data of bulk R chondrites is 18.62, which is identical to the CI chondritic Al/Ti ratio of 18.79, and close to the Al/Ti ratios of 16.14 and 15.88 for bulk NWA 753 type 3 lithology. Mean chondrule Al/Ti ratios are always sub-chondritic, with 12.24 in NWA 2446, 10.43 in NWA 753 and 11.47 in Hughes 030. Mean matrix Al/Ti ratios are always super-chondritic, with 31.93 in NWA 2446, 34.71 in NWA 753 and 19.31 in Hughes 030. The lower Al/Ti ratio of the Hughes 030 matrix results from slightly lower average Al concentrations (av. 0.89 wt.% compared to 1.37 wt.% in NWA 2446 or 1.1 wt.% in NWA 753), as well as from higher Ti concentrations in the Hughes 030 matrix (av. 0.05 wt.% compared to 0.04 wt. % in NWA 2446 and 0.03 wt. % in NWA 753).

The Al/Ti ratio is particularly significant because two refractory elements are involved and it is impossible to fractionate Al from Ti by aqueous alteration or at mild metamorphic temperatures. As discussed earlier (Lux et al., 1980; Floss et al., 1996;1998) this requires processes at high temperatures. The chondrule precursors may have preferentially included early condensed perovskite grains (Klerner, 2001; Palme et al., 2015). Although the abundance of Ti is close to the detection limit of the electron microprobe we want to stress that both components, matrix and chondrules, have rather low Ti concentrations and the difference between chondrules and matrix excludes a systematic error with sample Ti contents.

All chondrule Al/Ca ratios are sub-chondritic relative to the literature data of bulk R chondrites of 0.94: 0.66 in NWA 2446, 0.53 in NWA 753, and 0.46 in Hughes 030. Matrices in NWA 2446 and NWA 753 are super-chondritic, with Al/Ca ratios of 2.19 and 2.40, respectively, and the mean Al/Ca ratio in the Hughes 030 matrix is 0.48. The bulk R chondrite literature data for the Al/Ca ratio is with 0.94 basically identical to the CI-chondritic value of 0.92. Yet, the measured bulk Al/Ca ratios of 0.77 and 0.76 of the NWA 753 unequilibrated lithology is somewhat below the CI chondritic ratio. However, the Al value in the NWA 753 type 3 sample is comparatively strongly deviating from those in the other NWA 753 samples (Fig. 4.4). As the sample quantity was very low, we suggest that incomplete sampling, e. g. missing of an Al-rich phase, has caused that deviance. The Ca/Al ratios for the bulk lithology and the equilibrated lithology of NWA 753 are however 0.84 and 0.96 respectively.

No complementary distribution of Al and Ca exists in Hughes 030. Calcium, however, is known to get enriched during terrestrial weathering by formation of Ca-bearing phases (e.g. Stelzner et al., 1999; Lee and Bland, 2004). Hence, prior to terrestrial weathering, there may have also been a Ca/Al complementarity in Hughes 030.

### 4.4.4 Origin of major element complementarities

In NWA 753 chondrules, matrix, and sulphides, all with distinct Fe/Mg ratios, aggregated together just in the right proportions to produce a CI chondritic bulk ratio. The most sensible conclusion from this is that these components formed from a single reservoir, represented by the bulk composition of R chondrites, which is very similar to the composition of the solar photosphere or CI chondrites. An arbitrary mixture of chondrules, matrix, and sulphides formed at spatially separated locations could never achieve the photospheric bulk composition of major elements.

The parental reservoir of R chondrites has a slightly elevated Si/Mg ratio. Warren (2011) proposed, based on stable isotope data, that chondritic meteorites can be divided into carbonaceous (C) and non-carbonaceous material (NC). The two groups, of C and NC chondrites also have characteristic chemical differences (Palme et al., 1996). It has been suggested that C chondrites formed farther away from the Sun as NC chondrites (Warren, 2011). The extent of the complementarity, i.e. differences of characteristic element ratios between chondrules and matrix are similar in R chondrites to carbonaceous chondrites (e.g.



Hezel and Palme, 2008; Hezel and Palme, 2010; Palme et al., 2015), indicating that the chondrule forming process operated in the same way in C and in NC chondrite material.

The strong fractionation of Fe and Mg may reflect preferred incorporation of forsterite into chondrule precursors and separate formation of metallic iron grains, which were only partly incorporated in chondrule precursors. Both processes may have occurred at a single temperature, since forsterite and metal have similar condensation temperatures, the precise sequence depends on the ambient pressure (e.g, Lodders, 2003).

A strong support for complementarity comes from chemical and isotopic data of W and Mo. Becker et al. (2015) found low W/Hf ratios in chondrules and high ratios in matrix. The isotope ratios  $^{182}\text{W}/^{184}\text{W}$  in both fractions are complementary, leading to a single isochron reflecting formation of chondrules and matrix at the same time, within the first 2.6 Gy after formation of the solar system (Becker et al., 2015; Budde et al., 2016a). Becker et al. (2015) and Budde et al. (2016a) further identified complementary relationship of  $^{183}\text{W}$  between chondrules and matrix in Allende. This is remarkable because all chondritic meteorites analysed so far have the same  $\delta^{183}\text{W}$  within limits of uncertainty, but far outside the measured  $\delta^{183}\text{W}$  of chondrules and matrix. There must be two sources of  $^{183}\text{W}$  with very different  $\delta^{183}\text{W}$  which add up to the remarkably constant solar system value of  $\delta^{183}\text{W}$  (Hubbard, 2016). Similar results are found for Mo (Budde et al. 2016b). The Mo stable isotopes are, however, less constant in chondritic meteorites than those of W.

#### 4.4.5 Addition of Si in bulk R chondrites

Figure 4.8a shows main element ratios of R chondrites (Bischoff et al., 2011) and of ordinary chondrites (H, L and LL; Wasson and Kallemeyn, 1988), normalised to the CI chondritic ratios. The Si/Mg ratios are always super-CI chondritic, with R chondrites having the highest Si/Mg ratios. The Fe/Mg ratios are sub-chondritic in L and LL chondrites, but are CI chondritic in R and H chondrites. Ratios of Fe/Si are sub-chondritic in all chondrite groups in the increasing order: H, R, L, LL.

The non-chondritic Si/Mg ratio in LL and L ordinary chondrites can be explained by removal of early formed forsteritic olivine from the region of ordinary chondrite formation (e.g. Petaev and Wood, 1998; Dauphas et al. 2015). Such a removal of forsteritic olivine should not only change the Si/Mg ratio in the remaining reservoir, but also the Fe/Mg ratio, which would need to increase. The Fe/Mg ratio in R chondrites is, however, unchanged from

the CI chondritic ratio, although the Si/Mg and the Si/Fe ratios are super-chondritic. This could be achieved by simply adding Si to the reservoir, in which R chondrites formed. Hence, rather the addition of Si than the removal of Mg seems likely to explain the main element ratios of Si/Mg, Si/Fe and Fe/Mg observed in R chondrites. A similar process might also have led to the super-chondritic Si/Mg ratio in H chondrites, and even also in all OC, and not the removal of forsteritic olivine.

Figure 4.8b displays the average Si/Mg ratios of bulk chondrules and of matrices in different carbonaceous chondrite groups and in R chondrites. The figure shows that the mean Si/Mg ratio of matrix in R chondrites is in the range of the mean Si/Mg ratios of matrices in

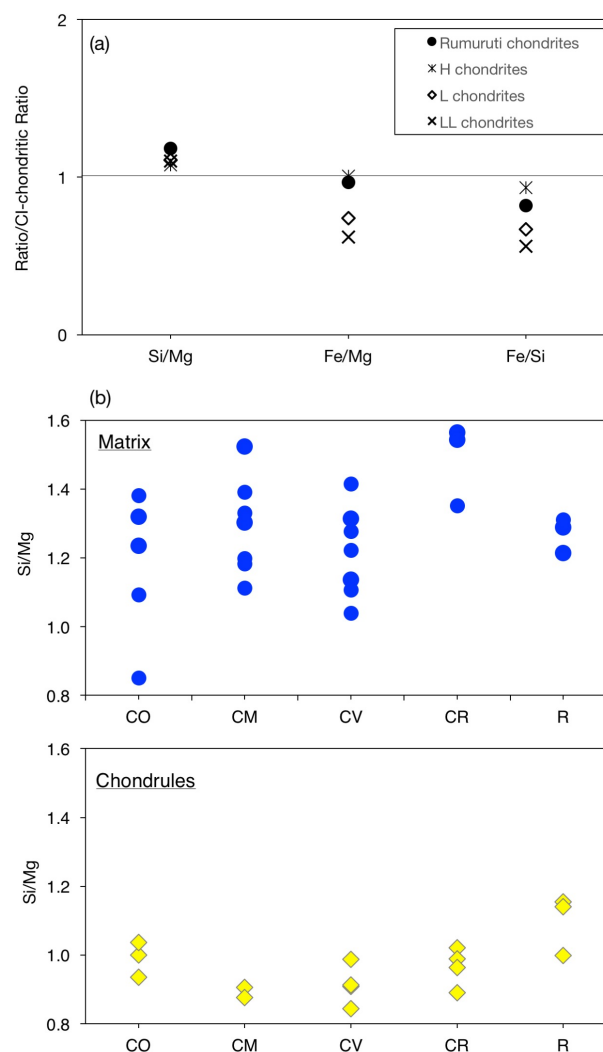


Figure 4.8: (a) All main element ratios of bulk meteorite composition are deviating from the CI- chondritic ratios for L and LL ordinary chondrites, while the Fe/Mg ratio in R chondrites and in H ordinary chondrites is CI chondritic. (b) Matrices in R chondrites have similar Si/Mg ratios, but chondrules have higher Si/Mg ratios than the according components in carbonaceous chondrites. Data for ordinary chondrites are from Wasson and Kallemeyn, 1988; data for R chondrites are from Bischoff et al., 2011, and data for carbonaceous chondrites are from Hezel and Palme, 2010; and references therein; Friend et al.2016, and Friend et al., submitted for publication.

carbonaceous chondrite. Yet, the chondrules in R chondrites are enriched in Si compared to carbonaceous chondrites. Hence, the excess of Si in bulk R chondrites is most probably carried by the chondrules, not by the matrix.

### 4.4.6 Origin of refractory element complementarities

The refractory elements Ca, Al and Ti are unfractionated in bulk R chondrites, and the ratios of Al/Ti and Al/Ca are CI chondritic (Fig. 4.5c and 4.5d). However, they are different between chondrules and matrix, with chondrules being generally enriched in Ca and Ti and depleted in Al, while the matrix has the according reverse composition. A fractionation of the elements with respect to distinct condensation temperatures can be ruled out as the condensation temperatures for Al, Ti and Ca bearing minerals are very close to each other (Ebel, 2006; and references therein). Further, the refractory elements are not supposed to have been fractionated from thermally induced chemical reactions between gases and grains in the solar nebula during chondrule formation. We rather propose that different minerals served as carriers for the individual elements and were fractionated between chondrule precursors and the surrounding nebula gas. For example, Al dominated hibonite, corundum or spinel could have been concentrated in the material that formed the matrix, while perovskite minerals were incorporated in chondrule precursors. Ebert and Bischoff (2016) suggest that some precursors of Na-rich chondrules were most likely perovskite minerals. Such a distribution of refractory minerals was probably responsible for the enrichments of Al in the matrix and of Ti and Ca in chondrules of R chondrites. Possibly sorting due to grain sizes or different grain sticking coefficients controlled this sorting.

## 4.5 Conclusions

The chemical complementarity between matrix and chondrules was so far only observed in carbonaceous chondrites. Here we report complementary element compositions in a non-carbonaceous chondrite group, the Rumuruti chondrites. The complementary relationships between matrix and chondrules in R chondrites is qualitatively the same as in carbonaceous chondrites: strongly fractionated Fe/Mg and a preference of Ti and Ca for chondrules,

resulting in low Al/Ti and Al/Ca ratios in chondrules and high ratios in matrix. We explain the complementarity in R chondrites similar carbonaceous chondrites: chondrules and matrix formed from the same reservoir.

The super-chondritic Si/Mg ratio in bulk R chondrites must be explained by the addition of Si. As the bulk Fe/Mg ratio is chondritic, removal of forsteritic olivine is unlikely. The super-chondritic Si/Mg ratio is most probably carried by the chondrules.

### **Acknowledgements**

P. F. is grateful for a fellowship grant No. GSGS-2016B-F01 from the Graduate School of Geosciences (GSGS) of the University of Cologne.

## References

- Berlin J., Jones R. H., and Brearley A. J. 2006. Determining the bulk chemical composition of chondrules by electron microprobe: a comparison of different approaches(Abstract). *37<sup>th</sup> Lunar and Planetary Science Conference*: 2370.
- Becker M., Hezel D. C., Schulz, T., Elfers B. M., and Münker C. 2015. Formation timescales of CV chondrites from component specific Hf-W systematics. *Earth and Planetary Science Letters* 432: 472-482.
- Bischoff A. 2000. Mineralogical characterization of primitive, type 3 lithologies in Rumuruti chondrites. *Meteoritics and Planetary Science* 35: 699-706.
- Bischoff A., Vogel N., and Roszjar J. 2011. The Rumuruti chondrite group. *Chemie der Erde* 71: 101-133.
- Bland P. A., Alard O., Benelux G. K., Kearsley A. T., Menzies O. N., Watt L. E., and Rogers N. W. 2005. Volatile fractionation in the early solar system and chondrule/matrix complementarity. *Proceeding of the National Academy of Sciences* 102: 13755-13760.
- Budde G., Kleine T., Kruijjer T. S., Burkhardt C., and Metzler K. 2016a. Tungsten isotopic constraints on the age and origin of chondrules. *Proceeding of the National Academy of Sciences* 113: 2886-2891.
- Budde G., Burkhardt C., Brennecke G. A., Fischer-Gödde A., Kruijjer T. S., Kleine T. 2016b. Molybdenum isotopic evidence for the origin of chondrules and a distinct genetic heritage of carbonaceous and non-carbonaceous meteorites. *Earth and Planetary Science Letters* 454: 293-303.
- Dauphas N., Poitrasson F., Burkhardt C., Kobayashi H., and Kurosawa K. 2015. Planetary and meteoritic Mg/Si and  $\delta^{30}\text{Si}$  variations inherited from solar nebula chemistry. *Earth and Planetary Science Letters* 427: 236-248.
- Ebel D. S. 2006. Condensation of rocky material in astrophysical environments. In *Meteorites and the Early Solar System II*. Edited by Lauretta D.S., McSween H. J. Jr., Univ. Arizona Press:253-277.
- Ebel D. S., Greenberg M., Rivers M. L., and Newville M. 2009. Threedimensional textural and compositional analyses of particle tracks and fragmentation history in aerogel. *Meteoritics and Planetary Science* 44: 1445-1463.
- Ebel D. S., Brunner C., Konrad K., Leftwich K., Erb I., Lu M., Rodriguez H., Crapster-Pregont E., Friedrich J.M., and Weisberg M. K. 2016. Abundance, major element composition and size of components and matrix in CV, CO and Acfer 094 chondrites.

- Geochimica et Cosmochimica Acta* 172: 322-356.
- Ebert S., and Bischoff A. 2016. Genetic relationship between Na-rich chondrules and Ca,Al-rich inclusions? –Formation of Na-rich chondrules by melting of refractory and volatile precursors in the solar nebula. *Geochimica et Cosmochimica Acta* 177: 182-204.
- Floss C., El Goresy A., Zinner E., Kransel G., Rammensee W., and Palme H. 1996. Elemental and isotopic fractionations produced through evaporation of Allende CV chondrite: Implications for the origin of HAL-type hibonite inclusions. *Geochimica et Cosmochimica Acta* 60: 1975-1997.
- Floss C., El Goresy A., Zinner E., Palme H., Weckwerth G., and Rammensee W. 1998. Corundum-bearing residues produced through the evaporation of natural and synthetic hibonite. *Meteoritics and Planetary Science* 33: 191-206.
- Franchi I. A. 2008. Oxygen isotopes in asteroidal materials. *Reviews in Mineralogy and Geochemistry* 68: 345-397.
- Friend P., Hezel D. C., and Mucerschi D. (2016). The conditions of chondrule formation, Part II: Open system. *Geochimica et Cosmochimica Acta* 173: 198-209.
- Friend P., Hezel D. C., Barrat J. A., Zipfel J., Palme H., and Metzler K.. Composition, petrology and chondrule-matrix complementarity of the recently discovered Jbilet Winselwan CM2 chondrite. Submitted for publication to *Meteoritical and Planetary Science*.
- Grossman J. N., and Brearley A. J. 2005. The onset of metamorphism in ordinary and carbonaceous chondrites. *Meteoritics and Planetary Science* 40: 87-122.
- Hezel D. C. 2010. A mathematica code to produce phase maps from two element maps. *Computers & Geosciences* 36: 1097-1099.
- Hezel D. C., and Palme H. 2008. Constrains for chondrule formation from Ca-Al distribution in carbonaceous chondrites. *Earth and Planetary Science Letters* 265: 716-725.
- Hezel D. C., and Palme H. 2010. The chemical relationship between chondrules and matrix and the chondrule matrix complementarity. *Earth and Planetary Science Letters* 294: 85-93.
- Hubbard A., 2016. Partitoning tungsten between matrix precursors and chondrule precursors through relative settling. *The Astrophysical Journal* 826: 151-158.
- Huss G. R., Keil K., and Taylor G. J. 1981. The matrices of unequilibrated ordinary chondrites: implications for the origin and history of chondrites. *Geochimica et Cosmochimica Acta* 45:33-51.

- Kadlag Y, and Becker H. 2016. Highly siderophile and chalcogen element constraints on the origin of components of the Allende and Murchison meteorites. *Meteoritics and Planetary Science* 51: 1136-1125.
- Kallemeyn G. W., Rubin A. E., and Wasson J. T. 1996. The compositional classification of chondrites: VII. The R chondrite group. *Geochimica et Cosmochimica Acta* 60: 2243-2256.
- Kita N. T., Tenner T. J., Ushikubo T., Nakashima D., and Bischoff A. 2013. Primitive chondrules in a highly unequilibrated clast in NWA 753 R chondrite (Abstract). *44<sup>th</sup> Lunar and Planetary Science Conference*: 1784.
- Klerner S. 2001. Materie im frühen Sonnensystem: die entstehung von chondren, matrix und refraktären forsteriten. Ph.D. thesis. Universität zu Köln.
- Klerner S., and Palme H. 2000. Large Titanium/Aluminium fractionation between chondrules and matrix in Renazzo and other carbonaceous chondrites. *Meteoritics and Planetary Science* (Supplement) 35: 89.
- Lee M. R., and Bland P. A. 2004. Mechanisms of weathering of meteorites recovered from hot and cold deserts and the formation of phyllosilicates. *Geochimica et Cosmochimica Acta* 68: 893-916.
- Lodders K. 2003. Solar system abundances and condensation temperatures of the elements. *The Astrophysical Journal* 591: 1220-1247.
- Lux G., Keil K., and Taylor G. J. 1980. Methamorphism of the H-group chondrites: implicatins from compositional and textural trend in chondrules. *Geochimica et Cosmochimica Acta* 44: 841-855.
- Palme H., Weckwerth G., and Wolf D. 1996. The composition of a new R-chondrite and the classification of chondritic meteorites (Abstract). *27<sup>th</sup> Lunar and Planetary Science Conference*: 991.
- Palme H., Spettel B., and Hezel D. C. 2014a. Siderophile elements in chondrules of CV chondrites. *Chemie der Erde–Geochemistry* 74: 507-516.
- Palme H., Lodders K., and Jones A. 2014b. Solar system abundances of the elements. In *Treatise on Geochemistry, 2<sup>nd</sup> edition*. Edited by Turekian, K. K., and Holland H., Elsevier: 15-36.
- Palme H., Hezel D. C., and Ebel D. S. 2015. The origin of chondrules: Constraints from matrix composition and matrix-chondrule complementarity. *Earth and Planetary Science Letters* 411:11-19.
- Petaev M. I., and Wood J. A. (1998). The condensation with partial isolation (CWPI) model



- of condensation in the solar nebula. *Meteoritics and Planetary Sciences* 33: 1123- 1137.
- Schneider C. A., Rasband W. S., Eliceiri K. W. NIH Image to ImageJ: 25 years of image analyses. *Nature Methods* 9: 671-675.
- Stelzner T., Heide K., Bischoff A., Weber D., Scherer P., Schultz L., Happel M., Schrön W., Neupert U., Michel R., Clayton R. N., Mayeda T. K., Bonani G., Haidas I., Ivy-Ochs S., and Suter M. 1999. An interdisciplinary study of weathering effects in ordinary chondrites from the Acfer region, Algeria. *Earth and Planetary Science* 34: 787-794.
- Warren P. H. 2011. Stable-isotopic anomalies and the accretionary assemblage of the Earth and Mars: A subordinate role for carbonaceous chondrites. *Earth and Planetary Science Letters* 311: 93-100.
- Wasson J. T., and Kallemeyn G. W. 1988. Compositions of chondrites. *Philosophical Transactions of the Royal Society of London A: Mathematical, Physical and Engineering Sciences* 325: 535-544.
- Wood J. A. 1985. Meteoritic constrains on processes in the solar nebula. In *Protostars and Planets II*. Edited by Black D. C. and Matthews M. S., The University of Arizona Press: 687-702.
- Wolf D., and Palme H. 2001. The solar system abundances of phosphorus and titanium and the nebular volatility of phosphorus. *Meteoritics and Planetary Science* 36: 559-571.

## Supplementary

Supplementary Table 4.1: Abundances of major and minor elements in three distinct samples of NWA 753, each of different equilibration degree, compared to literature data of R chondrites.

		CI	R chondrites	NWA 753				Allende		
			mean	Bulk sample		Type fragment	3	Equilibrated fragment		
Mg	wt.%	9.54	12.81 ±0.45	13.19	13.14	13.04	13.10	12.88	12.99	15.15
Al	wt.%	0.84	1.08 ±0.04	0.98	1.00	0.97	0.95	0.98	1.00	1.60
Si	wt.%	10.70	16.97 ±0.31	16.30	16.30	16.31	16.21	16.42	16.41	16.00
Ca	wt.%	0.91	1.15 ±0.08	1.18	1.18	1.26	1.25	1.03	1.03	1.77
Ti	wt.-ppm	447	580 ±10	660	660	600	600	660	660	840
Fe	wt.%	18.66	24.2 ±0.6	25.07	25.07	25	25.23	25.3	25.42	24.11
Na	wt.-ppm	4960	6475 ±337	-	-	-	-	-	-	-
K	wt.-ppm	546	806 ±140	580	500	580	580	580	1000	330
Cr	wt.-ppm	2623	3568 ±125	3790	3660	3670	3640	3700	3780	3600
Mn	wt.-ppm	1916	2271 ±146	2320	2320	2320	2250	2170	2320	1470
Ni	wt.%	1.09	1.46 ±0.11	1.73	1.80	1.55	1.80	1.38	1.73	1.33

Mean R chondrite data from Bischoff et al., 2011 and CI chondrite data from Palme et al., 2014.

#### 4 Complementary element relationships between chondrules and matrix in Rumuruti chondrites

Supplementary Table 4.2: Bulk chondrule compositions of chondrules in NWA 753, NWA 2446 and Hughes 030.

NWA 753										
	Chd#1 n=31	Chd#2 n=47	Chd#3 n=23	Chd#4 n=26	Chd#5 n=32	Chd#6 n=27	Chd#7 n=34	Chd#8 n=26	Chd#9 n=33	Chd#10 n=37
Si	22.89	20.30	18.83	24.90	24.57	22.59	21.31	21.96	23.33	21.14
Ti	0.11	0.06	0.01	0.07	0.07	0.07	0.09	0.07	0.10	0.12
Al	1.54	0.61	0.20	0.66	0.55	0.66	0.74	0.41	0.65	2.01
Cr	0.20	0.23	0.17	0.25	0.44	0.48	0.19	0.42	0.57	0.19
Mg	22.00	24.98	25.92	22.36	22.82	21.48	23.20	19.48	17.96	21.78
Fe	6.39	8.76	11.35	5.12	3.95	8.22	8.85	9.82	9.98	7.53
Ni	0.66	0.30	0.30	0.46	0.21	0.45	0.35	0.46	0.44	0.55
Mn	0.11	0.13	0.21	0.09	0.30	0.53	0.11	0.36	0.37	0.11
Ca	1.64	0.95	0.12	0.51	1.44	1.07	1.48	3.17	2.52	2.36
Na	0.04	0.03	0.03	0.06	0.05	0.09	0.03	0.13	0.09	0.03

NWA 2446										
	Chd#1 n=43	Chd#2 n=27	Chd#3 n=33	Chd#4 n=32	Chd#5 n=36	Chd#6 n=36	Chd#7 n=20	Chd#8 n=29	Chd#9 n=38	Chd#10 n=38
Si	21.39	24.02	21.32	22.38	20.84	25.54	24.95	24.52	20.42	23.17
Ti	0.16	0.04	0.25	0.08	0.05	0.04	0.02	0.10	0.06	0.08
Al	3.17	0.24	3.50	0.66	0.82	0.18	0.22	0.59	0.95	0.52
Cr	0.15	0.42	0.20	0.29	0.24	0.34	0.46	0.48	0.14	0.51
Mg	20.83	19.75	19.01	21.38	19.16	21.06	17.03	19.16	24.52	18.46
Fe	4.38	8.33	5.20	8.57	13.18	4.48	10.53	8.82	10.80	11.32
Ni	0.13	0.06	0.03	0.05	0.09	0.02	0.07	0.05	0.05	0.08
Mn	0.06	0.34	0.07	0.18	0.30	0.22	0.35	0.38	0.11	0.36
Ca	2.11	1.18	3.37	1.15	1.55	0.80	0.40	2.60	0.52	2.74
Na	1.64	0.13	2.04	0.24	0.53	0.08	0.14	0.08	0.58	0.12

Hughes 030							
	Chd#1 n=54	Chd#2 n=65	Chd#3 n=52	Chd#4 n=49	Chd#5 n=63	Chd#6 n=31	Chd#7 n=60
Si	26.05	25.04	23.84	23.63	19.86	26.23	21.43
Ti	0.08	0.12	0.06	0.20	0.04	0.07	0.03
Al	2.53	0.87	0.93	1.25	0.13	0.56	0.61
Cr	0.32	0.58	0.37	0.38	0.37	0.32	0.37
Mg	19.20	20.72	20.22	22.06	21.30	20.51	19.90
Fe	1.84	4.10	7.08	3.04	13.52	4.68	14.04
Ni	0.02	0.02	0.02	0.02	0.05	0.06	0.03
Mn	0.13	0.31	0.45	0.08	0.32	0.12	0.21
Ca	2.86	2.84	1.39	3.92	1.69	1.40	0.88
Na	0.20	0.07	0.63	0.02	0.08	0.02	0.02

#### 4 Complementary element relationships between chondrules and matrix in Rumuruti chondrites

Supplementary Table 4.3: Element ratios of bulk meteorites, chondrules and matrices in R chondrites

	<b>Bulk chondrites</b>			<b>Chondrules</b>			<b>Matrix</b>		
	CI	R chondrites (mean)	NWA 753 type 3 lithology	NWA 2446	NWA 753	Hughes 030	NWA 2446	NWA 753	Hughes 030
Fe/Mg	1.96	1.89	1.92	0.43	0.36	0.34	2.46	2.09	2.16
Si/Mg	1.12	1.32	1.24	1.14	1.00	1.15	1.31	1.29	1.21
Fe/Cr	71.77	67.83	67.81	26.62	25.47	17.82	98.10	89.76	78.38
Mg/Cr	36.69	35.90	35.32	62.30	70.69	53.10	39.90	42.88	36.26
Mn/Cr	0.73	0.64	0.62	0.74	0.74	0.60	0.77	0.90	0.78
Al/Ti	18.67	18.62	16.00	12.24	10.43	11.47	31.93	34.71	19.14
Fe/Ni	17.28	16.58	14.93	134.03	19.13	219.55	43.39	13.44	83.35
Al/Ca	0.92	0.94	0.77	0.66	0.53	0.46	2.19	2.40	0.48

Mean R chondrite data from Bischoff et al., 2011 and CI chondrite data from Palme et al., 2014.

## 5 Discussion

The data which are presented and discussed in chapters 2, 3, and 4 provide a coherent picture of chondrule formation. Most chondrules in C and in R chondrites are mineralogically zoned. A conservative count of the studied chondrules results in 72% of zoned chondrules. The pyroxene dominated chondrule rims formed during chondrule formation, whilst chondrules were open systems. Chondrule precursors presumably consisted of olivine minerals and to lesser amounts of diopside and refractory minerals, as these phases are among the first to form from a cooling gas of solar composition (e.g. Larimer 1967; Grossman, 1972; Lodders 2003). The condensation of Mg-rich olivines led to an enrichment of SiO in the surrounding nebula gas. When chondrule precursor were heated and (partially) melted, they reacted at their peripherals with the SiO of the nebula gas to form enstatite. The low-Ca pyroxenes in the chondrule rims often enclose olivine minerals poicilitically. This occurrence presumably developed because the low-Ca pyroxene rims prevented olivine cores from further reaction with the gas.

After chondrule formation, the surrounding nebula gas condensed as fine-grained matrix material. The enrichment in SiO of the nebula gas is still reflected in the Si/Mg complementarity between chondrules and matrix. As shown in chapters 3 and 4, matrices in C and R chondrites (the same chondrites as investigated in chapter 2) have higher Si/Mg ratios than chondrules. These chemical differences would be even bigger without the described addition of Si from the gas to the chondrules. However, chondrules and matrix have not only different Si contents. Within this work, chemical complementarities have been found for Fe/Mg, Si/Mg, Al/Ti and Ca/Al in the studied chondrules. Matrices have super-chondritic ratios for Fe/Mg, Si/Mg, Al/Ti, and Al/Ca, and chondrules have sub-chondritic ratios, while bulk meteorites are CI chondritic (except R chondrites for Si/Mg). Those complementarities indicate that chondrules and matrix formed within a common reservoir. Since, when both components would have originated in different localities with diverse compositions, it would be unfeasible that they mixed up in just the right amounts to obtain CI chondritic element abundances for bulk meteorites. This reasoning is particularly conclusive, when considering (i) that the proportions of chondrules and matrix in different meteorites are highly variable, but (ii) Si/Mg ratios of bulk meteorite compositions are uniform on the gram-level (Stracke et. al., 2012; Palme et al., 2015, and references therein),

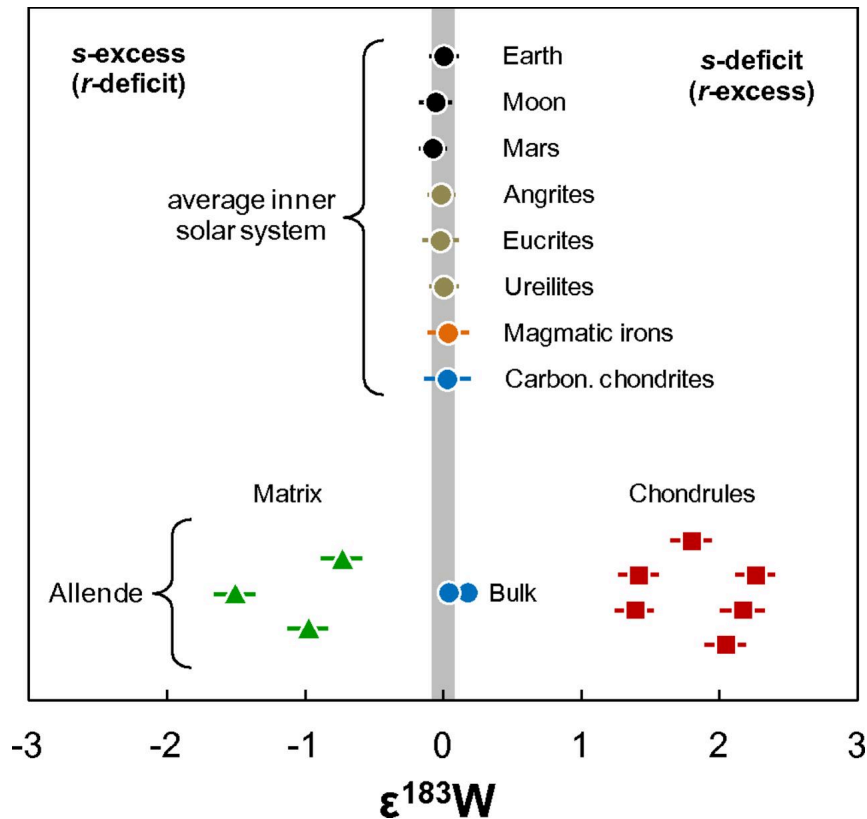


Figure 5.1: Values for  $\epsilon^{183}\text{W}$  of meteoritic and planetary material. Bulk meteorites and planets of the inner solar system show no, or only small nucleosynthetic W isotope variations. Chondrules and matrix from the Allende chondrite however, show large and complementary anomalies. (Figure from Budde et al., 2016a)

and (iii) that complementarities are so far already found for several different element ratios in numerous chondrite groups.

Recently, complementarity has also been found for W (Becker et al., 2015; Budde et al. 2016a) and Mo isotopes (Budde et al., 2016b). Figure 5.1 shows that bulk meteorites and inner solar system planets all have similar  $\epsilon^{183}\text{W}$  (parts per 10,000 deviations from terrestrial standard values normalised to the terrestrial  $^{186}\text{W}/^{183}\text{W}$ ). Chondrules and matrix in the CV chondrite Allende, however, have large anomalies, which are complementary. These isotope anomalies are of nucleosynthetic origin and indicate a different distribution of presolar material between chondrules and matrix. Regarding the nearly homogenous distribution of  $^{183}\text{W}$  in inner solar system materials, including bulk meteorites, the anomalies between chondrules and matrix can also only be explained by formation of both components in a single reservoir within the solar nebula.

## 5.1 Possible mechanisms of complementarities

The phenomena of chemical complementarities between chondrules and matrix in chondritic meteorites is getting more and more attention within the last years. Yet, it is still unclear how these element and isotope fractionations have been established. There is most probably not only one mechanism responsible for all observed complementarities. Some ideas about how the complementarities could have been established are outlined in the following.

### 5.1.1 Condensation, evaporation and recondensation

The Si/Mg complementarity is—as explained above—mainly the result of Mg removal from the nebula reservoir, due to condensation of Mg-rich olivines. These olivines aggregated together with other early nebula condensates to form the chondrule precursors and later chondrules, while the surrounding nebula gas became enriched in Si. Additional Si-enrichment to the nebula was probably caused by evaporation from the chondrule precursors/melts. Cohen et al. (2000) demonstrated experimentally that chondrule precursors most likely lost FeO as well as up to 40% of SiO<sub>2</sub> by evaporation during prolonged heating times. As shown in chapter 2, some of the Si recondensed during subsequent cooling back onto the chondrules to form pyroxene.

Loss of FeO from the chondrule precursors due to evaporation may have also caused Fe/Mg complementarities. In the experiments of Cohen et al. (2000), mineral mixtures of CI chondritic composition were evaporated for different lengths of time. Olivine minerals of charges that were only evaporated for up to 6 h, contained considerable amounts of Fe, resembling type II chondrules. After 12 h of evaporation, the olivine crystals were almost purely forsteritic, due to evaporation of FeO. Yet, especially among the R chondrites examined in chapter 4, several type II chondrules are present, but they all have considerably lower Fe/Mg ratios than matrix. Therefore, evaporation of Fe alone would probably only have increased the effect, but is unlikely the only mechanism to produce Fe/Mg complementarities.

Matrix material is generally enriched in volatile elements compared to the bulk meteorites. Chondrules must have the opposite, complementary composition. As bulk chondrites have volatile-depleted, non-CI chondritic bulk compositions, these chemical

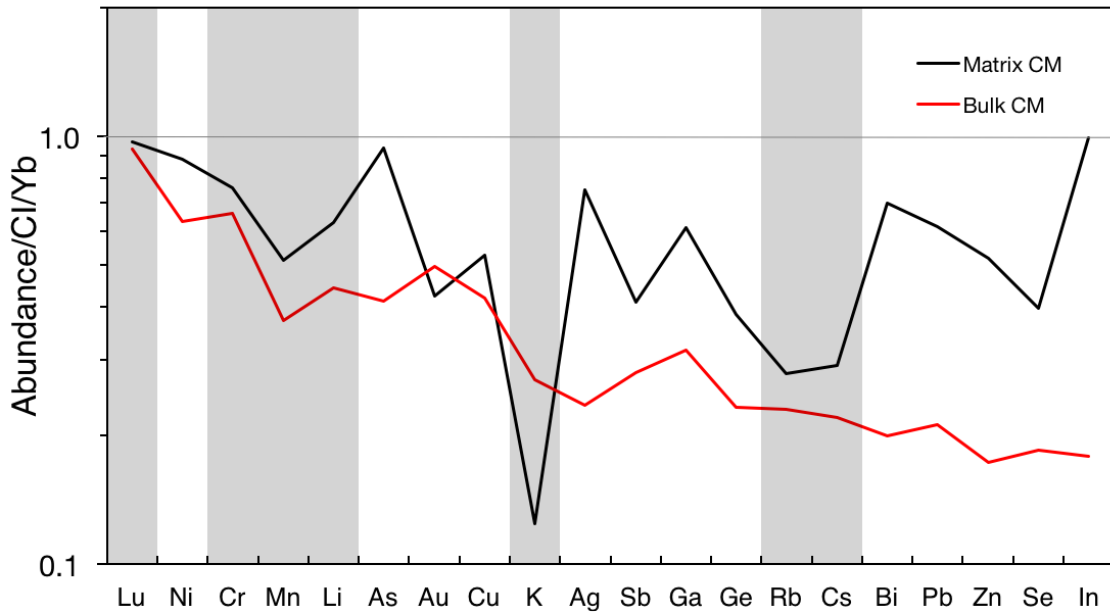


Figure 5.2: Distribution of moderately volatile elements in CM chondrite matrices and CM bulk meteorites, in order of increasing volatility (lithophile elements are indicated by grey vertical bars; Ni, Au, and Ge are siderophile; all other elements are chalcophile). Siderophile and chalcophile elements are generally more fractionated than lithophile elements. (Data are from Bland et al., 2005; and references therein)

differences cannot be referred to as complementarities. However, the general enrichment of volatile elements in the matrix supports the idea, that matrix chemistry is—at least partly—dominated by recondensed elements which evaporated during heating from the chondrule melts. In addition, Bland et al. (2005) found that the depletion trends of volatile elements in carbonaceous chondrite matrices (relative to CI) do not resemble the monotonic decreasing trend correlating with increasing volatility of the bulk chondrites (Fig. 5.2). Rather, elements with similar condensation temperatures show large variation in their abundances. Within the volatile elements, those with siderophile and chalcophile character are particularly enriched in the matrices relative to the respective bulk meteorites. Hence, there must have been a process responsible for the observed element pattern, which was not only volatility controlled. Elements were further separated due to their preferred host phases. Thus, siderophile and chalcophile elements were incorporated in metal and sulphide phases, which in turn were not or less integrated into chondrules than into matrix.



### 5.1.2 Separation of metal from chondrules

As explained above, the Fe/Mg complementarities cannot be explained only by evaporation and recondensation processes. Also the enrichment of siderophile and chalkophile volatile elements in C chondrite matrices, cannot be due to volatility controlled processes. Several authors suggested a loss of metal from chondrule melts (e.g. Dodd, 1978; Grossman, 1982; Grossman and Wasson, 1985; Hubbard, 2016). The FeO-rich olivines, typically observed in matrix, could then have formed by oxidation of the metals. Such a physical separation of metal and sulfide from chondrule melts seems necessary to obtain the differences of siderophile and chalkophile volatile element distribution in chondrite matrices (Bland et al., 2005).

The process of metal expulsion from chondrule melts is also likely to explain the distributions of W and Mo isotopes in chondrules and matrix (Budde et al., 2016a,b). As shown in Fig. 5.1, the enrichment of  $^{183}\text{W}$  in chondrules reflects a deficit of s-process material in chondrules. The depletion of  $^{183}\text{W}$  in the matrix indicates accordingly an excess of s-process material. Also, the complementary distribution of Mo isotopes in Allende chondrules and matrix reveals a deficit of s-process material in chondrules and an excess of s-process material in the matrix. The carrier phase of this s-process material is most likely a metal phase (Budde et al., 2016b). Hence, if metal was excluded from the chondrule melt, the s-process carrier metal phase would have accumulated in the matrix, establishing the observed complementarities.

There are several suggestions on possible mechanisms to expell metal from chondrule melts. According to Uesugi et al. (2008), metal can be ejected from the inside of molten chondrules by centrifugal forces, resulting from rotation of chondrules or by internal flows within melted chondrules.

### 5.1.3 Differences among precursors and sorting between chondrules and matrix

Complementarities of the refractory elements Al, Ti and Ca are more puzzling. Due to their high condensation temperatures, these elements are not supposed to have been affected by any evaporation and/or recondensation process. The chondritic meteorites studied in this work generally show a preference of Al in matrix and of Ti and Ca in chondrules. These complementarities of refractory elements could be explained by preferential incorporation of specific minerals in chondrules or matrix, respectively (Hezel and Palme, 2008). For

example, higher abundances of perovskite or early formed Al,Ti-diopside minerals among chondrule precursors could have been responsible for increased Ca and Ti contents in chondrules. Enrichments of Al in matrix could in turn be due to an excess of spinel minerals. Hezel and Palme (2008) as well as Ebel et al. (2016) found in several CV chondrites oppositional complementaries of Al, Ti and Ca between chondrites and matrices. According to Ebel et al. (2016) high Ti/Al and Ca/Al ratios in matrices and low Ti/Al and Ca/Al in chondrules are the typical complementarities in CV chondrites. The two CV chondrites Yamato 86751 and Tibooburra, however have the opposite composition, with high Al contents in the matrices. Hezel and Palme (2008) recognised tiny spinels dispersed in the matrix of the Yamato 86751, but not in the CV chondrite Allende, which has low Al contents in the matrix. These authors suggested that those spinel minerals are the source of the higher Al/Ca ratios in the matrix of Yamato 86751.

Additionally, in all cases, Ca and Ti seem to be linked. These two elements are either both depleted in the matrix and enriched in chondrules, or vice versa. Therefore, perovskite is a likely candidate for creating complementarities of the refractory elements. The complementarities of the refractory elements, however indicate that there must have been chemical differences among the precursor aggregates and between chondrule precursor and the surrounding nebula gas prior to chondrule formation. Different minerals in chondrules and matrix must have been responsible for the complementarities.

### **5.2 Complementarity and chondrule formation processes**

Matrix material was most probably partially vaporised. Yet, matrix in all chondrite groups contain thermally labile presolar grains, which would not have survived high temperatures. Chondrules and CAIs, in contrast, formed during high temperature events. Hence, in chondritic meteorites, high and low temperature materials are combined. The findings of this work support the premise that both components must have formed spatially and probably also temporally connected. Interactions between chondrules and the surrounding nebula gas which formed the matrix, is consistent with the idea of complementarity and the joined formation of both components. As the data include R chondrites, the resulting implications are not only true for the carbonaceous chondrites, but must also for the non-carbonaceous chondrites. Non-carbonaceous chondrites probably formed in a closer heliocentric distance

to the sun and also somewhat earlier, than carbonaceous chondrites (Warren et al., 2001; Budde et al., 2016b). The findings of this work show that the chondrule formation process must have been similar in both formation regions and times, regarding the joint formation of chondrules and matrix.

Many suggestions on the chondrule formation process include a local separation of chondrules and matrix within the protoplanetary disk and a mixing of these components afterwards. The x-Wind model from Shu et al. (2001) or the model from Cuzzi et al. (2003), which is based on turbulence driven transport, require that chondrules and refractory inclusions formed near the sun and consolidated with cold matrix dust in the outer parts of the disk. Any of these models are inconsistent with the chemical chondrule and matrix complementarities.

There exist also several scenarios of chondrule formation including collisions of molten, or partially molten planetesimals. In those concepts, the formation of matrix is often generally insufficiently considered. Sanders and Scott (2012) imply that matrix partially derived from unconsolidated dust at the surface of the planetesimals and from dust within the interplanetary space. In such a scenario, however, it is not only difficult to maintain up to 60 vol.% of matrix material as typical in carbonaceous chondrites, it is also extremely unlikely to retain the observed complementarities between chondrules and matrix. Especially the isotopic complementarities, which must be due to inhomogeneous distribution of presolar material, are impossible to combine with such a model, making chondrules of already processed planetesimals.

Only chondrule formation processes, which predict very local heating mechanisms to allow chondrules and matrix to remain together, are in agreement with complementarity. These conditions are so far only met by the shock heating model and the current sheet model. Shock waves could have been generated in the solar nebula in a variety of ways. For example, planetesimals driven bow shocks or shocks which were due to nebular spiral arms can be considered (Boss and Durison, 2005). These shocks convert a local low temperature and low density environment in short time into a high temperature and high density environment. Adiabatic expansion allows fast cooling of the gas (Boley et al. 2013). Matrix material could have been formed from unevaporated dust and some volatile elements that were lost from the chondrules during heating, hence the complementary element distribution of chondrules and matrix could also have been established. Current sheet heating is supposed to originate from magnetorotational instabilities and is predicted to be even more localised (Joung et al., 2004; Hubbard et al. 2012; McNally et al., 2013).

Hubbard and Ebel (2017) recently introduced a layered-disk model, which would also allow chondrules and matrix to form cogenetic. According to these authors, chondrules formed in the hotter upper regions of the disk and then settled down onto the midplane to mix with the unprocessed matrix material. Only short vertical distances between chondrules and matrix would be required, due to the low aspect ratio of protoplanetary disks, allowing chondrule and matrix complementarity to be established.

### 5.3 Conclusion

The complementary element distributions between chondrules and matrix of the CM chondrite Jbilet Winselwan and the Rumuruti chondrites found in this work support previous findings on complementarity. The contribution to the debate on possible chondrule formation process is, that it can be limited to those scenarios which allow chondrules and matrix to form from a single reservoir. This is so far only fulfilled by the shock wave model and the current sheet model. Possibly layered disk models can help to keep chondrules and matrix in the same region during formation.

The high abundance of mineralogically zoned chondrules in carbonaceous and in R chondrites also indicate, that chondrules and matrix did not only form in a single reservoir, but that chondrules operated as open systems. During formation, chondrules were in chemical exchange with the surrounding nebula gas, which later condensed to form matrix.

## References for chapter 1 and chapter 5

- Aléon J., Krot A. N., and McKeegan K. D. 2002. Calcium-aluminum-rich inclusions and amoeboid olivine aggregates from the CR carbonaceous chondrites. *Meteoritics and Planetary Science* 37: 1729-1755.
- Alexander C. M. O' D. 1996. Recycling and volatile loss in chondrule formation. In *Chondrules and the Protoplanetary Disk*. Edited by Hewins R. H., Jones R., and Scott E. R. D., Cambridge University: 233-241.
- Alexander C. M. O' D. 2005. Re-examining the role of chondrules in producing the elemental fractionations in chondrites. *Meteoritics and Planetary Science* 40: 943-965.
- Alexander C. M. O' D., Grossman J. N., Wang J., Zanda B., Bourot-Denise M., and Hewins R. H. 2000. The lack of potassium-isotopic fractionation in Bishunpur chondrules. *Meteoritics and Planetary Science* 35: 859-868.
- Alexander C. M. O' D., Grossman J. N., Ebel D. S., and Ciesla F. J. 2008: The formation conditions of chondrules and chondrites. *Science* 320: 1617-1619.
- Alves J. F., Lada C. J., and Lada E. A. (2001). Internal structure of a cold dark molecular cloud inferred from the extinction of background starlight. *Nature* 409: 159-161.
- Anders E., and Grevesse N. 1989. Abundance of the elements: meteoritic and solar. *Geochimica et Cosmochimica Acta* 53: 197-214.
- Asphaug E., Jutzi M., and Movshovitz N. (2011). Chondrule formation during planetesimals accretion. *Earth and Planetary Science Letters* 308: 369-379.
- Becker M., Hezel D. C., Schulz T., Elfers B. M., and Münker C. 2015. Formation timescales of CV chondrites from component specific Hf-W systematics. *Earth and Planetary Science Letters* 432: 472-482.
- Berlin J., Jones R.H., and Brearley A.J. 2006. Determining the bulk chemical composition of chondrules by electron microprobe (abstract). *37<sup>th</sup> Lunar and Planetary Science Conference* 37: 2370.
- Bischoff A., Rubin A. E., Keil K., and Stöffler D. 1983. Lithification of gas-rich chondrite regolith breccias by grain boundary and localized shock melting. *Earth and Planetary Science Letters* 66: 1-10.
- Bischoff A., Vogel N., and Roszjar J. 2011: The Rumuruti chondrite group. *Chemie der Erde –Geochemistry* 71: 101-133.

- Bland P. A., Alard O., Benedix G. K., Kearsley, A. T., Menzies, O. N., Watt L. E., and Rogers N. W. 2005. Volatile fractionation in the early solar system and chondrule/matrix complementarity. *Proceedings of the National Academy of Sciences of the United States of America* 102: 13755-13760.
- Bland P. A., Stadermann F. J., Floss C., Rost D., Vicenzi E. P., Kearsley A. T., and Benedix G. K. 2007. A cornucopia of presolar and early solar system materials at the micrometer size range in primitive chondrite matrix. *Meteoritics and Planetary Science* 42: 1417-1427.
- Boley A. C., Morris M. A., and Desch S. J. 2013. High-Temperature Processing of Solids Through Solar Nebular Bow Shocks: 3D Radiation Hydrodynamics Simulations with Particles. *Astrophysical Journal* 776: 101-124.
- Boss A. P., and Durisen R. H. 2005. Sources of shock waves in the protoplanetary disk. In *Chondrites and the Protoplanetary Disk*. Edited by Krot A. N., Scott E. R. D. and Reipurth B., Astronomical Society of the Pacific: 821-838.
- Bouvier A., and Wadhwa M., 2010. The age of the Solar System redefined by the oldest Pb-Pb age of a meteoritic inclusion. *Nature geoscience* 39: 637-641.
- Brauer F., Dullemond C. P., and Henning T. 2008. Coagulation, fragmentation and radial motion of solid particles in protoplanetary disks. *Astronomy and Astrophysics* 480: 859-877.
- Brearley A. J., and Jones R. H. 1998. Chondritic meteorites. In *Planetary Materials, Reviews in Mineralogy, vol. 36*. Edited by Papike J. J., The Mineralogical Society of America: 3-1-3-398.
- Brearley A. J. 2003. Nebular versus Parent-body Processing. In *Treatise on Geochemistry*. Edited by Holland H. D., and Turekian K. K., Elsevier: 247-268.
- Budde G., Kleine T., Kruijer T. S., Burkhardt C., and Metzler K. 2016a. Tungsten isotopic constraints on the age and origin of chondrules. *Proceeding of the National Academy of Science USA* 11: 2886-2891.
- Budde G., Burkhardt C., Brennecka G. A., Fischer-Gödde A., Kruijer T. S., Kleine T. 2016b. Molybdenum isotopic evidence for the origin of chondrules and a distinct genetic heritage of carbonaceous and non-carbonaceous meteorites. *Earth and Planetary Science Letters* 454: 293-303.
- Campbell A.J., Zanda B., Perron C., Meibom A., and Petaev M. I. 2005. Origin and thermal history of Fe-Ni Metal in primitive chondrites. In *Chondrites and the Protoplanetary*

- Disk*. Edited by Krot A. N., Scott E. R. D., and Reipurth B., Astronomical Society of the Pacific: 407-431.
- Chambers J. 2008. Oligarchic growth with migration and fragmentation. *Icarus* 198: 256-273.
- Chambers J. 2014. Forming Terrestrial Planets. *Science* 344: 479-480.
- Chaussidon M., Libourel G. and Krot A. N. 2008. Oxygen isotope constrains on the origin of magnesian chondrules and on the gaseous reservoir in the early Solar System. *Geochimica et Cosmochimica Acta* 72: 1924-1938.
- Chizmadia L. J., Rubin A. E., and Wasson J. T. 2002. Mineralogy and petrology of amoeboid olivine inclusions in CO<sub>3</sub> chondrites: Relationship to parent-body aqueous alteration. *Meteoritics and Planetary Science* 40(supplement): A29.
- Christophe M. 1968. Un chondre exceptionnel dans la meteorite de Vigarano. *Bulletin de la Société Française de Mineralogie et de Cristallographie* 91: 212-214.
- Clayton R. N. 2003. Oxygen Isotopes in Meteorites. In *Treatise on Geochemistry*. Edited by Holland H. D., and Turekian K. K., Elsevier: 129-142.
- Clayton R. N., and Mayeda T. K. 1996. Oxygen isotope studies of achondrites. *Geochimica et Cosmochimica Acta* 60: 1999-2017.
- Clayton R. N., and Mayeda T. K. 1999. Oxygen isotope studies of carbonaceous chondrites. *Geochimica et Cosmochimica Acta* 63: 2089-2104.
- Clayton R. N., Mayeda T. K., Goswami J. N., and Olsen E. J. 1991. Oxygen isotope studies of ordinary chondrites. *Geochimica et Cosmochimica Acta* 55: 2317-2337.
- Cohen B. A., Hewins R. H., and Yu Y. 2000. Evaporation in the young solar nebula as the origin of 'just-right' melting of chondrules. *Nature* 406: 600-602.
- Connelly J. N., Bizzarro M., Krot A. N., Nordlund A., Wielandt D., and Ivanova M. A. 2012. The Absolute Chronology and thermal Processing of Solids in the Solar Protoplanetary Disk. *Science* 388: 651-655.
- Connelly J. N., Bollard J., and Bizzarro M., 2017. U-Pb chronology of chondrules (abstract). In *Workshop on Chondrules and the Protoplanetary disk*. LPI Contribution No. 1963, Lunar and Planetary Institute: 2025.
- Conolly H. C. Jr., Jones B. D., and Hewins 1998. The flash melting of chondrules: An experimental investigation into the melting history and physical nature of chondrule precursors. *Geochimica et Cosmochimica Acta* 65: 4567-4588.

- Cuzzi J. N., Davis S. S., and Dobrovolskis A. R. 2003. Blowing in the wind. II. Creation and redistribution of refractory inclusions in a turbulent protoplanetary nebula. *Icarus* 166: 358-402.
- Desch S. J., and Connolly H. C. Jr. 2002. A model for the processing of the thermal processing of particles in solar nebula shocks: application to cooling rates of chondrules. *Meteoritics and Planetary Sciences* 37: 183-208.
- Desch S. J., and Cuzzi J. N. 2001. The generation of lightning in the solar nebula. *Icarus* 143: 87-105.
- Dodd R. T. 1978. The composition and origin of large microporphyritic chondrules in the Manych (L-3) chondrite. *Earth and Planetary Science Letters* 39: 52-66.
- Ebel D. S., Brunner C., Konrad K., Leftwich K., Erb I., Lu M., Rodriguez H., Crapster-Pregnont E., Friedrich J. M., and Weisberg M. K. 2016. Abundance, major element composition and size of components and matrix in CV; CO and Acfer 094 chondrites. *Geochimica et Cosmochimica Acta* 172: 322-356.
- Grossman J. N. 1972. Condensation in the primitive solar nebula. *Geochimica et Cosmochimica Acta* 36: 597-619.
- Grossman J. N. 1982. Mechanisms for the depletion of metal in chondrules (abstract). *Conference on Chondrules and their Origins*: 23.
- Grossman J. N. 1988. Origin of chondrules. In *Meteoritics and the early solar system*. Edited by Kerridge J. F., and Matthews M. S., The University of Arizona Press: 680-696.
- Grossman J. N. 1996. Zoning of mesostasis in FeO-poor Sermakona chondrules (abstract). *Meteorite and Planetary Science Conference* 31: A55-A56.
- Grossman J. N., and Wasson J. T. 1985. The origin and history of the metal and sulfide components of chondrules. *Geochimica et Cosmochimica Acta* 49: 925-939.
- Grossman J. N., Alexander C. M.O'D., Wang J., and Brearley A.J. 2002. Zoned chondrules in Sermakona: Evidence for high- and low-temperature processing. *Meteoritics and Planetary Science* 37: 49-73.
- Grossman L. 1972. Condensation in the primitive solar nebula. *Geochimica et Cosmochimica Acta* 36: 597-619.
- Grossman L., Becket J. R., Fedkin A. V., Simon S. B., and Ciesla F. 2008. Redox Conditions in the Solar Nebula: Observational, Experimental, and Theoretical Constraints. *Reviews in Mineralogy and Geochemistry* 68: 93-140.



- Harju E. R., Kohl I. E., Rubin A. E., and Young E. D. 2014. Evaluating silicon condensation in type 1AB chondrules using in-situ silicon isotopes (abstract). *37<sup>th</sup> Lunar and Planetary Science Conference*: 2370.
- Hewins R. H., and Connolly H. C. Jr. 1996. Peak Temperatures of Flash-melted Chondrules. In *Chondrules and the Protoplanetary Disk*. Edited by Hewins R. H., Jones R. H., and Scott E. R. D., Cambridge University Press: 197-209.
- Hewins R. H., and Zanda B. 2012. Chondrules: Precursors and interactions with the nebular gas. *Meteoritics and Planetary Science* 47: 1120-1138.
- Hewins R. H., Connolly H. C. Jr., Lofgren G. E., and Libourel G. 2005. Experimental Constraints on Chondrule Formation. In *Chondrites and the Protoplanetary Disk*. Edited by Krot A. N., Scott E. R. D., and Reipurth B., Astronomical Society of the Pacific: 286-316.
- Hezel D. C., and Palme H. 2008. Constraints for chondrule formation from Ca-Al distribution in carbonaceous chondrites. *Earth and Planetary Science Letters* 265: 716-725.
- Hezel D. C., and Palme H. 2010. The chemical relationship between chondrules and matrix and the chondrule matrix complementarity. *Earth and Planetary Science Letters* 294: 85-93.
- Hezel D.C., Palme H., Brenker F.E., and Nasdala L. 2003. Evidence for fractional condensation and reprocessing at high temperatures in CH-chondrites. *Meteoritics and Planetary Science* 38:1199-1216.
- Hezel D.C., Palme H., Nasdala L., and Brenker F. E. 2006. Origin of SiO<sub>2</sub>-rich components in ordinary chondrites. *Geochimica et Cosmochimica Acta* 70:1548-1564.
- Hezel D. C., Russel S. S., Ross A. J. and Kearsley A. T. 2008. Modal abundances of CAIs: Implications for bulk chondrite element abundances and fractionations. *Meteoritics and Planetary Science* 43: 1879-1894.
- Hezel D. C., Needham A. W., Armytage R., Georg B., Abel R. L., Kurahashi E., Coles B. J., Rehkämpfer M., and Russel S. S. 2010. A nebula setting as the origin for bulk chondrule Fe isotope variations in CV chondrites. *Earth and Planetary Science Letters* 296: 423-433.
- Hirota T., Bushimata T., Choi Y. K., Honma M., Imai H., Iwadate K., Jike T., Kamenno S., Kameya O., Kamohara R., and Kan-Ya Y. 2007. Distance to Orion KL measured with VERA. *Publications of the Astronomical Society of Japan* 59: 897-903.
- Hubbard A. I. 2016. Ferromagnetism and particle collisions: applications to protoplanetary

- disks and the meteoritical record. *The Astrophysical Journal* 826: 152-162.
- Hubbard A. I., and Ebel D. S. 2017. Combining Dynamical and Cosmochemical Constraints on the Process of Chondrule Formation: Layered Disks (abstract). In *Workshop on Chondrules and the Protoplanetary disk*. Lunar and Planetary Institute: 2036.
- Hubbard A. I., McNally C. P., and Mac Low M.-M. 2012. Short circuits in thermally ionized plasmas: a mechanism for intermittent heating of protoplanetary disks. *Astrophysical Journal* 761: 58-68.
- Huss G. R., Alexander C. M. O' D., Palme H., Bland P. A., Wasson J. T. 2005. Genetic Relationships between Chondrules, Fine-grained Rims, and Interchondrule Matrix. In *Chondrites and the Protoplanetary Disk*. Edited by Krot A. N., Scott E. R. D. and Reipurth B., Astronomical Society of the Pacific: 701-731.
- Jacquet E., Alard O., and Gounelle M. 2012. Chondrule trace element geochemistry at the mineral scale. *Meteoritics and Planetary Science* 47: 1-20.
- Johnson B. C., Minton D. A., Melosh H. J., and Zuber M. T. 2015. Impact jetting as the origin of chondrules. *Nature* 517: 339-341.
- Jones R. H. 2012. Petrographic constraints on the diversity of chondrule reservoirs in the protoplanetary disk. *Meteoritics and Planetary Science* 47: 1176-1190.
- Joung M. K. R., Mac Low M.-M., and Ebel D. S. 2004. Chondrule formation and protoplanetary disk heating by current sheets in non-ideal magnetohydrodynamic turbulence. *Astrophysical Journal* 606: 532-541.
- Kadlag Y., and Becker H. 2016. Highly siderophile element constraints on the origin of components of the Allende and Murchison meteorites. *Meteoritics and Planetary Science* 51: 1136-1152.
- Kallemeyn G. W., Rubin A. E., and Wasson J. T. 1996. The compositional classification of chondrites: VII. The R chondrite group. *Geochimica et Cosmochimica Acta* 60: 2243-2256.
- Kita, N. T., Huss G. R., Tachibana S., Amelin Y., Nyquist L. E., and Hutcheon I. D. 2005. Constraints on the origin of chondrules and CAIs from short-lived and long-lived radionuclides. In *Chondrites and the Protoplanetary Disk*. Edited by Krot A. N., Scott E. R. D. and Reipurth B., Astronomical Society of the Pacific: 558-587.
- Klerner S., and Palme H. 1999. Origin of chondrules and matrix in carbonaceous chondrites(abstract). *30<sup>th</sup> Lunar and Planetary Science Conference*: 1272.
- Kleine, T., Mezger K., Palme H., Scherer E., and Münker C. 2005. Early core formation in asteroids and late accretion of chondrite parent bodies: Evidence from <sup>182</sup>Hf-<sup>182</sup>W in

- CAIs, metal-rich chondrites, and iron meteorites. *Geochimica et Cosmochimica Acta* 69: 5805-5818.
- Krot A.N., Libourel G., Goodrich C., and Petaev M.I. 2004. Silica-igneous rims around magnesian chondrules in CR carbonaceous chondrites: evidence for fractional condensation during chondrule formation. *Meteoritics and Planetary Science* 39:1931–1955.
- Krot A. N., Keil K., Goodrich C. A., Scott E. R. D., and Weisberg 2014. Classification of meteorites. Meteorites, Comets and Planets. In *Treatise on Geochemistry*, 2<sup>nd</sup> edition. Edited by Turekian, K. K., and Holland H., Elsevier: 1-63.
- Komatsu M., Krot A. N., Petaev M. I., Ulyanov A. A., Keil K., and Miyamoto M. 2001. Mineralogy and petrography of amoeboid olivine aggregates from the reduced CV3 chondrites Efremovka, Leoville, and Vigarano: Products of nebular condensation, accretion, and annealing. *Meteoritics and Planetary Science* 36: 629-641.
- Larimer J. W. 1967. Chemical fractionation in meteorites-1. Condensation of the elements. *Geochimica et Cosmochimica Acta* 31: 1215-1238.
- Lauretta D.S., Nagahara H., and Alexander C.M.O'D. 2006. Petrology and Origin of Ferromagnesian Silicate Chondrules. In *Meteorites and the Early Solar System II*. Edited by Lauretta D.S., McSween H. J. Jr., Univ. Arizona Press: 431-459.
- Libourel G., Krot A. N., and Tissandier L. 2006. Role of gas-melt interaction during chondrule formation. *Earth and Planetary Science Letters* 251: 232-240.
- Lodders K. 2003. Solar system abundances and condensation temperatures of the elements. *The Astrophysical Journal* 591: 1220-1247.
- Lofgren A. 1996. A dynamic crystallization model for chondrule melts. In *Chondrules and the Protoplanetary Disk*. Edited by Hewins R. H., Jones R. H., and Scott E. R. D., Cambridge University Press: 187-196.
- Lord H. C., III 1965. Molecular equilibria and condensation in a solar nebula and cool stellar atmospheres. *Icarus* 4: 279-288.
- Matsunami S., Ninagawa K., Nishimura S., Kubono N., Yamamoto I., Kohata M., Wada T., Yamashita Y., Lu J., Sears D. W. G., and Nishimura H. 1993. Thermoluminescence and compositional zoning in the mesostasis of a Sermakona group A1 chondrule and new insights into the chondrule-forming process. *Meteoritics* 57: 2101-2110.
- Markowski A., Qitté G., Halliday A. N., and Kleine T. 2006. Tungsten isotopic compositions of iron meteorites: chronological constraints vs. cosmogenic effects. *Earth and Planetary Science Letters* 242: 1-15.

- McNally C. P., Hubbard A., Mac Low M. M., Ebel D. S., and D'Alessio P. 2013. Mineral processing by short circuits in protoplanetary disks. *Astrophysical Journal* 767: L2-L7.
- McSween H. Y., and Richardson S. M. 1977. The composition of carbonaceous chondrite matrix. *Geochimica et Cosmochimica Acta* 41: 1145-1161.
- Morris M. A., and Desch S. J. 2010. Thermal histories of chondrules in the solar nebula. *The Astrophysical Journal* 722: 1474-1494.
- Mostefaoui S., Kita N. T., Togashi S., Tachibana S., Nagahara H., and Morishita Y. 2002. The relative formation ages of ferromagnesian chondrules inferred from their initial aluminum-26/aluminium-27 ratios. *Meteoritics and Planetary Science* 37: 421-438.
- Nagahara H., Kita N. T., Ozawa K., and Morishita Y. 1999. Condensation during chondrule formation: elemental and Mg isotopic evidence (abstract). *30<sup>th</sup> Lunar and Planetary Science Conference*: 1342.
- Olsen M. B., and Wielandt D., Schiller M., Van Kooten E. M., and Bizzarro M. (2016). Magnesium and <sup>54</sup>Cr isotope compositions of carbonaceous chondrite chondrules—Insights into early disk processes. *Geochimica et Cosmochimica Acta* 191: 118-138.
- Ostriker E. C., Stone J. M., and Gammie C. F. (2001). Density, velocity and magnetic field structure in turbulent molecular cloud models. *The Astrophysical Journal* 546: 980-1005.
- Palme H. 2000. Are there chemical gradients in the inner solar system?. In *From dust to terrestrial planets*. Edited by Benz W., Kallenbach R., and Lugmair G., Springer: 237-262.
- Palme H, and Wlotzka F. 1976. A metal particle from a Ca, Al-rich refractory inclusion from the meteorite, Allende, and the condensation of refractory siderophile elements. *Earth and Planetary Science Letters* 33: 45-60.
- Palme H., Lodders K., and Jones A. 2014a. Solar System Abundances of the Elements. In *Treatise on Geochemistry, 2<sup>nd</sup> edition*. Edited by Turekian, K. K., and Holland H., Elsevier: 15-36.
- Palme H., Spettel B., and Hezel D. C. 2014b. Siderophile elements in chondrules of CV chondrites. *Chemie der Erde* 74: 507-516.
- Palme H., Hezel D. C., and Ebel D. S. 2015. The origin of chondrules: Constraints from matrix composition and matrix-chondrule complementarity. *Earth and Planetary Science Letters* 411: 11-19.
- Petaev M. I., and Wood J. A. 1998. The condensation with partial isolation (CWPI) model of condensation in the inner solar system. *Meteoritics and Planetary Science* 33: 1123-1137.

- Rambaldi E. R. 1981. Relict grains in chondrules. *Nature* 293: 558-561.
- Rubin A. E. 2000. Petrologic, geochemical and experimental constraints on models of chondrule formation. *Earth-Science Reviews* 50: 3-27.
- Rubin A. E., Keil K., and Scott E. R. D. 1997. Shock metamorphism of enstatite chondrites. *Geochimica et Cosmochimica Acta* 61:847-858.
- Ruzicka A., Floss C., and Hutson M., 2012. Agglomeratic olivine (AO) objects and Type II chondrules in ordinary chondrites: Accretion and melting of dust to form ferroan chondrules. *Geochimica et Cosmochemical Acta* 76: 103-124.
- Sanders I. S., and Scott E. R. D. 2012. The origin of chondrules and chondrites: Debris from low-velocity impacts between molten planetesimals? *Meteoritics and Planetary Science* 47: 2170-2192.
- Sanders I. S., and Scott E. R. D. 2012. The origin of chondrules and chondrites: Debris from low-velocity impacts between molten planetesimals?. *Meteoritics and Planetary Science* 47: 2170-2192.
- Sanders I. S., and Taylor G. J. 2005. Implications of  $^{26}\text{Al}$  in nebular dust: Formation of chondrules by disruption of molten planetesimals. In *Chondrites and the Protoplanetary Disk*. Edited by Krot A. N., Scott E. R. D. and Reipurth B., Astronomical Society of the Pacific: 821-838.
- Schersten A., Elliot T., Hawkesworth C., Russell S., and Masarik J. 2006. Hf-W evidence for rapid differentiation of iron meteorite parent bodies. *Earth and Planetary Science Letters* 241: 530-542.
- Scott E. R. D., and Krot A. N. 2003. Chondrites and their Components. In *Treatise on Geochemistry*. Edited by Holland H. D., and Turekian K. K., Elsevier: 1-72.
- Scott E. R. D., and Krot A. N. 2014. Chondrites and their components. In *Treatise on Geochemistry, 2<sup>nd</sup> edition*. Edited by Turekian, K. K., and Holland H., Elsevier: 65-136.
- Scott E.R.D., and Taylor G.J. 1983. Chondrules and other components in C, O, and E chondrites: Similarities in their properties and origins. *Journal of Geophysical Research: Solid Earth* (Supplement)88: B275–B286.
- Scott E. R. D.; Barber D. J., Alexander C. M. O.'D., Hutchison R., and Peck J. A. 1988. Primitive material surviving in chondrites: Matrix. In *Meteorites and the Early Solar System*. Edited by Kerridge J. F., and Matthews M. S., University of Arizona Press: 718-745.

- Scott E. R. D., Love S. G., and Krot 1996. Formation of chondrules and chondrites in the protoplanetary nebula. In *Chondrules and the Protoplanetary Disk*. Edited by Hewins R. H., Jones J., and Scott E.R.D., Cambridge University Press: 45-55.
- Shu F.H., Shang H., and Lee T. 1996. Toward an astrophysical theory of chondrites. *Science* 271: 1545-1552.
- Shu F. H., Shang H., Gounelle M., Glassgold A. E., and Lee T. 2001. The origin of chondrules and refractory inclusions in chondritic meteorites. *The Astrophysical Journal* 548: 1029-1050.
- Stöffler D., Keil K., and Scott E. R. D. 1991. New shock classification for chondrites: Implication for parent body impact histories. *Meteoritics* 26: 398.
- Stracke A., Palme H., Gellissen M., Münker C., Kleine T., Birbaum K., Günther D., Bourdon B., and Zipfel J. 2012. Refractory element fractionation in the Allende meteorite: implications for nebula condensation and the chondritic composition of planetary bodies. *Geochimica et Cosmochimica Acta* 85: 114-141.
- Swindle T. D., Davis A. M., Hohenberg C. M., MacPherson G. J., and Nyquist L. E. 1996. Formation times of chondrules and Ca-Al-rich inclusions: constraints from short-lived radionuclides. In *Chondrules and the Protoplanetary Disk*. Edited by Hewins R. H., Jones R., and Scott E. R. D., Cambridge University Press: 77-86.
- Tissandier L., Libourel G., and Robert F. 2002. Gas-melt interactions and their bearing on chondrule formation. *Meteoritics and Planetary Sciences* 37: 1377-1389.
- Uesugi M., Sekiya M., and Nakamura T. 2008. Kinetic stability of a melted iron globule during chondrule formation. I. Non-rotating model. *Meteoritics and Planetary Science* 43: 717-730.
- Van Schmus W. R., and Wood J. A. 1967. A chemical-petrological classification for the chondritic meteorites. *Geochimica et Cosmochimica Acta* 31: 747-765.
- Wänke H., Dreibus G., Jagoutz E., Palme H., and Rammensee W. 1981. Chemistry of the Earth and the significance of primary and secondary objects for the formation of planets and meteorite parent bodies (abstract). *12<sup>th</sup> Lunar and Planetary Science Conference*: 1139.
- Wänke H., Dreibus G., and Jagoutz E. 1984. Mantle chemistry and accretion history of the Earth. In *Archean geochemistry*. Edited by Kröner A., Hanson G. N., and Goodwin A. M., Springer Verlag: 1-24.

- Warren P. H. 2011. Stable-isotopic anomalies and the accretionary assemblage of the Earth and Mars: A subordinate role for carbonaceous chondrites. *Earth and Planetary Science Letters* 311: 93-100.
- Wasson J. T. 1993. Constrains on chondrule origins. *Meteoritics* 28: 14-28.
- Wasson J. T. 1996. Chondrule formation energetics and length scales. In *Chondrules and the Protoplanetary Disk*. Edited by Hewins, R. H., Jones R., and Scott E. R. D., Cambridge University Press: 45-55.
- Weisberg M. K., McCoy T. J., and Krot A. N. 2006. Systematics and evaluation of meteorite classification. In *Meteorites and the Early Solar System II*. Edited by Lauretta D.S., McSween H. J. Jr., Univ. Arizona Press:19-52.
- Wlotzka F. 1993. A weathering scale for the ordinary chondrites. *Meteoritics* 28: 460.
- Wolf D., and Palme H. 2001. The solar system abundances of phosphorus and titanium and the nebular volatility of phosphorus. *Meteoritic and Planetary Science* 36: 559-571.
- Wood J. A. 1962. Chondrules and the origin of terrestrial planets. *Nature* 197: 127-130.
- Wood J. A. 1963. On the origin of chondrules and chondrites. *Icarus* 2: 152-180.
- Woolfson M. 2000. The origin and evolution of the solar system. *Astronomy & Geophysics* 41: 12-19.
- Zanda B. 2004. Chondrules. *Earth and Planetary Science Letters* 224: 1-17.
- Zanda B., Zanetta P. M., Leroux H., Le Guillou C., Lewin É., S. Pont, Deldicque D., and Hewins R. H. 2017. The chondritic Assemblage(abstract). In *Workshop on Chondrules and the Protoplanetary disk*. LPI Contribution No. 1963, Lunar and Planetary Institute: 2035.
- Zook H. A. 1980. A new impact model for the generation of ordinary chondrites (abstract). *Lunar and Planetary Institute Contribution* 412: 143.
- Zook H. A. 1981. On a new model for the generation of chondrules (abstract). *12<sup>th</sup> Lunar and Planetary Science Conference*: 1242.
- Zsom A., Ormel C. W., Guttler C., Blum J., and Dullemond C. P. 2010. The outcome of protoplanetary dust growth: Pebbles, boulders, or planetesimals? -II. Introducing the bouncing barrier. *Astronomy and Astrophysics* 531: A57.

## List of abbreviations

AOA	amoeboid olivine aggregate
AU	astronomical unit
BO	barred olivine chondrule
CAI	calcium-aluminium-rich inclusion
CB	Bencubbin-like (carbonaceous chondrites)
CC	cryptocrystalline chondrule
CH	ALH 85085-like (carbonaceous chondrites)
chd	chondrule
CI	Ivuna-like (carbonaceous chondrites)
CK	Karoonda-like (carbonaceous chondrites)
CM	Mighei/Murchison-like (carbonaceous chondrites)
CO	Ornans-like (carbonaceous chondrites)
CR	Renazzo-like (carbonaceous chondrites)
CV	Vigarano-like (carbonaceous chondrites)
d.l.	detection limit
EH	high iron enstatite (chondrites)
EL	low iron enstatite (chondrites)
Fa	fayalite
FGR	fine-grained rim
Fo	forsterite
Fs	ferrosilite
H	high iron (ordinary chondrites)
ICP-AES	inductively coupled plasma-atomic emission spectrometry
ICP-MS	inductively coupled plasma-mass spectrometry
JW	Jbilet Winselwan
K	Kagangari-like (chondrites)
K	Kelvin
L	low iron (ordinary chondrites)
LL	low iron low metal (ordinary chondrites)
Myr	million years
n	number



## List of abbreviations

---

PO	porphyritic olivine (chondrule)
POP	porphyritic olivine pyroxene (chondrule)
PP	porphyritic pyroxene (chondrule)
ppm	parts per million
R	Rumuruti-like (chondrites)
REE	rare earth elements
RP	radial pyroxene (chondrule)
s.d.	standard deviation
TCI	tochilinite-cronstedtite intergrowths
TFL	terrestrial fractionation line
vol.	volume
wt.	weight
XRF	x-ray fluorescence

## Danksagung

Mein erster Dank an dieser Stelle gilt *Dominik Hezel* und *Herbert Palme*. Herbert Palme hat mich im Rahmen meiner Diplomarbeit mit der Welt der Kosmochemie vertraut gemacht. Er hat das Thema der vorliegenden Dissertation ausgesucht und auf seine Unterstützung und Hilfe konnte ich mich immer verlassen. Außerdem hat er mich mit Dominik zusammengebracht, welcher sich als wohl bester Promotionsbetreuer diesseits des Asteroidengürtels herausgestellt hat. Insbesondere, weil er sich immer viel Zeit für meine Angelegenheiten genommen und mir stets gute Ratschläge und Anregungen gegeben hat.

*Carsten Münker* danke ich natürlich für seine Hilfsbereitschaft in den vergangenen Jahren. Aber ganz besonders dankbar bin ich ihm eigentlich dafür, dass er *all die netten Menschen der Geo-und Kosmochemie Arbeitsgruppe* zusammengeführt hat, in der ich lauter richtig coole Leute -und sicherlich den ein oder anderen Freund gefunden habe!

*Reiner Kleinschrodt* hat nicht nur zeitweise unermüdlich die Mikrosonde repariert, sondern mich auch immer mal wieder wissen lassen, dass er es bewundert, wie ich Promotion und Familie vereinbare -ich möchte ihm hiermit mitteilen, wie hilfreich er mit beidem gewesen ist!

*Karin Boessenkool* und ihrem Engagement im Rahmen der GSGS möchte ich an dieser Stelle ganz besonders herzlich danken –einige Reisestipendien und vor allem der „Fellowship Grant“ haben mich sehr motiviert!

Meinen Koautoren, insbesondere *Addi Bischoff*, *Jutta Zipfel* und *Knut Metzler* danke ich für die sehr gute Zusammenarbeit an den hier eingebundenen Arbeiten.

*Andreas Vogt* danke ich für wahrscheinlich mindestens 1.000 Kleinigkeiten.

*Almuth Katzemich* und *Marko Gellissen* danke ich außerdem für die Hilfe beim Probenaufbereiten und an der RFA.

Ohne die gute Arbeit von *Steffi Lemke*, sowie der *Teams des Zwergenland Kindergartens und der Offenen Ganztagsbetreuung der Grundschule Gerberstraße* wäre ich nicht weit gekommen –mein wärmster Dank dafür!

Bei den *freundlichen Mitarbeitern der Dacom West GmbH* bedanke ich mich herzlich für das gewährte Arbeitsplatzasyl.

Aus *meiner Familie* möchte ich mich vor allem bei denen bedanken, welche wahrscheinlich allesamt die Worte „kumulativ“ und „Paper“, „Chondren“ oder gar „Doktorarbeit“ nicht mehr hören können.

Als da wären:

Die *UFFLs* –alias *Uschi, Frank und Lisa-Lynn Neeff!* Wo soll ich anfangen? Liebe UFFLs, ich denke ihr wisst noch so in etwa, was ihr alles für mich getan habt –all die UFFL'schen rundum-sorglos-Pakete! Sowie *Tante Karin und Onkel Klaus Breuer*, die immer für einen da sind.

*Helen und Alan Friend* (besser bekannt als Grannie und Grappie), den allerbesten Schwiegereltern. Ihnen danke ich besonders dafür, dass Sie mir mit beispielloser und unermüdlicher Freude an ihren beiden Enkeltöchtern so oft den Rücken freigehalten haben! Aber auch für die vielen schönen kleinen Auszeiten in „Little Britain“, Schwalmthal.

Meine Eltern *Jörg und Petra Köhnen*. Denn sie haben nicht nur mit ihrer Erziehung den Grundstein für mein naturwissenschaftliches Interesse gelegt, sondern mich außerdem Selbstvertrauen gelehrt. Ohne ihre vielseitige Unterstützung wäre diese Arbeit überhaupt gar nicht möglich gewesen.

Meine seelenverwandte und große Schwester *Melanie Köhnen*. Wahrscheinlich keine wichtigere Entscheidung in meinem Leben habe ich ohne ihren Einfluss getroffen. Und *Martin*, er hat mir meine Schwester wiedergegeben.

*Tristan* -für seine uneingeschränkte Liebe! Mehr Unterstützung hätte ich mir nicht wünschen können.

Mein „Ein und Alles“, den wundervollen Landplagen Leni und Alba danke ich an dieser Stelle nicht –ohne sie wäre die Arbeit an meiner Dissertation bestimmt unkomplizierter und schneller gewesen.

Zu guter Letzt danke ich *Beppo Straßenkehrer* dem Freund der kleinen Momo, aus Michael Endes gleichnamigen Roman für seine weise Aussage:

„Manchmal hat man eine sehr lange Straße vor sich. Man denkt, die ist so schrecklich lang; das kann man niemals schaffen, denkt man.“ ... „Man darf nie an die ganze Straße auf einmal denken, verstehst du? Man muss immer nur an den nächsten Schritt denken, an den nächsten Atemzug, an den nächsten Besenstrich. Dann macht es Freude; das ist wichtig, dann macht man seine Sache gut. Und so soll es sein. Auf einmal merkt man, dass man Schritt für Schritt die ganze Straße gemacht hat. Man hat gar nicht gemerkt wie, und man ist nicht außer Puste. Das ist wichtig.“

## **Erklärung zum Eigenanteil an den Publikationen**

Als Erstautor habe ich in jeder der nachfolgenden Publikationen den Inhalt zu verantworten.

1. „The conditions of chondrule formation, Part II: Open system”

Der Hauptteil der Mineralphasenbilder, welche den Aussagen dieser Veröffentlichung zugrunde liegen, habe ich selbst erhoben. Die übrigen Mineralphasenbilder wurden ursprünglich zu anderen Zwecken erstellt und erst von mir zusammengetragen und gesichtet, sowie im Kontext der Publikation neu ausgewertet.

2. „Composition, petrology and chondrule-matrix complementarity of the recently discovered Jbilet Winselwan CM2 chondrite”

Alle Daten zur Gesamtchondrenzusammensetzung sowie der Zusammenstzung der Matrix wurden von mir erhoben. Des Weiteren habe ich die Gesamtgesteinsbestimmung basierend auf Röntgenfluoreszenzanalytik durchgeführt. Diese Daten bilden die Hauptaussage des Artikels. Die Rückstreuerelektronenbilder, welche den Größenbestimmungen der Chondren zugrundeliegenden, habe ich ebenfalls erstellt. Beiträge von Co-Autoren, in Form von Daten oder Text, habe ich in die Arbeit integriert.

3. „Complementary element relationships between chondrules and matrix in Rumuruti chondrites”

Alle in dieser Arbeit vorgestellten Daten, wurden von mir selber erhoben und ausgewertet.

## Erklärung

"Ich versichere, dass ich die von mir vorgelegte Dissertation selbständig angefertigt, die benutzten Quellen und Hilfsmittel vollständig angegeben und die Stellen der Arbeit – einschließlich Tabellen, Karten und Abbildungen –, die anderen Werken im Wortlaut oder dem Sinn nach entnommen sind, in jedem Einzelfall als Entlehnung kenntlich gemacht habe; dass diese Dissertation noch keiner anderen Fakultät oder Universität zur Prüfung vorgelegen hat; dass sie – abgesehen von unten angegebenen Teilpublikationen – noch nicht veröffentlicht worden ist, sowie, dass ich eine solche Veröffentlichung vor Abschluss des Promotionsverfahrens nicht vornehmen werde. Die Bestimmungen der Promotionsordnung sind mir bekannt. Die von mir vorgelegte Dissertation ist von Dominik Hezel betreut worden."

Teilpublikationen:

- Friend P., Hezel D. C., and Mucerschi 2016. The conditions of chondrule formation, Part II: Open system. *Geochimica et Cosmochimica Acta* 173: 198-209.
- Friend P., Hezel D. C., Barrat J. A., Zipfel J., Palme H., and Metzler K. (submitted for publication). Composition, petrology and chondrule-matrix complementarity of the recently discovered Jbilet Winselwan CM2 chondrite. *Meteoritics and Planetary Science*.
- Friend P., Hezel D. C., Palme H., Bischoff A., and Gellissen M. (submitted for publication). Complementary element relationships between chondrules and matrix in Rumuruti chondrites. *Earth and Planetary Science Letters*.

Datum:

Unterschrift:

## Lebenslauf

**Pia Friend, geb. Köhnen**

Staatsangehörigkeit: Deutsch

Geburtsort: Solingen

Geburtsdatum: 13.12.1982

Familienstand: Verheiratet, 2 Kinder

### Schulbildung

1988-1992                      Grundschule Gerberstraße, Solingen

1992-1998                     August-Dicke-Schule, Solingen

1999-2003                    Herder Schule Wuppertal

### Studium und Promotion

2004-2007                    Universität zu Köln, Geowissenschaftliche Fakultät, Grundstudium  
Geologie und Paläontologie

2007-2009                    Universität zu Köln, Geowissenschaftliche Fakultät, Hauptstudium  
Geologie und Paläontologie

2009-2010                    Elternzeit

2010-2011                    Universität zu Köln, Geowissenschaftliche Fakultät, Diplomarbeit „*Ein  
ungewöhnlicher Chondrit –petrographische und petrologische  
Erläuterungen zu NWA 5492*“

Abschluss: Diplom Geologin, Note „sehr gut“ (1,27)

2011-2013                    Elternzeit

Seit 2013                     Universität zu Köln, Geowissenschaftliche Fakultät, Arbeitsgruppe  
Geochemie und Kosmochemie, Promotion